Akademia Górniczo-Hutnicza
im. Stanisława Staszica w Krakowie

Wydział Fizyki i Informatyki
Stosowanej

Rozprawa doktorska

Unconventional Superconductivity in Correlated Itinerant Magnetic Systems

Michał Zegrodnik

Promotor: prof. dr hab. Józef Spałek

Kraków, czerwiec 2013

Declaration of the author of this dissertation:

Aware of legal responsibility for making untrue statements I hereby declare that I have written this dissertation myself and all the contents of the dissertation have been obtained by legal means.

data, podpis autora

Declaration of the thesis Supervisor:

This dissertation is ready to be reviewed.

data, podpis promotora rozprawy

Abstract

In this Thesis the universal aspects of the Hund's-rule induced spin-triplet pairing are analyzed within the two-band extended Hubbard model for the case of square lattice. In the presented considerations, two physically distinct regions of parameters have been singled out. Namely, the so-called attractive-interaction regime when the intraatomic interorbital Coulomb repulsion magnitude is smaller than the Hund's coupling ($U' < J$) and the purely repulsive-interaction regime ($U' > J$).

First, the emphasis is placed on the $U' < J$ regime for which the phase diagram is calculated with the use of the Hartree-Fock (HF) approximation combined with the Bardeen-Cooper-Schrieffer (BCS) approach. Within this treatment the stable pure superconducting phase, as well as coexistent with either ferromagnetism or antiferromagnetism are obtained. Influence of the intersite hybridization on the stability of the paired phases, as well as the temperature dependences of both the magnetic moment and the superconducting gaps are discussed. The approach supplements the diagrams established earlier which now contain not only magnetically ordered phases, but also the spin-triplet paired states treated on equal footing. According to the performed calculations, the nonzero magnetization can appear slightly below the Stoner threshold when it is induced by the onset of the paired phase which leads to the conclusion that the spin-triplet pairing of A1 type enhances the magnetism.

To analyze the influence of interelectronic correlations, the so-called statistically consistent Gutzwiller approximation (SGA), which has been developed recently, is used for the same model. The results obtained within the HF and SGA methods are often similar from the qualitative point of view. The main difference is that in the SGA the region of stability of the spin-triplet paired phase coexisting with ferromagnetism is absent, whereas it appears in the HF-BCS situation.

Next, it was discovered that for the purely repulsive interactions regime the spin-triplet paired phases, both pure and coexisting with antiferromagnetism, can become stable but only when the calculations are performed within the SGA method. The absence of the stable paired states in that regime within the HF approximation shows explicitly, that the electron correlations, in conjunction with the Hund's-rule exchange, play a crucial role in stabilizing the spin-triplet superconducting state. Furthermore, even though the model contains only the intrasite interactions, an intersite pairing appears in the correlated regime that leads to the $\mathbf{k}$-dependent superconducting gap (extended s-wave).

Finally, the problem of the average particle number conservation with respect to the Gutzwiller projection operation is discussed. A modification of the previously used method (SGA) is proposed and consists of inclusion of an additional term in the effective Hamiltonian which enforces the conservation of the average particle number when carrying out the Gutzwiller projection, without introducing the so-called fugacity factors in the projection operator. It is shown, that this modification leads to a significant reduction of the superconducting gap in the situation when the pairing is strong. Nevertheless, the qualitative trends remain the same. Concluding, it is claimed that the SGA method can be regarded as a realistic method of approach also when extended to concrete materials, which should be analyzed separately.

Streszczenie

W niniejszej rozprawie przeprowadzono rozważania dotyczące uniwersalnych aspektów parowania trypletowego zaindukowanego regułą Hunda w dwupasmowym modelu Hubbarda na sieci kwadratowej. Dwa fizycznie różne obszary parametrów zostały przeanalizowane z osobna. Pierwszy z nich to tak zwany region oddziaływań przyciągających, który odnosi się do sytuacji, gdy międzyorbitalne wewnątrzatomowe odpychanie kulombowskie jest mniejsze od całki oddziaływań wymiennych typu Hunda ($U' < J$), natomiast dla drugiego z nich mamy do czynienia z czysto odpychajacymi oddzialywaniami ($U' > J$).

W pierwszej części rozprawy rozważano sytuację, w której $U' < J$. Za pomocą przybliżenia Hartree-Focka (HF) połączonego z podejściem Bardeena-Coopera-Schrieffera (BCS) wyznaczone zostały diagramy fazowe, zawierające obszary stabliności fazy nadprzewodzącej, a także fazy nadprzewodzącej współistniejacej z ferromagnetyzmem lub antyferromagnetyzmem. Przeanalizowany został wpływ miedzywęzłowej hybrydyzacji na stabilność rozważanych faz, a także na zależność temperaturową momentu magnetycznego i przerwy nadprzewodzącej. Dzięki przedstawionemu podejściu diagramy fazowe wyznaczone wcześniej i zawierające jedynie fazy o uporządkowaniu magnetycznym zostały uzupelnione o obszary stabilności faz sparowanych trypletowo. Jak wynika z przeprowadzonej analizy, niezerowe namagnesowanie może wystąpić poniżej progu Stonera, jeśli faza ferromagnetyczna współistnieje z nadprzewodnictwem, co z kolei prowadzi do konkluzji, że nadprzewodnictwo trypletowe typu A1 wspomaga uporządkowanie ferromagnetyczne.

W celu przeanalizowania wpływu korelacji miedzyelektronowych na rozważane fazy użyto tzw. statystycznie konsystentego przyblizenia Gutzwillera (SGA), które zostało opracowane w ostatnich latach. Wyniki otrzymane w ramach przybliżeń HF oraz SGA są często podobne z jakościowego punktu widzenia. Główna różnica polega na tym, że dla metody SGA obszar stabilności fazy nadprzewodzącej typu A1 z fazą ferromagnetyczną nie wystepuje, natomiast jest on obecny gdy obliczenia przeprowadzi się zgodnie z przybliżeniem HF.

Następnie, odkryto, iż faza nadprzewodząca oraz faza antyferromagnetyczna współistniejąca z nadprzewodnictwem, mogą być stabline dla obszaru parametrów, który odpowiada czysto odpychającym oddziaływaniom, gdy obliczenia przeprowadzone są zgodnie z metodą SGA. W przybliżeniu Hartree-Focka fazy nadprzewodzące nie wystepują dla tego obszaru parametrów, co prowadzi do stwierdzenia, że korelacje międzyelektronowe wraz z regułą Hunda odgrywają najistotniejszą rolę w stablilizacji nadprzewodnictwa trypletowego. Co więcej, pomimo że w rozważanym modelu wystepują jedynie oddziaływania wewnatrzwęzłowe, to parowanie trypletowe ma charakter miedzywęzłowy w stanie skorelowanym, co z kolei prowadzi do przerwy nadprzewodzącej zależnej od wektora falowego $\mathbf{k}$ (extended s-wave).

W ostatniej części rozprawy, rozważany jest problem zachowania średniej ilości cząstek przy wykonywaniu projekcji Gutzwillera wielocząstkowej funkcji falowej. Zaproponowano modyfikacje poprzednio użytej metody SGA, która polega na dodaniu wyrazu do Hamiltonianu effektywnego, który to wyraz wymusza zachowanie średniej ilosci cząstek bez wprowadzania odpowiednich współczynnikow wariacyjnych Fukushimy (fugacity factors) w operatorze projekcji Gutzwillera. Pokazano, że zaproponowana modyfikacja prowadzi do silnej redukcji wartości przerwy nadprzewodzącej w sytuacjach, dla których nadprzewodnictwo trypletowe jest silne. Niemniej jednak, trendy jakościowe pozostaja bez zmiany. Konkludując metoda SGA może zostać uznana za realistyczną do zastosowania do konkretnych meteriałów, które wymagają jednak odrębnej analizy ilościowej.

Contents

Acknowledgements

I would like to express my gratitude to Prof. Józef Spałek for supervising the research which is presented in this Thesis, as well as for inspiration and motivation during my PhD studies. Apart from that, I am very grateful to him for critical reading of the text of this Thesis.

Discussions with Dr hab. Jörg Bünemann, Dr Jan Kaczmarczyk, and Dr Jakub Jędrak are also appreciated.

This PhD thesis has been completed within the framework of the Human Capital Operational Program POKL.04.01.01-00-434/08-02 co-financed by the European Union.

I would also like to acknowledge the partial financial support from the Foundation for Polish Science (FNP) within project TEAM/2010-6/7, carried out within the TEAM programme, cofinanced from the European Union under the European Regional Development Fund.

Preface

According to the amendment of the law on higher education introduced on 18.03.2011, a PhD Thesis can be constituted of a thematically coherent set of papers published or accepted for publication in scientific journals. The following papers constitute this PhD Thesis:

A.1 M. Zegrodnik and J. Spałek, *Spin-triplet pairing induced by Hund's rule exchange in orbitally degenerate systems: Hartree-Fock approximation*, Acta Phys. Pol. A **121**, 1051 (2011)

A.2 M. Zegrodnik and J. Spałek, *Coexistence of spin-triplet superconductivity and antiferromagnetism in orbitally degenerate systems: Hartree-Fock approximation*, Acta Phys. Pol. A **121**, 801 (2011)

A.3 M. Zegrodnik and J. Spałek, *Coexistence of spin-triplet superconductivity with magnetic ordering in an orbitally degenerate system: Hartree-Fock-BCS approximation revisited*, Phys. Rev. B **86**, 014505 (2012)

A.4 M. Zegrodnik, *Hund's rule induced spin-triplet superconductivity coexisting with magnetic ordering in the degenerate band Hubbard model*, Proceedings of the ISD Workshops, 49-52 (2013)

A.5 M. Zegrodnik, J. Spałek, and J. Bünemann, *Coexistence of spin-triplet superconductivity with magnetism within a single mechanism for orbitally degenerate correlated electrons: Statistically-consistent Gutzwiller approximation*, submitted to New J. Phys.

A.6 M. Zegrodnik, J. Bünemann, and J. Spałek, *Even-parity spin-triplet pairing for orbitally degenerate correlated electrons by purely repulsive interactions*, submitted to Phys. Rev. Lett.

A.7 J. Spałek and M. Zegrodnik *Spin-triplet paired state induced by the Hund's rule coupling and correlations: fully statistically consistent Gutzwiller approach*, submitted to J. Phys: Condens. Matter

List of abbreviations and symbols

A	pure type A superconducting phase (equal-spin paired state)
A1+FM	superconducting phase type A1 coexisting with ferromagnetism
SC+AF	superconducting phase coexisting with antiferromagnetism
FM	Pure ferromagnetic phase
AF	Pure antiferromagnetic phase
NS	paramagnetic phase
HF	Hartree-Fock
BCS	Bardeen-Cooper-Schrieffer
SGA	statistcally consistant Gutzwiller approximation
GA	Gutzwiller approximation
DMFT	dynamical mean field theory
FFLO	Fulde-Ferrell-Larkin-Ovchinnikov
GWF	Gutzwiller wave function
VMF	variational Monte Carlo
RMFT	venormalized mean field theory
DMFG	density matrix renormalization group
QMC	quantum Monte Carlo
SB	slave boson
MF	mean field
U	intrasite intraorbital Coulomb repulsion magnitude
U'	intrasite interorbital Coulomb repulsion magnitude
J	Hund's coupling
n	band filling
T_N	Néel temperature
T_C	Curie temperature
T_S	superconducting critical temperature
μ	chemical potential
S_u^z	uniform magnetic moment per site per band
S_s^z	staggered magnetic moment per site per band
Δ_1	Superconducting gap that corresponds to $l = 1$
Δ_{-1}	Superconducting gap that corresponds to $l = -1$
Δ_0	Superconducting gap that corresponds to $l = 0$
$\Delta^{(0)}$	intrasite component of the superconducting gap
$\Delta^{(1)}$	intersite component of the superconducting gap
F	free energy

Chapter 1

Introduction

Unconventional superconductivity

In recent years the unconventional superconductivity has become one of the main topics in condensed matter physics. The term "unconventional" is used with respect to all superconductors, in which the pairing mechanism has either a non-phononic origin or the structure of the superconducting gap and other physical properties are of non-BCS character. There is a wide range of materials which fulfill either of the conditions. They are: the heavy fermion superconductors [1, 2], the high-T_C cuprates [3, 4] and the iron-pnictide [5, 6, 7] superconductors, the organic superconductors [8, 9], the uranium based superconductors [10, 11], and the ruthenate superconductors [12, 13]. In the mentioned compounds one distinguishes between the spin-singlet and the spin-triplet pairing. The latter has been observed in UGe_2 [10, 14] and UIr [15, 16] at high pressure, as well as in URhGe [17, 18] and UCoGe [19, 20] at ambient pressure. The enhanced linear coefficient γ of the electronic specific heat shows that these materials are moderately correlated metals. What is interesting, the paired phase coexists with itinerant ferromagnetism in all four of them. Furthermore, they share the feature that the uranium $5f$ magnetic moments hybridized with conduction-electron states are responsible for the ferromagnetic order and it is believed that the same hybridized $5f$ electrons form Cooper pairs in the superconducting state. What is more, the paired phase appears close to the magnetic instability and, except UCoGe, the region of stability of this phase is completely contained inside the region of stability of the ferromagnetic phase on the (p, T) diagram. At this point, one should note that the first evidence of coexistence of itinerant ferromagnetism and superconductivity has been reported for the d-band metal Y_9Co_7 [21]. The spin-triplet superconductivity can also coexist with antiferromagnetic ordering which is the case in the heavy fermion UNi_2Al_3 [22, 23, 24] and UPt_3 [25, 26].

A pure spin-triplet superconductivity has been observed in Sr_2RuO_4 [12], which has the same layered structure as high-T_C cuprates. Because of the fact that this material gives a set of Fermi liquid parameters comparable to those of the superfluid ^{3}He, some analogies are drawn between these two systems. It should be noted that ^{3}He was the first case of the spin-triplet pairing in a quantum liquid. The electronic structure of Sr_2RuO_4 is characterized by three cylindrical Fermi surfaces (α, β and γ) and it is suggested from experiment (neutron scattering) that it is a correlated electron system with dominant incommensurate antiferromagnetic correlation. Due to similarities between Sr_2RuO_4 and the layered compound $LaFeAsO_{1-x}F_x$ [27, 28], it is believed that this iron-based material

can also be a spin-triplet superconductor. The mother compound LaFeAsO is metallic and shows antiferromagnetic ordering at about 150 K. The paired phase is induced by the doping, similarly as in the case of the cuprate superconductors. Furthermore, among the organic compounds one can also find candidates for the spin-triplet pairing. In this respect the $(TMTSF)_2PF_6$ has attracted much attention due to observation of large H_{c_2} [29], as well as unusual Knight shift results [30]. However, the pairing mechanism in this compound is most likely different than that proposed in Sr_2RuO_4.

The microscopic origin of spin-triplet pairing

The question of the microscopic origin of pairing in the mentioned systems still remains open. Different scenarios are considered and it may be the case that not all of the spin-tiplet superconductors can be described by a unified approach. One of the possible mechanisms is the pairing due to ferromagnetic spin fluctuations or paramagnon exchange (similarly as in superfluid ^{3}He) [31, 32, 33, 34, 35]. Such approach results in the odd parity (p-wave) gap symmetry and is limited to weak correlations. One could also consider the incommensurate antiferromagnetic spin-fluctuations [36] or charge/orbital [37] fluctuations as the origin of a spin-triplet pairing. Moreover, it has been suggested that the intra atomic Hund's rule exchange can lead in a natural manner to the triplet paired phase [38, 39, 40, 41], both pure, as well as coexisting with magnetic ordering. Some theoretical investigations put aside the question of the microscopic mechanism for Cooper pair creation and apply a phenomenological or semi-phenomenological approach [42, 43, 44, 45].

Since there are already more than a few candidates for the spin-triplet pairing, many different models are examined by authors considering this unconventional type of superconductivity. In this respect, one can distinguish between the single- and the multi-band models. Earlier, the spin-triplet pairing in ^{3}He [46, 47] and that of the neutron star crust [48] has been successfully described with the use of a single band Landau Fermi-liquid picture. This approach has been applied to weakly ferromagnetic superconductors [49] and to Sr_2RuO_4 [31]. A single band model was also used, together with a phenomenological approach, relating to the uranium based compound UGe_2 [43]. However, in order to describe in a realistic manner the spin-triplet superconductivity one should often consider a multiband model. The two- [44, 45, 50, 51] and three- [42, 52] band models were examined to study both the pnictides and Sr_2RuO_4, as well as the spin-triplet pairing in general [50, 52]. A number of theoretical investigations of multiband models are carried out with the help of mean-field approximation [42, 43, 44, 45, 52], but the influence of correlations has also been examined by few authors using DMFT+quantum Monte Carlo method [50, 51].

The gap symmetry

Another important aspect is the symmetry of the superconducting gap parameter. As the gap symmetry arises from the pairing mechanism, the crystal structure and the microscopic properties of the considered compound, also in this context different situations are being considered. The constant $a - b$ plane Knight shift [53] and the spin susceptibility [54] measurements below T_C in Sr_2RuO_4, suggest that in this compound the gap

function of the chiral p-wave state is realized. This kind of state is an analog of the unitary A phase of ^{3}He and it breaks the time reversal symmetry. However, the experimental research indicates [55, 56, 57] that the gap function should have lines of zeros on the Fermi surface which is not consistent with the p-wave type of pairing. In this respect, it has been proposed by Zhitomirsky et al [58] that a specific p-wave type of pairing with a circular horizontal line nodes at $k_z = \pm\pi/c$ on the α and β Fermi surface sheets can be induced by an interband-proximity effect between the α and β bands and the γ band in which a nodeless p-wave type of pairing is due to an attractive interaction. For these calculations the two-band model has been used in the weak coupling limit. The same type of p-wave pairing with line nodes has been earlier considered by Hasegawa et al [59] by using a one band model and assuming a repulsive interaction between electrons in a single Ru-O plane, as well as an attraction between electrons in adjacent layers. Furthermore, suggestions of the f-wave gap functions for the Sr_2RuO_4 can also be found [60, 61]. Investigations concerning possible p-wave and f-wave internal symmetries for Sr_2RuO_4 have been performed by Annett et al [42, 62] for the three-band model, with the pairing due to two nearest neighbors negative-U Hubbard interactions (intraplane and the interplane). These calculations have been preformed in the mean field approximation and gave a good agreement with selected experimental data. In contraposition to these considerations, the fully open gap close to the BCS value for Sr_2RuO_4 has been reported by Suderow et al [63]. The measurments have been performed by the tunneling spetroscopy using a scanning tunneling microscope (STM) and it seems reasonable to say, that they suggest a realization of an s-wave or extended s-wave gap symmetry in the paired state. However, as far as the author of this thesis is concerned so far no theoretical investigations applying directly the even-parity symmetry (of s-wave character) to this compound have been carried out.

What concerns UGe_2, the non-unitary p-wave type superconducting phase coexisting with ferromagnetism has been considered [43]. This choice of gap symmetry was motivated by the experimental results form the ^{73}Ge-nuclear-quadrupole-resonance under pressure [64] which revealed, that the spin-up band is gapped with line nodes, but the spin-down band remains gapless at the Fermi level.

The p and f-wave symmetries are examples of the so-called odd-parity pairing which has an intersite character. On the other hand, some general investigations concerning s-wave or extended s-wave (even-parity) pairing in the correlated electron systems were presented in Refs. [50] and [51]. In these calculations, only the on-site interactions were included in the two-band Hubbard model and the pairing was due to the Hund's rule coupling. Both intra- (s-wave) and inter- (extended s-wave or d-wave) site type of pairing have been proposed to describe the superconductivity of the iron based superconductor $LaFeAsO_{1-x}F_x$ [44]. In this case, also a two-band model has been used, however the analysis was performed in the mean field approximation and the superconducting phase has occurred due to an effective paring term which has been introduced in the Hamiltonian. This kind of approach should be considered as a phenomenological one. Furthermore, the considerations regarding even parity type of superconductivity have been presented by Puetter et al [52] for t_{2g} orbital (3-band) system. In this approach, the spin-orbit and Hund's rule couplings jointly give rise to the superconducting state in the mean filed approximation.

Calculation methods for correlated electron systems

For the case of weakly-correlated electron systems, when the interaction energy is much smaller than the kinetic energy, the standard Hartree-Fock approximation provides often satisfactory results, at least from a qualitative point of view. Unfortunately, many of the realistic compounds which are of interest in the modern-day solid state physics, are considered to be moderately or strongly correlated. In those systems the magnitude of the electron-electron interaction is comparable to or larger than the kinetic energy. In such situation, the Gutzwiller variational approach has received a great deal of interest. It uses the so-called variational many-particle wave function (Gutzwiller wave function, GWF) which describes the correlated state and is constructed by action of a projection operator (which, in turn, contains the variational parameters determined by optimizing the energy) on a non-correlated state. Due to the variational principle this approach provides the upper bound for the ground state energy of the initial Hamiltonian. The GWF was proposed for a single-band Hubbard model by Gutzwiller [65] (see also [66]). Because the approach which uses GWF can be quite cumbersome even for simple models, the Gutzwiller approximation (GA) has been developed which is a straightforward method to handle GWF. This method provides a prescription for constructing the effective single-particle Hamiltonian, in which the so-called band-narrowing factors are introduced. However, additional simplifications have to be made in the GA which lead to a reduced quality of the solution.

As it has been shown by Metzner and Vollhardt [67, 68] in the limit of infinite dimensions, the GA gives the same results as the GWF approach. An approximation-free solution for the GWF was obtained in one spatial dimension [69, 70], however for a long time the most important cases of $d = 2$ and 3 could not be solved without additional simplifications. Recently, a diagrammatic method allowed for obtaining the GWF paramagnetic [71] and superconducting [72] solutions for the two-dimensional Hubbard model. Alternatively, the variational Monte Carlo (VMC) techniques [73] have been developed which allow for an accurate evaluation of the expectation values for the Gutzwiller projected wave function in two and three dimensions. Unfortunately, they are restricted to small systems. The Gutzwiller variational approach was extended to the multi-band case [74, 75, 76], as well as applied to the periodic Anderson model [77] and also used to perform a full out-of-equilibrium time-dependent calculations [78]. Moreover, on the basis of GA the so-called renormalized mean-field theory (RMFT) for the $t - J$ model has been derived by Zhang et al [79].

Recently, the so-called statistically consistant Gutzwiller approximation (SGA) has been developed [80] which is a modification of the original GA approach. As argued in Ref. [80], in the standard Gutzwiller approximation the mean fields should be treated as viariational parameters to obtain a fully-minimazed energy of the system. This is due to the fact that the mentioned band-narrowing factors depend explicitly on the mean-fields. However, to make the self-consistency condition fulfilled during the minimization procedure, one has to impose additional constraints. These constraints, together with invocation of the maximum entropy principle, which allow to work in the nonzero-temperature regime, are the novelties introduced within the SGA method. Such an approach was applied to the $t - J$ model [81, 82] as well as to the Anderson-Kondo lattice model [83, 84]. As one can see from this brief overview, the original concept of Gutzwiller has been developed further over the years and is still widely used.

With respect to the quantitative analysis of correlated electron systems, one should also mention other non-variational methods. One of them is the density matrix renormalization group (DMRG) method [85], which yields very accurate results but for quasi-one dimensional ladder systems. The approach based on the tensor network states [86], which is the generalization of the DMRG to two-dimensions has also been used in recent years but have similar limitations as the VMC calculations. In general, the VMC is the variational alternative for the so-called Quantum Monte Carlo (QMC) [87] techniques, which are very efficient for bosons but suffer from the negative sign problem [88] when applied, in the non-variational form, to interacting fermions. This weakness does not allow for an accurate QMC simulations of large systems at low temperatures.

Another method is the dynamical mean-field theory (DMFT), which is based on mapping the lattice model (such as the Hubbard model) onto a quantum impurity model which constitutes a many-body local problem and is solvable through various schemes (usually the QMC simulations are used at this point $\rightarrow$ DMFT+QMC). The mapping is exact in the infinite-dimension limit which means that it leads to a similar approximation as the GA. However, the DMFT has not been often applied to the unconventional superconductivity as the off-site anisotropic pairing (d or p wave) cannot be treated by it. Instead, it has been used with respect to the s-wave type of pairing [50, 51].

One should also mention the slave boson (SB) approach which has been used to treat the infinite-U Anderson model as well as large-U Hubbard model for description of high-T_C superconductors. This method is based on introducing bosonic degrees of freedom on each lattice site of the system and formulating a new Hamiltonian in the extended bosonic-fermionic Hilbert space. The resulting Hamiltonian can be treated by means of the mean field theory (MF), as it has been proposed by Kotliar and Ruckenstein [89] for a one-band situation, and extended subsequently to the multi-band case by Lechermann et al [90]. When it comes to the computational complexity, limitations, and applicability, the SB approach can be considered as comparable in quality to the GA method. This is why the topic of the GA and SB equivalence has been addressed in the series of papers [77, 91, 92]. As argued in Ref. [80], the so-called SGA variant of the GA approach gives results equivalent to the SB+MF in the simplest one-band and multi-band situations. As it is pointed out in the mentioned paper, all features of the latter method may be obtained in a alternative simpler manner within SGA, without introducing the "ghost" condensed-Bose fields introducing spurious Bose-Einstein condensation points into the thermodynamic description of the system at hand.

Aim and scope of this Thesis

As one can notice from previous Sections, the evidence for the spin-triplet superconductivity is not completely clear as yet and different types of approaches are developed in order to describe theoretically this fundamental phenomenon. In this Thesis the emphasis is placed on the Hund's rule as the primary source of the spin-triplet pairing which was proposed in 1999 [38]. This concept originated form drawing an analogy between the spin-triplet superconductors and the cuprate high-T_C superconductors, where the antiferromagnetic kinetic exchange is regarded as a source of not only antiferromagntism but also the spin-singlet pairing. Hence, the question of ferromagnetic interactions as leading to spin-triplet pairing comes out naturally. Within the approach itinerant magnetism,

as well as superconductivity, can be induced by the Hund's rule interaction. As a result, both pure superconducting and coexisting superconducting-ferromangetic states can appear as stable. It should be noted at the start that most of the compounds in which the spin-triplet pairing has been observed or proposed represent multiband systems with strongly or moderately correlated electrons. Moreover, the magnetic instabilities are significant in them and the paired phase often coexists with magnetic ordering. A complete phase diagram of a model with Hund's rule induced spin-triplet pairing and magnetism has not been determined until now and the influence of the interband hybridization on the stability of the considered phases has not been analyzed. Another important topic is the influence of the correlations. There are only few theoretical papers that investigate the spin-triplet pairing in the correlated regime. In the paper from Klejnberg et al a slave boson approach (for the Coulomb interaction terms) combined with the mean-field-BCS approximation (for the pairing part) has been discussed. In this manner the correlations have been included only partly. The DMFT method has been also applied [50, 51] with regard to the considered mechanism of pairing, but no comparison with the mean field results for the same model has been performed, which would allow to scrutinize the effect of correlations. Moreover, in these papers the complete phase diagram including superconducting and magnetic phases in the correlated case has not been determined. Also, the DMFT method was applied to calculate the instablility of the normal state with respect to the pairing only. To the best knowledge of the author of this Thesis, the GA approach (and in particular SGA) has not been applied for a multi-band model with spin-triplet pairing due to the Hund's rule, until now.

The principal aims of this thesis are as follows:

1. To investigate the global stability of the Hund's rule induced spin-triplet paired phase against the onset of either magnetism (ferromagnetism and antiferromagnetism) or coexistent states and to construct a proper phase diagram comprising the stable phases.

2. To determine the influence of the interband hybridization on the relative stability of the considered phases.

3. To analyze in detail the influence of the interelectronic correlations on the formation of the paired and coexistent phases.

In order to achieve the goals written above the extended two-band Hubbard model is used for the case of square lattice within both the Hartree-Fock approximation and the Statistically Consistent Gutzwiller Approximation (SGA). In the process of executing this project it has been discovered that a purely repulsive interactions regime ($U' > J$) can also yield a stable phase of type A (i.e., with equal spin pairing), as well as coexistent spin-triplet superconducting-antiferromagnetic phase. This new feature is important as the approach encompasses now the regime of parameters regarded as canonical situation for appearance of itinerant magnetism only. Nevertheless, the approach still awaits application to real materials. A possibility of its direct application to the analysis of superfluid cold-atom systems should also be noted.

Chapter 2

Synopsis of the papers

2.1 Paper A.1, Spin-triplet pairing induced by Hund's rule exchange in orbitally degenerate systems: Hartree-Fock approximation

As said in the Introduction, it is important to determine the location of the paired and magnetically ordered phases on the phase diagram. The calculations have been performed using the Hartree-Fock approximation for the cases of flat density of states and for the square lattice. The paper reflects the initial stage of the research, and no antiferromagnetism has been included as yet. In the Section 2 of the paper, a detailed theoretical approach is presented in the mean-field approximation (HF+BCS) including the A, A1, and B superconducting phases, as well as the ferromagnetic phase.

Next, the ground-state phase diagrams on the (n, J) plane are provided for the cases with and without the interband hybridization. The results show sizable regions of stability of the pure paired phase of type A, as well as of the superconducting A1 phase coexisting with ferromagnetism (FM), for both shapes of the density of states considered. The pure ferromagnetic phase is stable only for the half filled band situation ($n = 2$) in the case with no hybridization. The regions of stability of A and A1+FM phases narrow down with the increasing strength of the hybridization in favor of the normal phase and the pure ferromagnetic phase, respectively. The results show that hybridization has a negative influence on the considered kind of spin-triplet superconductivity.

For the sake of completeness, the temperature dependences of the gap parameter, magnetic moment, and chemical potential have been provided for the coexistent superconducting-ferromagnetic phase, for different hybridization strengths. It can be seen from the plots that as the temperature is increased the system undergoes two phase transitions. The first one is from the A1+FM phase to the pure ferromagnetic phase (at the temperature T_S) and the second corresponds to the transition from the ferromagnetic phase to the paramagnetic phase (at the temperature T_C). The calculated transition temperature ratio was $T_C/T_S \approx 5$. With the increasing hybridization the critical temperature T_S decreases, while the Curie temperature T_C increases.

To summarize, in this paper the results from the first stage of the research have been presented. The initial phase diagram without antiferromagnetsim has been determined in the mean field approximation and the influence of the hybridization on the paired phases has been analyzed. In the next step of the research the antiferromagnetically

ordered phase is considered.

2.2 Paper A.2, Coexistence of spin-triplet superconductivity and antiferromagnetism in orbitally degenerate systems: Hartree-Fock approximation

In this paper it is presented how to incorporate the antiferromagnetic phase into consideretions contained in this Thesis. In particular, the coexistant Hund's rule induced spin-triplet paired phase in coexistance with antiferromagnetism (SC+AF) has been proposed. First, the theoretical discription of such a phase in the mean-field approxaimation is presented in detail. To make it possible for the paired phase to coexist with antiferromagnetism, four sublattice gap parameters (two sublattices and two spin orientations) have been inroduced. For symmetry reasons the gap parameters that correspond to intersite Cooper pairs with the spin aligned in the same direction as the magnetic moment on the sublattice are equal. As a result one obtains effectively two gap parameters.

Next, in the results section, the free energy of the considered phase as a function of temperature is presented and compared to the free energies of four other phases which were considered in the previous paper (A.1). The gap parameters, the staggered magnetic moment, and the specific heat have been analyzed, all as functions of temperature. The results show that as the temperature is being raised the system undergoes two phase transitions, similarly as in the case of A1+FM phase form A.1 paper. It should be noted that both gap parameters which have been introduced in this paper vanish for a single phase transition temperature. The transitions can be also seen from the calculated specific heat plots where there are two discontinuities in the critical temperature (T_C) and Néels temperature (T_N). The calculated transition temperature ratio is $T_N/T_S \approx 9$.

From the determined band filling dependences one can see that the SC+AF phase is stable close to the half filled band situation, however for $n = 2$ the superconducting gap parameters vanish and the pure antiferrromagnetism becomes stable. Furthermore, it is transparent from Figs. 3a and 3b that the division into two sublattice gap parameters is accompanied by the creation of the staggered structure in the system.

In conclusion, in this paper the spin-triplet superconducting antiferromagnetic phase has been proposed and it has been shown that this phase is stable for the proper range of model parameters. The calculations have been performed in the mean field approximation, however the hybridization has not been included yet. In the next step of the research the complete phase diagrams and the influence of hybridization are examined.

2.3 Paper A.3, Coexistence of spin-triplet superconductivity with magnetic ordering in an orbitally degenerate system: Hartree-Fock-BCS approximation revisited

In this paper, a fairly complete theoretical description of the spin-triplet paired phases pure and coexisting with magnetic ordering (ferromagnetism and antiferromagnetism) is

provided in the mean field approach for the case with nonzero interband hybridization. Next, the phase diagrams are constructed including the pure spin-triplet superconducting phase of type A, as well as superconductivity coexisting with both ferro- and antiferromagnetism. The evolution of the phase diagrams are presented with increasing strength of the interband hybridization. The diagrams show that practically all magnetically ordered phases are in fact the coexistent phases with superconductivity except the half filled band situation, where only the pure antiferromagnetism survives. A negative influence of the hybridization on the paired phase of type A is clearly visible. However, the magnetically ordered phases are not that much affected by the increasing hybridization strength.

The emphasis has been placed on the relation between the appearance of the A1 phase and the onset of ferromagnetism. The results show that the ferromagnetic phase coexisting with superconductivity becomes stable for slightly lower J values than the Stoner threshold for the appearance of pure ferromagnetic phase (cf. Fig. 2). Moreover, the superconducting gap increases rapidly in the range of model parameters where the magnetization also changes rapidly (Fig. 4). This leads to the conclusion that the spin-triplet superconductivity and magnetism enhance each other. The temperature dependences of the order parameters and the specific heat corresponding to the A, A1+FM, and SC+AF phases, have been analyzed for various strengths of the hybridization.

The concluding section of this paper contains the discussion of the effect of model parameters on the stability of the considered phases. It is emphasized that the necessary condition for the pairing to appear in the HF+BCS limit is $U' - J < 0$. This condition turned out to be unnecessary in the correlated regime as explained in papers A.6 and A.7.

Additionally in the Appendix C a brief discussion is provided on how to include the spin fluctuations within the considered model. It is outlined briefly, that by making the Hubbard-Stratonovich transformation for the interaction parts of the Hamiltonian the mean-field part and the fluctuation part can be incorporated into a single scheme.

This paper gives the fairly complete Hartree-Fock+BCS analysis of the given problem. Apart from that, one short additional paper has been written concerning the Hartree-Fock approximation. In the next stage of the research the so-called statistically consistent Gutzwiller approximation is applied for the same model Hamiltonian to examine the effect of correlations.

2.4 Paper A.4, Hund's rule induced spin-triplet superconductivity coexisting with magnetic ordering in the degenerate band Hubbard model

This paper should be considered as a small amendment to the Hartree-Fock analysis performed so far. It contains a brief revision of the main results presented in the earlier papers, as well as the calculated phase diagrams on (n, T) plane which have not been analyzed previously. The diagrams show the evolution of the stable paired phases and the corresponding critical temperature with increasing band filling. It can be seen that the coexistent paired and magnetically ordered phases remain stable for much larger temperatures than the pure spin-triplet superconducting phase which again leads to the

conclusion that magnetism and this type of unconventional superconductivity enhance each other. Also, the influence of the hybridization on the stability regions on the diagrams is shown.

2.5 Paper A.5, Coexistence of spin-triplet superconductivity with magnetism within a single mechanism for orbitally degenerate correlated electrons: Statistically-consistent Gutzwiller approximation

This paper discusses in detail the central issues of the Thesis. Namely, the statistically consistent Gutzwiller approximation is introduced for the first time for the-two band model with spin-triplet pairing. Before the results are presented, the details of the theoretical approach are given. In this approach the multiband extension of the Gutzwiller approximation is used to derive the so called renormalization factors for the considered two-band model. Next, the effective Hamiltonian is constructed within the framework of the SGA method, in which additional terms are added to the standard Gutzwiller approximation. These terms play the role of basic constraints, thanks to which all the mean fields, that are evaluated by minimizing the energy of the system, coincide with the corresponding values obtained from the self-consistent procedure. As this approach, in the present two-band case involves up to 256 variational parameters, the symmetry relations have been used for each phase considered reducing the number of these parameters significantly.

The results are compared to those obtained from the Hartree-Fock+BCS approximation. In this manner, the role of electronic correlations can be singled out explicitly. The free energy, the superconducting gaps, and the magnetic moments, all plotted as functions of either band filling n or Hund's coupling J have been analyzed. In general, the results for the HF and SGA methods appear to be similar from the qualitative point of view. However, the free energy calculated in the SGA is lower than the one for the HF situation, as expected. The main difference between the two compared methods is that in SGA the region of stability of the A1+FM phase is absent and only the pure spin-triplet superconductivity of type A and superconductivity coexistent with antiferromagnetism become stable for proper ranges of the model parameters, whereas in the HF approximation a sizable region of stability of the A1+FM phase is present.

Also, the band narrowing factors have been analyzed as functions of both band filling n and the interaction constants U,U', and J. The results show that for low values of the band filling and of the interaction parameters, the renormalization factors have values close to unity, as it should be, because the correlations are very weak then. Similarly, in the antiferromagnetically ordered phase, when the staggered magnetic moment is close to saturation, the renormalization factor is approaching to unity as in that situation the configurations with two electrons of opposite spin on the same orbital, are being ruled out. The influence of the hybridization is similar in the correlated case as it was in the non-correlated, at least from a qualitative point of view.

Summarizing, in this paper an original many-particle (SGA) method has been formulated which allows to investigate the spin-triplet real-space pairing in two-band correlated systems. By comparing the results obtained in this method with those calculated with

the use of Hartree-Fock+BCS approximation the effect of inter-electronic correlations have been analyzed and thus the results have been put on a firmer basis for a discussion of concrete meterials or cold-atom optical-lattice systems.

2.6 Paper A.6, Even-parity spin-triplet pairing for orbitally degenerate correlated electrons by purely repulsive interactions

In this paper we concentrate on a entirely new idea. Namely, that the spin-triplet pairing can originate from purely repulsive interactions. It should be noted again, that the discussion presented so far was for the case when the intraatomic interorbital Coulomb repulsion magnitude is smaller than the Hund's coupling ($U' < J$). This limit can be called as that with attractive interactions. It is important to investigate if it is possible that the paired phase can be stable in the more realistic regime of purely repulsive interactions ($U' > J$). This is the main topic of this and the next papers. The regime of purely repulsive interactions corresponds to a canonical situation of studying the correlated or itinerant magnetism within the whole class of extended Hubbard models.

By considering the same method and selection of phases as in the paper A.5, the phase diagram has been calculated, which shows that the paired phase (pure and coexisting with antiferromagnetism) is stable for the purely repulsive interactions regime. From the comparison with Hartree-Fock results, in which the paired phases are absent in the considered regime, it is seen that the correlations play a crucial role in stabilizing the superconducting state in this limit. The coexistent SC+AF phase appears close to half filling only, similarly as in the case of pnictide superconductors, whereas the pure A phase appears for $n \approx 1.2$ which corresponds roughly to the case of Sr_2RuO_4 in the hole language.

It has also been shown, that in the correlated regime the considered pairing mechanism can lead to intersite pairing in spite of the fact that all the interactions are of intrasite character in the starting model. The intersite pairing term in the effective Hamiltonian is non-zero only when the intrasite pairing is also present, which shows a direct connection between this two contributions to the pairing. The $\mathbf{k}$-dependent gap parameter that corresponds to this intersite pairing is of the same character as the form of the band dispersion relation. As a result, in the considered case one obtains the s-wave gap symmetry (intrasite) with an admixture of the extended s-wave gap symmetry (intersite). As before, the interband hybridization is detrimental to the superconducting A-phase stability when the spin-triplet pairing condensation energy is smaller than the Pauli principle-allowed kinetic energy gain.

Summarizing, in this paper the combined Hund's rule and correlation-induced pairing has been proposed. This kind of mechanism is operative in the purely repulsive interactions regime and leads to both intra- and inter-site contributions to the pairing. The considered kind of superconductivity can appear as a pure SC phase, as well as coexist with antiferromagnetism for the proper range of model parameters.

2.7 Paper A.7, Spin-triplet paired state induced by the Hund's rule coupling and correlations: fully statistically consistent Gutzwiller approach

In this paper the matter of conservation of the average particle number is elaborated with respect to the Gutzwiller projection operation, of the starting wave function, which is performed within the SGA method. The variant of this method which has been used to obtain the results presented in two preceding papers, leads to the situation, in which the average particle number is reduced while carrying out the Gutzwiller projection for certain states. Similar feature was also present in the original Gutzwiller formulation and it may raise doubts since the conservation of the average particle number should be a characteristic of the Fermi liquid. This matter has already been discussed by a number of authors with respect to the one band Hubbard model and Anderson model. To compensate the particle number reduction in the correlated state, the projection operator has been modified by Fukushima by introducing the so-called fugacity factors. A different approach to handle this problem is proposed here.

In the theoretical section the modification of the previously used method is described in detail. As it is shown, the particle number conservation constraint can be imposed by adding a supplementary term to the effective Hamiltonian in the spirit of the Lagrange-multiplier method. It should be noted, that this term does not contain any operators, but only the expectation values. In this manner, the projection operator is not modified, in contrast with the approach incorporating the fugacity factors, but the changes are made on the stage of the effective Hamiltonian construction.

The proposed method has been used for the discussion of the Hund's-rule and correlation induced spin-triplet paired phase of type A. It has been shown, that the gap magnitude obtained, when incorporating the particle number constraint, is essentially reduced. The differences between the situation with and without the particle number constraint are not significant when the superconducting pairing is weak (for low J values). The differences in the free energy between the two compared approaches is of the order of 1meV in the favor of the solution when the particle number is not conserved as expected, since for this case the variational space is richer. What is interesting that such a small energy difference leads to a significant quantitative differences of the physically meaningful parameters, although their qualitative trends remain the same. The influence of the interband hybridization appears to be similar for both methods considered.

In the last part of the paper the Fermi-surface topology of the normal state, as well as the quasi-particle energies in the normal and paired phases have been analyzed. It has also been argued that the Fermi vector mismatch between the hybridized bands can be the source of a transition to a spontaneous inhomogeneous spin-triplet state of the FFLO type. The last suggestion requires a further analysis.

Chapter 3

Conclusions

To conclude the Thesis, in the present analysis the fundamental aspects of the proposed microscopic real-space spin-triplet pairing mechanism has been discussed in the regime of weak to moderate correlations. Both the pure superconducting and the coexistent superconducting-magnetic phases have been analyzed and the proper phase diagrams have been constructed in the ground state. Moreover, the temperature dependences of the order parameters have been investigated. The calculations have been carried out by using the HF+BCS approach, as well as the SGA method, which have been applied for the first time to the two-band model with the spin-triplet pairing.

For the so-called attractive interactions regime ($U' < J$), a robust stability regions of the paired phases have been obtained by using using both HF+BCS and SGA approximations. As it has been shown, the Hund's rule induced spin-triplet superconductivity and magnetism enhance each other. In the correlated case (SGA) the paired phase in coexistence with antiferromegnetism appeared, however, the coexistence with ferromagnetism turn out not to be stable, in distinction with repsect to to the non-correlated situation (HF+BCS).

An important finding presented in this Thesis is that in the correlated regime the paired phases, both pure and coexistent with antiferromagnetism, can become stable for the case of purely repulsive interactions, which corresponds to a canonical situation of studying magnetism in the extended Hubbard model. It has been argued that this phenomenon takes place due to the combined effect of the Hund's-rule and the correlations. Moreover, as shown in detail, the considered mechanism can lead to both intra- and inter-site contributions to the pairing, even though the starting model contains only interactions of the intrasite character. Some connotations between this result and the pairing in the one-band Hubbard model, obtained in Ref. [72], can be mentioned at this point. As it has been shown there, the one-band model with intrasite repulsion can also lead to an intersite pairing. Similarly, in that case the correlations have to play the crucial role in the pairing mechanism. In fact, a more precise method of taking into account the correlations has to be applied (GWF) in the one-band situation to obtain the paired states. Also, for strong Coulomb repulsion the one-band model can be transformed to the $t - J$ model, in which the pairing is intensively investigated. However, in contrast to these considerations, in the case considered here, the pairing has both intra- and inter-site character and apart from the correlations, the Hund's rule is very important for the appearance of the superconducting phase, as it favors the spin-triplet states by decreasing their energy on a single atomic site. Nevertheless, the total energy including Coulomb repulsion is still positive (purely repulsive interactions). It should be

also noted that according to the performed analysis the inter- and intra-site pairing have strong connection, as they appear for the same values of the model parameters.

Furthermore, the influence of the intersite hybridization on the stability of the paired phases has been analyzed. The hybridization introduces the inequivalence of the bands and has a negative influence on the considered kind of paired states which is due to the Fermi wave-vector mismatch that appears. However, when the mismatch is not very large the paired state can still be stable, which means that the considered kind of pairing mechanism could be applied to some of the realistic situations. One of the possibilities is the compound $LaFeAsO_{1-x}F_x$, in which upon doping the superconductivity occurs. It is suggested, that the two bands β_1 and β_2 in this system are responsible for the appearance of the paired phase. Hence, a two-band model has been considered [44] for the discription of s-wave (and extended s-wave or d-wave) superconducting state, in a phenomenological manner. The approach presented in this Thesis can be used to construct a microscopic model of superconductivity also in a two-band approximation of this iron-based compound.

On the other hand, in the case of strongly inequivalent bands (as are the α and β bands in Sr_2RuO_4), the Cooper pair creation within the analyzed mechanism can be inhibited. However, as suggested here, the stable paired state in such a situation can also occur provided that the Fermi wave-vector mismatch can be compensated by the non-zero center-of-mass momentum of the Cooper pairs. This would lead to the spontaneous creation of the inhomogeneous spin-triplet FFLO phase. Such a scenario should definitely be considered as a continuation of the work presented in this Thesis. In particular, this kind of orbital-inequivalence-induced FFLO state could be applied for investigations regarding superconductivity in Sr_2RuO_4 in a two-band approximation including both α and β bands (as in Ref. [45]).

Futhermore, extension to the three-band case, even though may require cumbersome calculations, should be attempted and would allow to study other real materials within the approach considered here. Moreover, application of the findings obtained here to the cold atom fermionic systems in the optical lattices [93, 94, 95], where the two-equivalent-band situation can be realized, is also a promising route of further research.

Bibliography

[1] For first report on superconductivity in heavy fermion system:
F. Steglich, J. Aarts, C. D. Bredl, W.Lieke, D. Meschede, W. Franz, and H. Schäfer, Phys. Rev. Lett. **43**, 1892 (1979).

[2] For review on heavy fermion superconductors:
P. S. Reisborough, G. M. Schmiedeshoff, J. L. Smith in *Superconductivity*, volume 1 (Springer-Verlag Berlin Heidelberg 2008).

[3] For first report on high T_C superconductivity in cuprates:
J. G. Bednorz and K. A. Müller, Z. Phys. B **64**, 189 (1986).

[4] For review on high T_C cuprate superconductors:
N. Plakida, *High-Temperature Cuprate Superconductors: Experiment, Theory, and Applications* (Springer-Verlag Berlin Heidelberg 2010).

[5] For first report on high T_C iron-based superconductor:
Y. Kamihara, T. Watanabe, M. Hirano, and H. Hosono, J. Am. Chem. Soc. **130**, 3296 (2008).

[6] For first report on iron-based superconductor:
Y. Kamihara, H. Hiramatsu, M. Hirano, R. Kawamura, H. Yanagi, T. Kamija, and H. Hosono, J. Am. Chem. Soc. **128**, 10012 (2006).

[7] For overview on iron-based superconductors:
P. M. Aswalthy, J. B. Anooja, P. M. Sarun, and U. Syamaprasad, Supercond. Sci. Technol. **23**, 073001 (2010)

[8] For first report on organic superconductors:
D. Jérome, A. Mazaud, M. Ribault, and K. Bechgaard, J. Phys. Lett. **41**, 95 (1980).

[9] For revew on organic superconductors:
T. Ishiguro, K. Yamaji, G. Saito, *Organic Superconductors*, (Springer-Verlag Berlin Heidelberg 1998).

[10] For first report on uranium based ferromagnetic superconductor:
S. S. Saxena, P. Agarwal, K. Ahilan, F. M. Grosche, R. K. W. Haselwimmer, M. J. Steiner, E. Pugh, I. R. Walker, S. R. Julian, P. Monthoux, G. G. Lonzarich, A. Huxley, I. Sheikin, D. Braithwaite and J. Flouquet, Nature **406**, 587 (2000)

[11] For review on uranium based ferromagnetic superconductors:
A. de Visser in *Encyklopedia of Materials: Science and Technology* (Elsevier 2010) pp 1-6.

[12] For first report on superconductivity in Sr_2RuO_4:
Y. Maeno, H. Hashimoto, K. Yoshida, S. Nishizaki, T. Fujita, J, G. Bednorz and F. Lichtenberg, Nature **372**, 532 (1994).

[13] For review on superconductivity in Sr_2RuO_4:
Y. Maeno, S. Kittaka, T. Nomura, S. Yonezawa, and K. Ishida, J. Phys. Soc. Jpn **81**, 011009 (2012).

[14] C. Pfleiderer and A. D. Huxley, Phys. Rev. Lett. **89**, 147005 (2002).

[15] T. Akazawa, H. Hidaka, H. Kotegawa, T. C. Kobayashi, T. Fujiwara, E. Yammamoto, Y. Haga, R. Settai, and Y. Onuki, J. Phys. Soc. Jpn **73**, 3129 (2004).

[16] T. C. Kobayashi, S. Fukushima, H. Hidaka, H. Kotegawa, T. Akazawa, E. Yamamoto, Y. Haga, R. Settai, and Y. Onuki, Physica B **378-80**, 355-8 (2006).

[17] D. Aoki, A. Huxley, E. Ressouche, D. Braithwaite, J. Flouquet, J.-P. Brison, E. Lhotel, and C. Paulsen, Nature (London) **413**, 613 (2001).

[18] F. Hardy, A. D. Huxley, J. Flouquet, B. Salce, G. Knebel, D. Braithwaite, D. Aoki, M. Uhlarz, C. Pfleiderer, Physica B **359-61**, 1111-13 (2005).

[19] N. T. Huy, A. Gasparini, D. E. de Nijs, Y. Huang, J. C. P. Klaasse, T. Gortenmulder, A. de Visser, A. Hamann, T. Görlach, and H. v. Löhneysen, Phys. Rev. Lett. **99**, 067006 (2007).

[20] E. Slooten, T. Naka, A. Gasparini, Y. K. Huang, and A. de Visser, Phys. Rev. Lett. **103**, 097003 (2009).

[21] A. Kołodziejczyk, B. V. B. Sarkissian, B. R. Coles, J. Phys. F: Met. Phys. **10**, L333 (1980).

[22] C. Geibel, S. Thies, D. Kaczorowski, A. Mehner, A. Grauel, B. Seidel, U. Ahlheim, R. Helfrich, K. Petersen, C. D. Bredl, and F. Staglich, Z. Phys. B **83**, 305 (1991).

[23] A. Schröder, J. G. Lussier, B. D. Gaulin, J. D. Garrett, W. J. L. Buyers, L. Rebelski, and S. M. Shapiro, Phys. Rev. Lett. **72**, 136 (1994).

[24] K. Ishida, D. Ozaki, T. Kamatsuka, H. Tou, M. Kyogaku, Y. Kitaoka, N. Tateiwa, N. K. Sato, N. Aso, C. Geibel, and F. Steglich, Phys. Rev. Lett. **89**, 037002 (2002).

[25] G. Aeppli, D. Bishop, C. Broholm, E. Bucher, K. Siemensmeyer, M. Steiner, and N. Stüsser, Phys. Rev. Lett. **63**, 676 (1989)

[26] H. Tou, Y. Kitaoka, K. Asayama, N. Kimura, Y. Onuki, E. Yamamoto, and K. Maezawa, Phys. Rev. Lett. **77**, 1374 (1996)

[27] H. Takahashi, K. Igawa, K. Arii, Y. Kamihara, M. Hirano, and H. Hosono, Nature (London) **453**, 376 (2008).

[28] Y. Nakai, S. Kitagawa, K. Ishida, Y. Kamihara, M. Hirano, and H. Hosono, New J. Phys. **11**, 045004 (2009).

[29] I. J. Lee, M. J. Naughton, G. M. Danner, and P. M. Chaikin, Phys. Rev. Lett. **78**, 3555 (1997).

[30] I. J. Lee, D. S. Chow, W. G. Clark, M. J. Stouse, M. J. Naughton, P. M. Chaikin, and S. E. Brown, Phys. Rev. B **68**, 092510 (2003)

[31] I. I. Mazin and D. J. Singh, Phys. Rev. Lett. **79**, 733 (1997).

[32] P. Monthoux, G. G. Lonzarich, Phys. Rev. B **71**, 054504 (2005).

[33] T. R. Kirkpartick, D. Belitz, T. Vojta, and R. Narayanan, Phys. Rev. Lett. **87**, 127003 (2001).

[34] Z. Wang, W. Mao, and K. Bedell, Phys. Rev. Lett. **87** 257001 (2001).

[35] R. Roussev and A. J. Millis, Phys. Rev. B **63**, 140504 (2001).

[36] T. Kuwabara and M. Ogata, Phys. Rev. Lett. **85**, 4586 (2000).

[37] T. Takimoto, Phys. Rev. B **62**, R14641 (2000).

[38] A. Klejnberg and J. Spałek, J. Phys.: Condens. Matter **11**, 6553 (1999).

[39] A. Klejnberg and J. Spałek, Phys. Rev. B **61**, 15542 (2000).

[40] J. Spałek, Phys. Rev. B **63**, 104513 (2001).

[41] J. Spałek, P. Wróbel, and W. Wójcik, Phys. C (Amsterdam) **387**, 1 (2003).

[42] J. F. Annet, B. L. Görffy, G. Litak, K. I. Wysokiński, Eur. Phys. J. B 36, 301-312 (2003).

[43] J. Linder, I. B. Sperstad, A. H. Nevidomskyy, M. Cuoco, and A. Sudbø, Phys. Rev. B **77**, 184511 (2008).

[44] X. Dai, Z. Fang, Y. Zhou, and F.-C. Zhang, Phys. Rev. Lett. **101**, 057008 (2008).

[45] Y. Imai, K. Wakabayashi, M. Sigrist, Phys. Rev. B **85**, 174532 (2012).

[46] P. W. Anderson and W. F. Brinkman, Phys. Rev. Lett. **30**, 1108 (1973).

[47] P. W. Anderson and W. F. Brinkman in *Physics of Liquid and Solid Helium*, edited by K. H. Bennemann, and J. B. Ketterson (J. Wiley & Sons, New York, 1978) Part II, pp. 177-286.

[48] D. Pines and A. Alpar, Nature **316**, 27 (1985).

[49] D. Fay and J. Appel, Phys. Rev. B **22**, 3173 (1980).

[50] J. E. Han, Phys. Rev. B **70**, 054513 (2004).

[51] S. Sakai, R. Arita, and H. Aoki, Phys. Rev. B **70**, 172504 (2004).

[52] C. M. Puetter and H.-Y Kee, Eur. Phys. Lett. **98**, 27010 (2012).

[53] K. Ishida, H. Mukuda, Y. Kitaoka, K. Asayama, Z. Q. Mao, Y. Mori, and Y. Maeno, Nature **396**, 658 (1998).

[54] J. A. Duffy, S. M. Hayden, Y. Maeno, Z. Mao, J. Kulda, and G. J. McIntyre, Phys. Rev. Lett. **85**,5412 (2000).

[55] S. Nishizaki, Y. Maeno, Z. Mao, J. Phys. Jpn **69**, 336 (2000).

[56] I. Bonalde, B. D. Yanoff, M. B. Salamon, D. J. Van Harlingen, and E. M. E. Chia, Phys. Rev. Lett. **85**, 4775 (2000).

[57] K. Izawa, H. Takahashi, H. Yamaguchi, Y. Matsuda, M. Suzuki, T. Sasaki, F. Fukase, Y. Yoshida, R. Settai, and Y. Onuki, Phys. Rev. Lett. **86**, 2653 (2001).

[58] M. E. Zhitomirsky and T. M. Rice, Phys. Rev. Lett. **87**, 057001 (2001).

[59] Y. Hasegawa, K. Machida, M. Ozaki, J. Phys. Jpn **69**, 336 (2000).

[60] M. J. Graf and A. V. Balatsky, Phys. Rev. B **62**, 9697 (2000).

[61] H. Won, K. Maki, Europhys. Lett. **52**, 427 (2000).

[62] J. F. Annett, G. Litak, B. L. Gyöffy, and K. I. Wysokiński, Phys. Rev. B **66**, 134514 (2002).

[63] H. Suderow, V. Crespo, I. Guillamon, S. Vieira, F. Servant, P. Lejay, J. P. Brison, and J. Flouquet, New J. Phys. **11**, 093004 (2009).

[64] A. Harada, S. Kawasaki, H. Mukuda, Y. Kitaoka, Y. Haga, E. Yamamoto, Y. Ōnuki, K. M. Itoh, E. E. Heller, and H. Harima, Phys. Rev. B **75**, 140502(R) (2007).

[65] M. C. Gutzwiller, Phys. Rev. Lett. **10**, 159 (1963).

[66] W. F. Brinkman, T. M. Rice, Phys. Rev. B **2**, 4302 (1970).

[67] W. Metzner, D. Vollhardt, Phys. Rev. Lett. **62**, 324 (1989).

[68] W. Metzner, Z. Phys. B **77**, 253 (1989).

[69] W. Metzner and D. Vollhardt, Phys. Rev. Lett. **59**, 121 (1987).

[70] F. Gebhard and D. Vollhardt, Phys. Rev. Lett. **59**, 1472 (1987).

[71] J. Bünemann, T. Schickling, and F. Gebhard, Europhys. Lett. **98**, 27006 (2012).

[72] J. Kaczmarczyk, J. Spałek, T. Schickling, F. Gebhard, J. Bünemann, arxiv:1210.6249.

[73] B. Edegger, V. N. Muthukumar, and C. Gros, Advances in Physics **56**, 927 (2007).

[74] J. Bünemann and W. Weber, Phys. Rev. B **55**, 4011 (1997).

[75] J. Bünemann, W. Weber, and F. Gebhard, Phys. Rev. B **57**, 6896 (1998).

[76] Jörg Bünemann, Florian Gebhard, Torsten Ohm, Stefan Weiser, and Werner Weber in *Frontiers in Magnetic Materials* (Springer, Berlin 2005).

[77] F. Gebhard, Phys. Rev. B **44**, 992 (1991).

[78] M. Schiró, M. Fabrizio, Phys. rev. Lett. **105**, 076401 (2010).

[79] F.-C. Zhang, C. Gros, T. M. Rice, and H. Shiba, Supercond. Sci. Technol. **1**, 36 (1988).

[80] J. Jędrak, J. Kaczmarczyk and J. Spałek, arXiv:1008:0021v2 [cond-mat.str-el] 18 May 2011.

[81] J. Jędrak and J. Spałek, Phys. Rev. B **81** 073108 (2010).

[82] J. Kaczmarczyk and J. Spałek, Phys. Rev. B **84** 125140 (2011).

[83] O. Howczak and J. Spałek, J. Phys.: Condens. Matter **24** 205602 (2012).

[84] O. Howczak, J. Kaczmarczyk, and J. Spałek, Phys. Status Solidi **250**, 609-614 (2013).

[85] S. R. White, Phys. Rev. Lett **69**, 2863 (1992).

[86] P. Corboz, S. R. White, G. Vidal, and M. Troyer, Phys. Rev. B **84**, 041108(R) (2011).

[87] E. Dogotto, Rev. Mod. Phys. **66**, 763 (1994).

[88] M. Troyer, U.-J. Wiese, Phys. Rev. Lett. **94**, 170201 (2005).

[89] G. Kotliar and A. N. Ruckenstein, Phys. Rev. Lett. **57**, 1362 (1986).

[90] F. Lechermann, A. Georges, G. Kotliar, O. Parcollet, Phys. Rev. B **76**, 155102 (2007).

[91] J. Bünemann, F. Gebhard, Phys. Rev. B **76**, 193104 (2007).

[92] J. Bünemann, Phys. Status Solidi B **248**, 203-211 (2011).

[93] R. W. Cherng, G. Refael, and E. Demler, Phys. Rev. Lett. **99**, 130406 (2007).

[94] A. V. Gorshkov, M. Hermele, V. Gurarie, C. Xu, P. S. Julienne, J. Ye, P. Zoller, E. Demler, M. D. Lukin, A. M. Rey, Nature Physics **6**, 289 (2010).

[95] C. Wu, J. Hu, S.-C. Zhang, Int. J. Mod. Phys. B **24**, 311 (2009).

Papers

Vol. **121** (2012) *ACTA PHYSICA POLONICA A* No. 5–6

Proceedings of the European Conference Physics of Magnetism 2011 (PM'11), Poznań, June 27–July 1, 2011

Spin-Triplet Pairing Induced by Hund's Rule Exchange in Orbitally Degenerate Systems: Hartree–Fock Approximation

M. Zegrodnik[a,*] and J. Spałek[a,b]

[a]AGH University of Science and Technology, Faculty of Physics and Applied Computer Science
al. A. Mickiewicza 30, 30-059 Krakow, Poland

[b]Marian Smoluchowski Institute of Physics, Jagiellonian University
W.S. Reymonta 4, 30-059 Kraków, Poland

We discuss the spin-triplet pairing mechanism induced by the Hund rule ferromagnetic exchange. We include explicitly the effect of interband hybridization and treat the problem by starting from an extended Hubbard model for a doubly degenerate band, making the simplest Hartree–Fock approximation for the part involving the pairing and the Hubbard interaction. The conditions of stability of various phases are determined as a function of both band filling and microscopic parameters. The phase diagram contains regions of stability of the spin-triplet superconducting phase coexisting with either saturated or non-saturated ferromagnetism. Phase diagrams for the cases of constant density of states and that of square lattice have been provided. The influence of hybridization on the stability of considered phases, as well as the temperature dependences of magnetic moment and the superconducting gap are also discussed.

PACS: 74.20.–z, 74.25.Dw, 75.10.Lp

1. Introduction

The candidates for the spin-triplet superconductors have been discovered in the last two decades. They are Sr_2RuO_4 [1], UGe_2 [2], and URhGe [3]. Particularly interesting are the last two as the paired state appears inside the ferromagnetic phase and, in the case of UGe_2, disappears at the critical pressure together with ferromagnetism.

The question we posed for the first time a decade ago [4–7] was whether the two phenomena may have the same origin — the intra-atomic ferromagnetic Hund rule exchange. This question originated from drawing an analogy between the present systems and cuprate high-temperature superconductors where the antiferromagnetic kinetic exchange is often regarded as the source of both antiferromagnetism (in parent Mott–Hubbard insulating compound) and spin-singlet superconductivity when the metallic state is stabilized by doping the insulator with holes. Namely, if the exchange interaction induced superconductivity is a reasonable mechanism, not just an accident, one has to explore other possibilities such as the ferromagnetic interaction.

One should note a principal limitation for the exchange interaction to represent a feasible mechanism of pairing, which takes place in direct space. Namely, this is the pairing induced by interparticle exchange. Therefore one may think that the hopping (bare band) energy has to become comparable to the exchange-interaction strength. This idea is tested in the present paper in the simplest Hartree–Fock approximation. It turns out that even in the weak-coupling limit, the paired state (the so-called A phase) may appear below the Stoner threshold for the onset of ferromagnetism, as well as coexist with it above that threshold (in the form of A1 phase). The result is independent of the form of the density of states taken and when interband hybridization is included.

2. Theoretical model

We consider the extended orbitally degenerate Hubbard Hamiltonian, which has the form

$$\hat{H} = \sum_{ij(i\neq j)l\sigma} t_{ij} a^{\dagger}_{il\sigma} a_{jl\sigma} + \sum_{ij(i\neq j)ll'(l\neq l')\sigma} t^{12}_{ij} a^{\dagger}_{il\sigma} a_{jl'\sigma} + U\sum_{il} \hat{n}_{il\uparrow}\hat{n}_{il\downarrow} - J \sum_{ill'(l\neq l')} \left(\hat{\boldsymbol{S}}_{il}\cdot\hat{\boldsymbol{S}}_{il'} + \frac{3}{4}\hat{n}_{il}\hat{n}_{il'} \right), \tag{1}$$

where $l = 1, 2$ and the first term describes electron hopping between atomic sites i and j. The second term introduces hybridization into the system. The third term describes the Coulomb interaction between electrons on the same orbital. The fourth term introduces the Hund rule ferromagnetic exchange between electrons localized on the same site, but on different orbitals. In this model we neglect the interaction-induced intra-atomic singlet-pair

* corresponding author; e-mail: michal.zegrodnik@gmail.com

hopping $\sim J$ and the correlation induced hopping [8], as we deal with the triplet-paired and ferromagnetic phases only. It can be shown that [5] one can represent the full exchange term with the help of the real-space pair operators, i.e.,

$$J \sum_{ill'(l\neq l')} \left(\hat{\boldsymbol{S}}_{il} \cdot \hat{\boldsymbol{S}}_{il'} + \frac{3}{4} \hat{n}_{il} \hat{n}_{il'} \right) \equiv 2J \sum_{i,m} \hat{A}^{\dagger}_{im} \hat{A}_{im}, \quad (2)$$

which are defined in the following way [9, 10]:

$$\hat{A}^{\dagger}_{i,m} \equiv \begin{cases} a^{\dagger}_{i1\uparrow} a^{\dagger}_{i2\uparrow}, & m=1, \\ a^{\dagger}_{i1\downarrow} a^{\dagger}_{i2\downarrow}, & m=-1, \\ \frac{1}{\sqrt{2}} \left(a^{\dagger}_{i1\uparrow} a^{\dagger}_{i2\downarrow} + a^{\dagger}_{i1\downarrow} a^{\dagger}_{i2\uparrow} \right), & m=0. \end{cases} \quad (3)$$

Hamiltonian (1) cannot be treated rigorously, apart from model situations [11, 12]. In present paper we treat the pairing and the Hubbard part in the mean-field approximation. Effectively, after making the Hartree–Fock approximation we can write down the Hamiltonian in the following way (in reciprocal space):

$$\begin{aligned} \hat{H}_{\mathrm{HF}} &= \sum_{\boldsymbol{k}l\sigma} (\epsilon_{\boldsymbol{k}} - \mu - \sigma I S^z) \hat{n}_{\boldsymbol{k}l\sigma} \\ &+ \sum_{\boldsymbol{k}ll'(l\neq l')\sigma} \epsilon_{12\boldsymbol{k}} a^{\dagger}_{\boldsymbol{k}l\sigma} a_{\boldsymbol{k}l'\sigma} \\ &+ \sum_{\boldsymbol{k},m=\pm 1} \left(\Delta^{*}_{m} \hat{A}_{\boldsymbol{k},m} + \Delta_{m} \hat{A}^{\dagger}_{\boldsymbol{k},m} \right) \\ &+ \sqrt{2} \sum_{\boldsymbol{k}} \left(\Delta^{*}_{0} \hat{A}_{\boldsymbol{k},0} + \Delta_{0} \hat{A}^{\dagger}_{\boldsymbol{k},0} \right) \\ &+ N \Bigg[\frac{|\Delta_1|^2 + |\Delta_{-1}|^2 + 2|\Delta_0|^2}{2J} \\ &+ \frac{n^2}{2} (3J - U) + 2I (S^z)^2 \Bigg], \end{aligned} \quad (4)$$

where $I = U + J$ is the effective magnetic coupling constant, N is the number of atomic sites and $\epsilon_{\boldsymbol{k}1} = \epsilon_{\boldsymbol{k}2} \equiv \epsilon_{\boldsymbol{k}}$ is the dispersion relation in the doubly degenerate band. For modeling purpose, we assume that the bands are identical. In the Hamiltonian written above we have introduced the superconducting spin-triplet gap parameters

$$\Delta_{\pm 1} \equiv -\frac{2J}{N} \sum_{\boldsymbol{k}} \langle \hat{A}_{\boldsymbol{k},\pm 1} \rangle, \quad \Delta_0 \equiv -\frac{2J}{\sqrt{2}N} \sum_{\boldsymbol{k}} \langle \hat{A}_{\boldsymbol{k},0} \rangle. \quad (5)$$

Moreover, as the bands are identical, we assume that the corresponding band fillings and magnetic moments are also identical, i.e. $n_1 = n_2 \equiv n/2$ and $S^z_1 = S^z_2 \equiv S^z$. The one-particle part of the H–F Hamiltonian can be easily diagonalized via unitary transformation which introduces hybridized quasi-particle operators

$$\tilde{a}_{\boldsymbol{k}1\sigma} = \frac{1}{\sqrt{2}} (a_{\boldsymbol{k}1\sigma} + a_{\boldsymbol{k}2\sigma}),$$

$$\tilde{a}_{\boldsymbol{k}2\sigma} = \frac{1}{\sqrt{2}} (-a_{\boldsymbol{k}1\sigma} + a_{\boldsymbol{k}2\sigma}), \quad (6)$$

with new dispersion relations

$$\tilde{\epsilon}_{\boldsymbol{k}1\sigma} = \epsilon_{\boldsymbol{k}} - \mu - \sigma I S^z + |\epsilon_{12\boldsymbol{k}}|, \quad (7)$$

$$\tilde{\epsilon}_{\boldsymbol{k}2\sigma} = \epsilon_{\boldsymbol{k}} - \mu - \sigma I S^z - |\epsilon_{12\boldsymbol{k}}|, \quad (8)$$

for $\sigma = +1, -1$ corresponding to spin orientation up and down, respectively.

In the calculations, we make a simplifying assumption that $\epsilon_{12\boldsymbol{k}} = \beta_{\mathrm{h}} \epsilon_{\boldsymbol{k}}$, where $\beta_{\mathrm{h}} \in [0, 1]$. Let us note that the two energies correspond to the antibonding and the bonding states, respectively.

A generalized Nambu–Bogolyubov–de Gennes scheme is used next in order to write down the H–F Hamiltonian in a matrix form allowing an easy determination of its eigenvalues. With the help of composite creation operator [5] $\tilde{\boldsymbol{f}}^{\dagger}_{\boldsymbol{k}} \equiv (\tilde{a}^{\dagger}_{\boldsymbol{k}1\uparrow}, \tilde{a}^{\dagger}_{\boldsymbol{k}1\downarrow}, \tilde{a}_{-\boldsymbol{k}2\uparrow}, \tilde{a}_{-\boldsymbol{k}2\downarrow})$, we can construct the 4×4 Hamiltonian matrix and write

$$\hat{H}_{\mathrm{HF}} = \sum_{\boldsymbol{k}} \tilde{\boldsymbol{f}}^{\dagger}_{\boldsymbol{k}} \tilde{\boldsymbol{H}}_{\boldsymbol{k}} \tilde{\boldsymbol{f}}_{\boldsymbol{k}} + \sum_{\boldsymbol{k}\sigma} \tilde{\epsilon}_{\boldsymbol{k}2\sigma} + N\{\ldots\}, \quad (9)$$

where

$$\tilde{\boldsymbol{H}}_{\boldsymbol{k}} = \begin{pmatrix} \tilde{\epsilon}_{\boldsymbol{k}1\uparrow} & 0 & \Delta_1 & \Delta_0 \\ 0 & \tilde{\epsilon}_{\boldsymbol{k}1\downarrow} & \Delta_0 & \Delta_{-1} \\ \Delta^{*}_1 & \Delta^{*}_0 & -\tilde{\epsilon}_{\boldsymbol{k}2\uparrow} & 0 \\ \Delta^{*}_0 & \Delta^{*}_{-1} & 0 & -\tilde{\epsilon}_{\boldsymbol{k}2\downarrow} \end{pmatrix}, \quad (10)$$

and $\tilde{\boldsymbol{f}}_{\boldsymbol{k}} \equiv (\tilde{\boldsymbol{f}}^{\dagger}_{\boldsymbol{k}})^{\dagger}$. We limit ourselves to the case of real gap parameters $\Delta^{*}_m = \Delta_m$, and distinguish between the following superconducting phases: $\boldsymbol{A}$ ($\Delta_1 \neq 0$, $\Delta_{-1} \neq 0$, $\Delta_0 = 0$) and $\boldsymbol{A1}$ ($\Delta_1 \neq 0$, $\Delta_{-1} = 0$, $\Delta_0 = 0$). The phase labeled as $\boldsymbol{B}$, i.e. that with $\Delta_1 \neq 0$, $\Delta_{-1} \neq 0$, $\Delta_0 \neq 0$ is not stable within this mechanism, so it does not appear in the subsequent discussion. After making the diagonalization transformation of (10) we can write the H–F Hamiltonian as follows:

$$\begin{aligned} \hat{H}_{\mathrm{HF}} &= \sum_{\boldsymbol{k}l\sigma} \lambda_{\boldsymbol{k}l\sigma} \alpha^{\dagger}_{\boldsymbol{k}l\sigma} \alpha_{\boldsymbol{k}l\sigma} + \sum_{\boldsymbol{k}\sigma} (\tilde{\epsilon}_{\boldsymbol{k}2\sigma} - \lambda_{\boldsymbol{k}2\sigma}) \\ &+ N\{\ldots\}. \end{aligned} \quad (11)$$

The transformed (quasi-particle) operators have the form

$$\begin{aligned} \alpha_{\boldsymbol{k}1\uparrow} &= \tilde{U}^{(+)}_{\boldsymbol{k}} \tilde{a}_{\boldsymbol{k}1\uparrow} + \tilde{V}^{(+)}_{\boldsymbol{k}} \tilde{a}^{\dagger}_{-\boldsymbol{k}2\uparrow}, \\ \alpha^{\dagger}_{-\boldsymbol{k}2\uparrow} &= -\tilde{V}^{(+)}_{\boldsymbol{k}} \tilde{a}_{\boldsymbol{k}1\uparrow} + \tilde{U}^{(+)}_{\boldsymbol{k}} \tilde{a}^{\dagger}_{-\boldsymbol{k}2\uparrow}, \\ \alpha_{\boldsymbol{k}1\downarrow} &= \tilde{U}^{(-)}_{\boldsymbol{k}} \tilde{a}_{\boldsymbol{k}1\downarrow} + \tilde{V}^{(-)}_{\boldsymbol{k}} \tilde{a}^{\dagger}_{-\boldsymbol{k}2\downarrow}, \\ \alpha^{\dagger}_{-\boldsymbol{k}2\downarrow} &= -\tilde{V}^{(-)}_{\boldsymbol{k}} \tilde{a}_{\boldsymbol{k}1\downarrow} + \tilde{U}^{(-)}_{\boldsymbol{k}} \tilde{a}^{\dagger}_{-\boldsymbol{k}2\downarrow}, \end{aligned} \quad (12)$$

where the so-called Bogolyubov coherence factors acquire the form

$$\tilde{U}^{(\pm)}_{\boldsymbol{k}} = \frac{1}{\sqrt{2}} \left(1 + \frac{\epsilon_{\boldsymbol{k}} - \mu \mp I S^z}{\sqrt{(\epsilon_{\boldsymbol{k}} - \mu \mp I S^z)^2 + \Delta^2_{\pm 1}}} \right)^{1/2},$$

$$\tilde{V}_{\boldsymbol{k}}^{(\pm)} = \frac{1}{\sqrt{2}}\left(1 - \frac{\epsilon_{\boldsymbol{k}} - \mu \mp IS^z}{\sqrt{(\epsilon_{\boldsymbol{k}} - \mu \mp IS^z)^2 + \Delta_{\pm 1}^2}}\right)^{1/2}. \quad (13)$$

The dispersion relations for the quasi-particles $\lambda_{\boldsymbol{k}l\sigma}$ are then

$$\begin{aligned}
\lambda_{\boldsymbol{k}1\uparrow} &= \sqrt{(\epsilon_{\boldsymbol{k}} - \mu - IS^z)^2 + \Delta_1^2} + \beta_{\rm h}|\epsilon_{\boldsymbol{k}}|,\\
\lambda_{\boldsymbol{k}1\downarrow} &= \sqrt{(\epsilon_{\boldsymbol{k}} - \mu + IS^z)^2 + \Delta_{-1}^2} + \beta_{\rm h}|\epsilon_{\boldsymbol{k}}|,\\
\lambda_{\boldsymbol{k}2\uparrow} &= \sqrt{(\epsilon_{\boldsymbol{k}} - \mu - IS^z)^2 + \Delta_1^2} - \beta_{\rm h}|\epsilon_{\boldsymbol{k}}|,\\
\lambda_{\boldsymbol{k}2\downarrow} &= \sqrt{(\epsilon_{\boldsymbol{k}} - \mu + IS^z)^2 + \Delta_{-1}^2} - \beta_{\rm h}|\epsilon_{\boldsymbol{k}}|. \quad (14)
\end{aligned}$$

Defining the gap parameters as $\Delta_{\pm 1}$, the average number of particles per atomic site as $n = \sum_l \langle \hat{n}_{il\uparrow} + \hat{n}_{il\downarrow}\rangle$, and the average magnetic moment per band per site as $S^z = \langle \hat{n}_{il\uparrow} - \hat{n}_{il\downarrow}\rangle/2$, the set of self-consistent equations can be constructed for calculating all unknown mean-field parameters

$$\begin{aligned}
1 &= -J\int_{-1/2}^{1/2} \frac{\rho(\epsilon)}{\sqrt{(\epsilon - \mu - IS^z)^2 + \Delta_1^2}}\\
&\quad \times (f(\lambda_{1\uparrow}) + f(\lambda_{2\uparrow}) - 1)\,{\rm d}\epsilon, \quad (15)\\
1 &= -J\int_{-1/2}^{1/2} \frac{\rho(\epsilon)}{\sqrt{(\epsilon - \mu + IS^z)^2 + \Delta_{-1}^2}}\\
&\quad \times (f(\lambda_{1\downarrow}) + f(\lambda_{2\downarrow}) - 1)\,{\rm d}\epsilon, \quad (16)\\
n - 2 &= \int_{-1/2}^{1/2} \rho(\epsilon)\left\{\frac{\epsilon - \mu - IS^z}{\sqrt{(\epsilon - \mu - IS^z)^2 + \Delta_1^2}}\right.\\
&\quad \times (f(\lambda_{1\uparrow}) + f(\lambda_{2\uparrow}) - 1) + \frac{\epsilon - \mu + IS^z}{\sqrt{(\epsilon - \mu + IS^z)^2 + \Delta_{-1}^2}}\\
&\quad \left.\times (f(\lambda_{1\downarrow}) + f(\lambda_{2\downarrow}) - 1)\right\}{\rm d}\epsilon, \quad (17)\\
S^z &= \frac{1}{4}\int_{-1/2}^{1/2} \rho(\epsilon)\left[\frac{\epsilon - \mu - IS^z}{\sqrt{(\epsilon - \mu - IS^z)^2 + \Delta_1^2}}\right.\\
&\quad \times (f(\lambda_{1\uparrow}) + f(\lambda_{2\uparrow}) - 1) - \frac{\epsilon - \mu + IS^z}{\sqrt{(\epsilon - \mu + IS^z)^2 + \Delta_{-1}^2}}\\
&\quad \left.\times (f(\lambda_{1\downarrow}) + f(\lambda_{2\downarrow}) - 1)\right]{\rm d}\epsilon, \quad (18)
\end{aligned}$$

where $\rho(\epsilon)$ is the bare density of states (per site per spin per orbital) and we have normalized all energies to the bare bandwidth, W, while $f(x)$ stands for the Fermi–Dirac distribution function. Using Eq. (11) we can calculate the free energy functional per site of the system

$$\frac{F}{N} = -T\int_{-1/2}^{1/2} \rho(\epsilon)\sum_{l\sigma} \ln\left(1 + \exp\left(-\frac{\lambda_{l\sigma}}{T}\right)\right){\rm d}\epsilon$$

$$+ \int_{-1/2}^{1/2} \rho(\epsilon)\sum_{\sigma}(\tilde{\epsilon}_{2\sigma} + \lambda_{2\sigma})\,{\rm d}\epsilon + \mu n + \{\ldots\}, \quad (19)$$

where $T \equiv k_{\rm B}T/W$ denotes the reduced temperature. Substituting the solutions for $\Delta_{\pm 1}$, μ and S^z coming from Eqs. (15)–(18) to Eq. (19), we obtain the physical free energy which determine relative stability of different magnetic and/or paired states which we discuss next.

3. Results and discussion

Phase diagrams on the plane (n, J) have been calculated for the case of constant density of states in the starting (non-hybridized) bands and for that appropriate for the square lattice. In both cases, regions of stability of the following six different phases have been determined and involve the states: NS — normal state, A — superconducting phase A, SFM — saturated ferromagnet, FM — nonsaturated ferromagnet, A1+FM — coexisting superconducting phase A1 and FM phase, A1+SFM — coexisting superconducting phases A1 and SFM phase. Exemplary phase diagrams for selected parameters are shown in Fig. 1 for the constant density of states and for

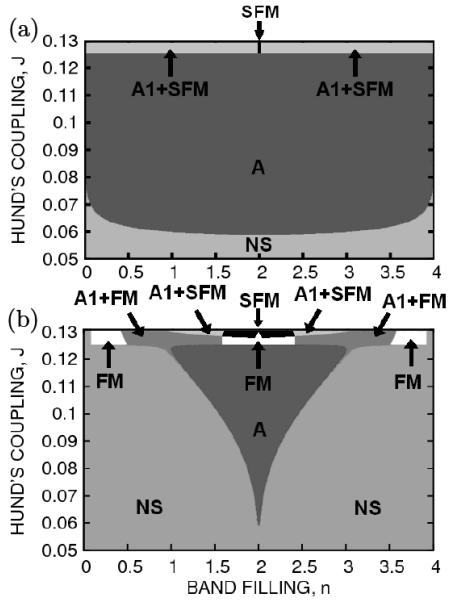

Fig. 1. Phase diagrams for $T = 10^{-4}$ for the case of constant density of states in the starting (non-hybridized) bands for $\beta_{\rm h} = 0.0$ (a) and $\beta_{\rm h} = 0.04$ (b). The Coulomb repulsion constant $U = 7$ J. No antiferromagnetism was included here.

hybridization parameter $\beta_{\rm h} = 0$ (a) and $\beta_{\rm h} = 0.04$ (b). The presence of hybridization enriches remarkably the phase diagram. Let us note that the Stoner threshold is reached for $J = 0.125$; only above this critical value the coexistent (S)FM+A1 phase appears. One has to emphasize that the pairing is induced by the exchange, not by any spin (moment) fluctuation. This is clearly seen from the fact that it can appear even in the ferromagnetically saturated state. The same type of phase diagrams

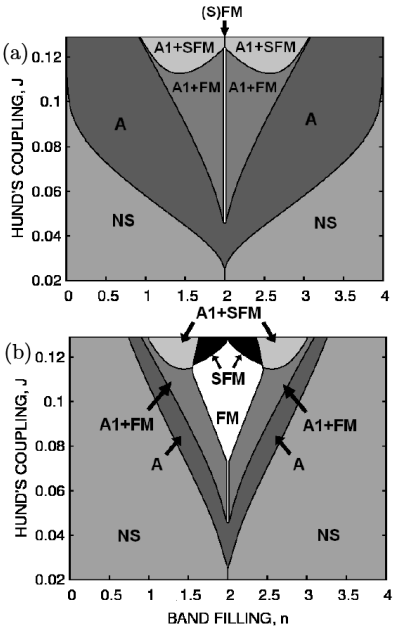

Fig. 2. Phase diagrams for $T = 10^{-4}$ for the case of square lattice for $\beta_{\rm h} = 0.0$ (a) and $\beta_{\rm h} = 0.04$ (b). The Coulomb repulsion constant $U = 7$ J. No antiferromagnetism was included here.

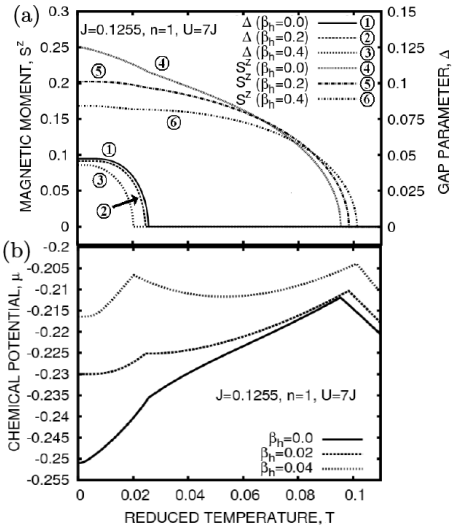

Fig. 3. Temperature dependence of the superconducting gap $\Delta \equiv \Delta_{\pm 1}$ and magnetic moment S^z (a), as well as the chemical potential μ (b), for selected values of $\beta_{\rm h}$ parameter. Figures correspond to a stable coexisting A1+(S)FM phase for the density of states in the starting (non-hybridized) bands appropriate for the square lattice.

but for a square lattice (with $W = 8|t|$) are exhibited in Fig. 2.

It can be seen in the presented diagrams that the stronger is the hybridization parameter the smaller are the regions of stability of the superconducting phases for both density-of-states functions considered. One has to note that these phase diagrams are still incomplete. This is because near the half-filling one can expect the appearance of stable antiferromagnetic phases [13]. Therefore, the regime of superconductivity stability may be restricted to even narrower strips on the phase diagrams. On the other hand, because of the peaked nature of the density of states in both cases, ferromagnetism may compete successfully with antiferromagnetism even close to $n \approx 2$. This question requires certainly further studies. One should notice that the A1+FM phase disappears for $n = 2$ even for the case where there is no hybridization, i.e., only the SFM phase survives then.

For the sake of completness, we display in Fig. 3 the thermodynamic quantities S^z, $\Delta \equiv \Delta_{\pm 1}$, and μ, all versus temperature, for selected values of $\beta_{\rm h}$. The values of microscopic parameters n and J have been chosen so that the A1+(S)FM phase would be the stable one. As the temperature of considered system is rising one can observe two phase transitions. The strength of hybridization influences the temperatures in which phase transitions occur. The increase of $\beta_{\rm h}$ parameter results in diminution of the critical temperature, $T_{\rm S}$, and increase of the Curie temperature, $T_{\rm C}$. What is more the hybridization makes the magnetic moment smaller in low temperatures. Let us note that the transition temperature ratio $T_{\rm C}/T_{\rm S} \approx 5$.

4. Conclusions

We have carried out the Hartree–Fock analysis of the phase diagrams involving the ferromagnetic and spin--triplet superconducting phases within the extended two--band degenerate Hubbard model. Stable and coexisting superconducting and ferromagnetic phases have been obtained. We have analyzed in detail the influence of inter--band hybridization on the stability of these phases, as well as have provided the temperature dependence of the order parameters. For particular set of microscopic parameters, one observes two separate phase transitions as a function of temperature. The first is the transition from A1+FM phase to FM at $T_{\rm S}$ and the second one is from FM to NS at $T_{\rm C} \sim 5T_{\rm S}$. According to our results, the hybridization has a negative influence on the spin-triplet superconductivity, as it decreases the critical temperature and reduces the regime of stability of the superconducting phases. On the contrary, $T_{\rm C}$ increases with the increasing hybridization parameter $\beta_{\rm h}$. The phase diagrams determined by us supplement the corresponding magnetic phase diagrams [13] with the A and coexistent A1+FM, A1+SFM phases for theoretical model of the same class.

Acknowledgments

M.Z. has been partly supported by the EU Human Capital Operation Program, Polish Project No. POKL.04.0101-00-434/08-00. J.S. acknowledges the financial support of the Foundation for Polish Science (FNP) within project TEAM. The authors thanks also for the support of the Ministry of Science and Higher Education through grant No. N N 202 128 736.

References

[1] Y. Maeno, H. Hashimoto, K. Yoshida, S. Nishizaki, T. Fujita, J.G. Bednorz, *Nature* **372**, 532 (1994).

[2] S.S. Saxena, P. Agarwal, K. Ahilan, F. M. Grosche, R.K.W. Haselwimmer, M.J. Steiner, E. Pugh, I. R. Walker, S.R. Julian, P. Monthoux, G.G. Lonzarich, A. Huxley, I. Sheikin, D. Braithwaite, J. Flouquet, *Nature* **406**, 587 (2000).

[3] N. Tateiwa, T.C. Kobayashi, K. Hanazono, K. Amaya, Y. Haga, R. Settai, Y. Onuki, *J. Phys., Condens. Matter* **13**, 117 (2001).

[4] For additional introduction see: J. Spałek, *Acta Phys. Pol. A* **111**, 409 (2007).

[5] K. Klejnberg, J. Spałek, *J. Phys., Condens. Matter* **11**, 6553 (1999).

[6] J. Spałek, *Phys. Rev. B* **63**, 104513 (2001).

[7] K. Klejnberg, J. Spałek, *Phys. Rev. B* **61**, 15542 (2000).

[8] T. Nomura, K. Yamada, *J. Phys. Soc. Jpn.* **71**, 1993 (2002).

[9] J. Spałek, P. Wróbel, W. Wójcik, *Physica C* **387**, 1 (2003).

[10] P. Wróbel, Ph.D. Thesis, Jagiellonian University, Kraków 2004, unpublished.

[11] Shun-Qing Shen, *Phys. Rev. B* **57**, 6474 (1998).

[12] J. Dukelsky, C. Esebagg, S. Pittel, *Phys. Rev. Lett.* **88**, 062501 (2002).

[13] S. Inagaki, R. Kubo, *Int. J. Magn.* **4**, 139 (1973).

Vol. **121** (2012) *ACTA PHYSICA POLONICA A* No. 4

Proceedings of the XV-th National School "Hundred Years of Superconductivity", Kazimierz Dolny, October 9–13, 2011

Coexistence of Spin-Triplet Superconductivity with Antiferromagnetism in Orbitally Degenerate System: Hartree–Fock Approximation

M. Zegrodnik[a,*] and J. Spałek[a,b]

[a]AGH University of Science and Technology, Faculty of Physics and Applied Computer Science al. Mickiewicza 30, 30-059 Kraków, Poland

[b]Marian Smoluchowski Institute of Physics, Jagiellonian University, ul. Reymonta 4, 30-059 Kraków, Poland

We consider the coexistence of the Hund's-rule-exchange induced spin-triplet paired state with the antiferromagnetic ordering by starting from the extended Hubbard model for a doubly degenerate band. We use the density of states appropriate for the square lattice and treat the problem in the Hartree–Fock approximation. The temperature dependences of the superconducting gaps, the magnetic moment, and the chemical potential are presented. The free energy in the considered phase is evaluated, as well as the corresponding free energies in four additional phases: paramagnetic, ferromagnetic, superconducting of type A and superconducting of type $A1$ coexisting with ferromagnetism; they occur in the proper range of parameters: band filling n and the interaction parameters U/W and J/W. The low temperature values of the superconducting gaps and staggered magnetic moment are also analyzed as a function of band filling.

PACS: 74.20.–z, 74.25.Dw, 75.10.Lp

1. Introduction

It is believed that the spin-triplet superconducting phase appears in Sr_2RuO_4 [1], UGe_2 [2] and URhGe [3]. In the last two compounds the considered type of superconducting phase occurs as coexisting with ferromagnetism. It has been shown [4–7] that the two phenomena may possibly have the same origin — the intra-atomic Hund's rule exchange, which can also lead to the coexistence of superconductivity with other type of magnetic ordering — antiferromagnetism. The coexisting superconducting and antiferromagnetic phase is discussed in this work for the extended two band Hubbard model with the use of the simplest Hartree–Fock approximation. For the sake of completeness, we also include some of the earlier results [7] concerning the superconducting phase of type A and the ferromagnetic phase coexisting with the superconducting phase of type $A1$.

2. Model

We consider the extended orbitally degenerate Hubbard Hamiltonian, which has the form

$$\hat{H} = \sum_{ij(i\neq j)l\sigma} t_{ij}\hat{a}^{\dagger}_{il\sigma}\hat{a}_{jl\sigma} + U\sum_{il}\hat{n}_{il\uparrow}\hat{n}_{il\downarrow} - J\sum_{ill'(l\neq l')}\left(\hat{\boldsymbol{S}}_{il}\cdot\hat{\boldsymbol{S}}_{il'} + \frac{3}{4}\hat{n}_{il}\hat{n}_{il'}\right), \quad (1)$$

where $l = 1, 2$ label the orbitals and the first term describes electron hopping between atomic sites i and j. The second term describes the intra-atomic Coulomb interaction between electrons on the same orbital. The third term introduces the (Hund's rule) ferromagnetic exchange between electrons localized on the same site, but on different orbitals. In this model we neglect the interaction-induced intra-atomic singlet-pair hopping $\sim J$ and the correlation induced hopping [8], as well as the inter-orbital Coulomb repulsion, as they should not introduce any important new feature in the considered here Hartree–Fock approximation. In this model for the sake of clarity, we neglect also the interorbital hybridization.

It can be shown that [4] one can represent the full exchange term with the help of the real-space pair operators, in the following manner

$$J\sum_{ill'(l\neq l')}\left(\hat{\boldsymbol{S}}_{il}\cdot\hat{\boldsymbol{S}}_{il'} + \frac{3}{4}\hat{n}_{il}\hat{n}_{il'}\right) \equiv 2J\sum_{i,m}\hat{A}^{\dagger}_{im}\hat{A}_{im}, \quad (2)$$

which are defined in the following way [9]

$$\hat{A}^{\dagger}_{i,m} \equiv \begin{cases} \hat{a}^{\dagger}_{i1\uparrow}\hat{a}^{\dagger}_{i2\uparrow} & m = 1 \\ \hat{a}^{\dagger}_{i1\downarrow}\hat{a}^{\dagger}_{i2\downarrow} & m = -1 \\ \frac{1}{\sqrt{2}}(\hat{a}^{\dagger}_{i1\uparrow}\hat{a}^{\dagger}_{i2\downarrow} + \hat{a}^{\dagger}_{i1\downarrow}\hat{a}^{\dagger}_{i2\uparrow}) & m = 0 \end{cases}. \quad (3)$$

In our considerations the antiferromagnetic state reflects the simplest form of the spin-density-wave state. In this state, we can divide our system into two interpenetrating sublattices. We name those sublattices A and B. In the antiferromagnetic phase, the average magnetic (staggered) moment of electons on each of $N/2$ sublattice A sites is equal $\langle S^z_i\rangle = \langle S^z_A\rangle$, whereas the electrons on the remaining $N/2$ sublattice B sites have magnetic moment $\langle S^z_i\rangle = \langle S^z_B\rangle \equiv -\langle S^z_A\rangle$. In accordance with the division

* corresponding author; e-mail: michal.zegrodnik@gmail.com

into the sublattices we define different annihilation operators for each sublattice, namely

$$\hat{a}_{il\sigma} = \begin{cases} \hat{a}_{il\sigma A} \\ \hat{a}_{il\sigma B} \end{cases}. \tag{4}$$

We do the same for the creation operators, $\hat{a}^{\dagger}_{il\sigma}$. For modeling purposes, we assume that the bands are identical and the charge ordering is absent. In this situation, we can write that

$$\langle \hat{S}^z_{i1A}\rangle = \langle \hat{S}^z_{i2A}\rangle \equiv \bar{S}^z, \quad \langle \hat{S}^z_{i1B}\rangle = \langle \hat{S}^z_{i2B}\rangle \equiv -\bar{S}^z, \tag{5}$$

$$\langle \hat{n}_{i1A}\rangle = \langle \hat{n}_{i2A}\rangle = \langle \hat{n}_{i1B}\rangle = \langle \hat{n}_{i2B}\rangle \equiv n/2. \tag{6}$$

In what follows, we treat the pairing and the Hubbard part in the mean field approximation. Applying (4) to (1) and making the Hartree–Fock approximation we can write down the Hamiltonian transformed to reciprocal ($\boldsymbol{k}$) space in the following form:

$$\begin{aligned}\hat{H}_{HF} = &\sum_{\boldsymbol{k}l\sigma}\Big(\epsilon_{\boldsymbol{k}}\big(\hat{a}^{\dagger}_{\boldsymbol{k}l\sigma A}\hat{a}_{\boldsymbol{k}l\sigma B} + \hat{a}^{\dagger}_{\boldsymbol{k}l\sigma B}\hat{a}_{\boldsymbol{k}l\sigma A}\big) \\ &-\sigma I\bar{S}^z\big(\hat{n}_{\boldsymbol{k}l\sigma A} - \hat{n}_{\boldsymbol{k}l\sigma B}\big)\Big) \\ &+\sum_{\boldsymbol{k},m=\pm1}\big(\Delta^*_{mA}\hat{A}_{\boldsymbol{k}mA} + \Delta_{mA}\hat{A}^{\dagger}_{\boldsymbol{k}mA}\big) \\ &+\sum_{\boldsymbol{k},m=\pm1}\big(\Delta^*_{mB}\hat{A}_{\boldsymbol{k}mB} + \Delta_{mB}\hat{A}^{\dagger}_{\boldsymbol{k}mB}\big) \\ &-\frac{\hat{N}}{4J}\big(|\Delta_{1A}|^2 + |\Delta_{-1A}|^2 + |\Delta_{1B}|^2 + |\Delta_{-1B}|^2\big) \\ &-\frac{\hat{N}}{8}(U-3J)n^2 + 2NI(\bar{S}^z)^2,\end{aligned} \tag{7}$$

where $I \equiv U + J$ is the effective magnetic coupling constant, N is the number of atomic sites and $\epsilon_{\boldsymbol{k}1} = \epsilon_{\boldsymbol{k}2} \equiv \epsilon_{\boldsymbol{k}}$ is the dispersion relation in the doubly degenerate band. One should note that the sum in (7) (and in all the corresponding equations below) is taken over N/2 independent $\boldsymbol{k}$ states. In the Hamiltonian above we also have introduced the superconducting spin-triplet gap parameters on the sublattices

$$\begin{aligned}\Delta_{\pm1A} &= -\frac{4J}{N}\sum_{\boldsymbol{k}}\langle\hat{A}_{\boldsymbol{k},\pm1A}\rangle, \\ \Delta_{\pm1B} &= -\frac{4J}{N}\sum_{\boldsymbol{k}}\langle\hat{A}_{\boldsymbol{k},\pm1B}\rangle.\end{aligned} \tag{8}$$

Because we are considering the superconducting phase coexisting with antiferromagnetism in which all lattice sites have a nonzero magnetic moment, the Cooper pairs in the spin-triplet state for $m = 0$ and spin $S^z = 0$ (that correspond to the pair operator $\hat{A}_{\boldsymbol{k},0}$) are not likely to be created. The phase, in which the gap parameters corresponding to the mentioned spin-triplet state of the Cooper pairs are nonzero, is not going to be stable, so we have neglected the term that contains $\Delta_{0A} = -\frac{4J}{\sqrt{2}N}\sum_{\boldsymbol{k}}\langle\hat{A}_{\boldsymbol{k},0A}\rangle$ and $\Delta_{0B} = -\frac{4J}{\sqrt{2}N}\sum_{\boldsymbol{k}}\langle\hat{A}_{\boldsymbol{k},0B}\rangle$.

By introducing the composite fermion creation operator

$$\begin{aligned}\hat{\boldsymbol{f}}^{\dagger}_{\boldsymbol{k}} \equiv \big(&\hat{a}^{\dagger}_{\boldsymbol{k}1\uparrow A}, \hat{a}^{\dagger}_{\boldsymbol{k}1\downarrow A}, \hat{a}_{-\boldsymbol{k}2\uparrow A}, \hat{a}_{-\boldsymbol{k}2\downarrow A}, \hat{a}^{\dagger}_{\boldsymbol{k}1\uparrow B}, \hat{a}^{\dagger}_{\boldsymbol{k}1\downarrow B}, \\ &\hat{a}_{-\boldsymbol{k}2\uparrow B}, \hat{a}_{-\boldsymbol{k}2\downarrow B}\big),\end{aligned} \tag{9}$$

we can construct the 8×8 Hamiltonian matrix and write

$$\hat{H}_{HF} - \mu\hat{N} = \sum_{\boldsymbol{k}}\hat{f}^{\dagger}_{\boldsymbol{k}}H_{\boldsymbol{k}}\hat{f}_{\boldsymbol{k}} - 4\mu\hat{N}, \tag{10}$$

where $\hat{f}_{\boldsymbol{k}} \equiv (\hat{f}^{\dagger}_{\boldsymbol{k}})^{\dagger}$, and

$$H_{\boldsymbol{k}} = \begin{pmatrix} -I\bar{S}^z-\mu & 0 & \Delta_{1A} & 0 & \epsilon_{\boldsymbol{k}} & 0 & 0 & 0 \\ 0 & I\bar{S}^z-\mu & 0 & \Delta_{-1A} & 0 & \epsilon_{\boldsymbol{k}} & 0 & 0 \\ \Delta^*_{1A} & 0 & I\bar{S}^z+\mu & 0 & 0 & 0 & -\epsilon_{\boldsymbol{k}} & 0 \\ 0 & \Delta^*_{-1A} & 0 & -I\bar{S}^z+\mu & 0 & 0 & 0 & -\epsilon_{\boldsymbol{k}} \\ \epsilon_{\boldsymbol{k}} & 0 & 0 & 0 & I\bar{S}^z-\mu & 0 & \Delta_{1B} & 0 \\ 0 & \epsilon_{\boldsymbol{k}} & 0 & 0 & 0 & -I\bar{S}^z-\mu & 0 & \Delta_{-1B} \\ 0 & 0 & -\epsilon_{\boldsymbol{k}} & 0 & \Delta^*_{1B} & 0 & -I\bar{S}^z+\mu & 0 \\ 0 & 0 & 0 & -\epsilon_{\boldsymbol{k}} & 0 & \Delta^*_{-1B} & 0 & I\bar{S}^z+\mu \end{pmatrix}. \tag{11}$$

In our considerations we limit to the case with the real gap parameters $\Delta^*_{\pm1A(B)} = \Delta_{\pm1A(B)}$. After diagonalization of (11), we can write down the Hamiltonian in the following form

$$\begin{aligned}\hat{H}_{HF} - \mu\hat{N} = &\sum_{\boldsymbol{k}d}(-1)^{d+1}\lambda_{\boldsymbol{k}d}\hat{\alpha}^{\dagger}_{\boldsymbol{k}d}\hat{\alpha}_{\boldsymbol{k}d} - 4\mu\hat{N} \\ &+\sum_{\boldsymbol{k}}(\lambda_{\boldsymbol{k}2}+\lambda_{\boldsymbol{k}4}+\lambda_{\boldsymbol{k}6}+\lambda_{\boldsymbol{k}8}),\end{aligned} \tag{12}$$

where $d = 1,2,3,\ldots,8$ and $\lambda_{\boldsymbol{k}d}$ are the eigenvalues of the matrix Hamiltonian (11) and $\hat{\alpha}_{\boldsymbol{k}d}$, $\hat{\alpha}^{\dagger}_{\boldsymbol{k}d}$ are the quasi-particle annihilation and creation operators, which can be expressed by the initial creation and annihilation operators via generalized Bogoliubov transformation, i.e.,

$$\hat{\boldsymbol{g}}_{\boldsymbol{k}} = U_{\boldsymbol{k}}\hat{\boldsymbol{f}}_{\boldsymbol{k}}, \tag{13}$$

with $\hat{\boldsymbol{g}}^{\dagger}_{\boldsymbol{k}} \equiv \big(\hat{\alpha}^{\dagger}_{\boldsymbol{k}1}, \hat{\alpha}_{-\boldsymbol{k}2}, \hat{\alpha}^{\dagger}_{\boldsymbol{k}3}, \hat{\alpha}_{-\boldsymbol{k}4}, \hat{\alpha}^{\dagger}_{\boldsymbol{k}5}, \hat{\alpha}_{-\boldsymbol{k}6}, \hat{\alpha}^{\dagger}_{\boldsymbol{k}7}, \hat{\alpha}_{-\boldsymbol{k}8}\big)$ and $\hat{\boldsymbol{g}}_{\boldsymbol{k}} = (\hat{\boldsymbol{g}}^{\dagger}_{\boldsymbol{k}})^{\dagger}$. Eigenvectors of the Hamiltonian matrix (11) are the columns of the diagonalization matrix $U_{\boldsymbol{k}}$. Using the definitions of gap parameters $\Delta_{\pm1A}$, $\Delta_{\pm1B}$, the average number of particles per atomic site $n = \sum_l\langle\hat{n}_{il\uparrow A} + \hat{n}_{il\downarrow A}\rangle$, and the average magnetic moment

per band per site $S^z = \langle \hat{n}_{il\uparrow A} - \hat{n}_{il\downarrow A} \rangle /2$, we can construct the set of self consistent equations for all mean-field parameters ($\Delta_{\pm 1A}$, $\Delta_{\pm 1B}$, $\bar{S}^z$) and the chemical potential. The averages that appear in the set of self consistent equations $\langle \hat{\alpha}^{\dagger}_{\boldsymbol{k}d} \hat{\alpha}_{\boldsymbol{k}d} \rangle$ can be replaced by the corresponding Fermi-Dirac distribution function

$$f((-1)^{d+1}\lambda_{\boldsymbol{k}d}) = 1/[\exp(\beta(-1)^{d+1}\lambda_{\boldsymbol{k}d}) + 1].$$

The eigenvalues and eigenvectors of matrix (11) are evaluated numerically during the procedure of solving the set of self consistent equations. The detailed procedure of calculating the free energies and corresponding order parameters is similar as in our previous work [7]. The numerical results are obtained by assuming the square lattice with the hopping t between the nearest neighbors.

3. Results and discussion

In all presented below figures the energies have been normalized to the bare band-width $W = 8|t|$, as well as T corresponds to the reduced temperature $T \equiv k_B T/W$.

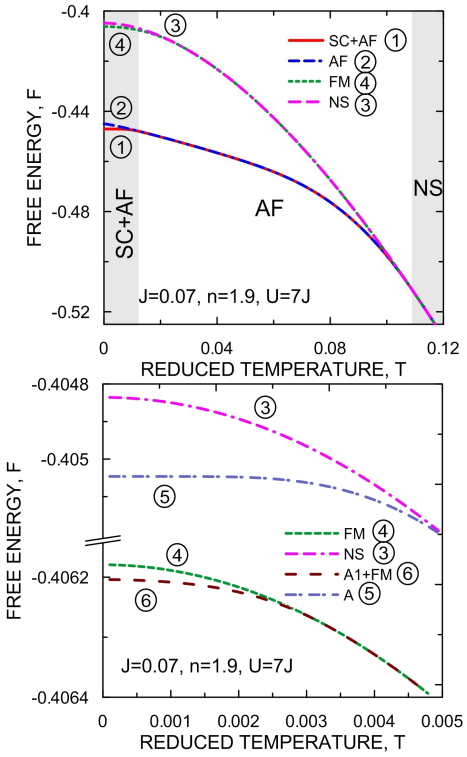

Fig. 1. (a) — temperature dependences of free energy in phases: coexisting superconducting–antiferromagnetic (SC+AF), antiferromagnetic (AF), normal state (NS), ferromagnetic (FM); (b) — free energies for A, NS, $A1$+FM and FM phases in the low-T regime. The free energy for A and $A1$+FM phases are not shown in Fig. 1a for the sake of clarity. For the selected parameters, AF+SC and AF phases are the only stable phases in proper temperature intervals.

In Fig. 1 we present the temperature dependence of free energies for the six different phases: NS — normal state, A — superconducting phase A ($\Delta_{\pm 1A} = \Delta_{\pm 1B} \neq 0$), $A1$+FM — coexistent superconducting phase $A1$ ($\Delta_{1A} = \Delta_{1B} \neq 0$ and $\Delta_{-1A} = \Delta_{-1B} = 0$) and the non-saturated ferromagnetic phase, $A1$+SFM — coexistent superconducting $A1$ and saturated ferromagnetic phase, SC+AF — coexistent superconducting and antiferromagnetic phase. Because the free-energy values of the A and NS phases are very close, we exhibit their temperature dependences zoomed in Fig. 1b). The same is shown for the phases $A1$+FM and FM (bottom part). As one can see from the Fig. 1, the phase SC+AF has the lowest free energy below the reduced temperature $T_S \approx 0.0123$ for the specified values of the microscopic parameters.

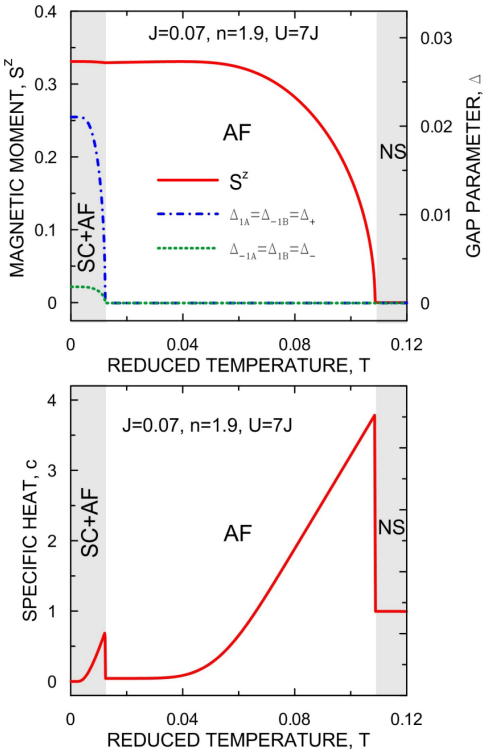

Fig. 2. (a) — temperature dependence of the superconducting gaps and the staggered magnetic moment; (b) — temperature dependence of the specific heat for the to the stable phases.

Temperature dependence of superconducting gaps and staggered magnetic moment in the SC+AF phase are shown in Fig. 2. Below T_S the staggered magnetic moment and the superconducting gaps, have all nonzero values. In the SC+AF phase the gap parameters that correspond to Cooper pairs with the spin aligned in the same direction as the magnetic moment on the sublattice have equal values ($\Delta_{1A} = \Delta_{-1B} \equiv \Delta_+$). Gap parameters that correspond to Cooper pairs with spin aligned in the opposite direction to the magnetic moment on the sublattice also have equal values ($\Delta_{-1A} = \Delta_{1B} \equiv \Delta_-$), but much smaller than the gap parameters Δ_{1A}, Δ_{-1B}.

In Fig. 2b one can observe that there are two discontinuities in the specific-heat temperature dependence. The

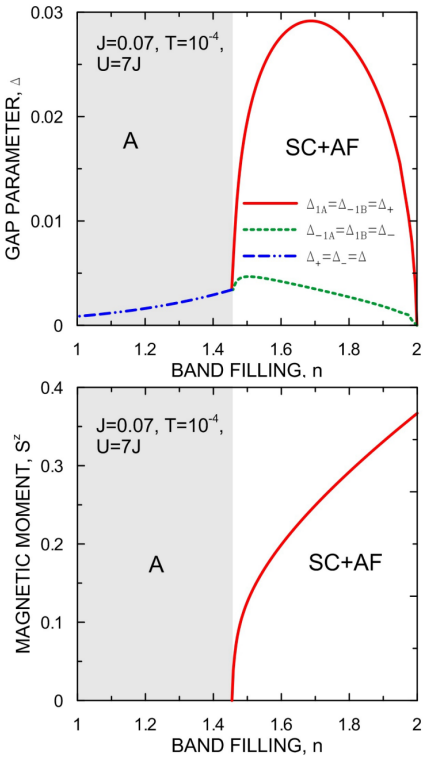

Fig. 3. (a) — gap parameters Δ_+ and Δ_- and (b) — staggered magnetic moment both as a function of band filling n. The coexistent phase appears near the half filling.

first, at lower T, corresponds to the phase transition from the SC+AF phase to the pure AF phase, while the second corresponds to the transition from the AF phase to the normal phase (NS). Near the Néel temperature, $T_N \approx 0.11$, the staggered magnetic moment decreases continuously to zero. The low temperature values of gap parameters for the AF+SC phase for different values of band filling are presented in Fig. 3. One can see that gap components Δ_+ and Δ_- tend to zero when the system is approaching the half filling ($n \to 2$). On the contrary, the staggered magnetic moment $\bar{S}^z$ reaches then maximum. Below the critical value of band filling, $n_c \approx 1.45$, the gap parameters Δ_+ and Δ_- become equal and the staggered magnetic moment vanishes. In this regime the superconducting phase of type A is the stable phase. One should mention that the easiness, with which the superconducting triplet state is accommodated within the antiferromagnetic phase stems from the fact that the SC gaps have an intra-atomic origin and the spins are parallel. Therefore, the pairs respect the Hund's rule and do not disturb the staggered-moment structure at the same time.

4. Conclusions

We have obtained the stable coexistent superconducting and antiferromagnetic phase within the extended two band Hubbard model using the Hartree–Fock approximation. For selected values of the microscopic parameters, that correspond to zero-temperature stability of SC+AF phase, with the rise of temperature, one can observe two phase transitions. The first is from the SC+AF phase to the antiferromagnetic phase and the second form the antiferromagnetic phase to paramagnetic state. The transition temperature ratio is $T_N/T_S \approx 9$. In the superconducting phase coexisting with antiferromagnetism we have introduced two different gap parameters on different sublattices. The calculated gap parameters fulfill the relations

$$\Delta_{1A} = \Delta_{-1B} \equiv \Delta_+, \ \Delta_{-1A} = \Delta_{1B} \equiv \Delta_-, \ \Delta_+ > \Delta_-.$$

Full discussion including details of the phase diagram that contains all considered here phases will be provided elsewhere.

Acknowledgements

M.Z. has been partly supported by the EU Human Capital Operation Program, Polish Project No. POKL.04.0101-00-434/08-00. J.S. acknowledges the financial support of the Foundation for Polish Science (FNP) within project TEAM and thanks also for the support of the Ministry of Science and Higher Education though Grant No. N N 202 128 736.

References

[1] Y. Maeno, H. Hashimoto, K. Yoshida, S. Nishizaki, T. Fujita, J.G. Bednorz, F. Lichtenberg, *Nature* **372**, 532 (1994).

[2] S.S. Saxena, P. Agarwal, K. Ahilan, F.M. Grosche, R.K.W. Haselwimmer, M.J. Steiner, E. Pugh, I.R. Walker, S.R. Julian, P. Monthoux, G.G. Lonzarich, A. Huxley, I. Sheikin, D. Braithwaite, J. Flouquet, *Nature* **406**, 587 (2000).

[3] N. Tateiwa, T.C. Kobayashi, K. Hanazono, K. Amaya, Y. Haga, R. Settai, Y. Onuki, *J. Phys. Condens. Matter* **13**, 117 (2001).

[4] K. Klejnberg, J. Spałek, *J. Phys. Condens. Matter* **11**, 6553 (1999).

[5] J. Spałek, *Phys. Rev. B* **63**, 104513 (2001).

[6] K. Klejnberg, J. Spałek, *Phys. Rev. B* **61**, 15542 (2000).

[7] M. Zegrodnik, J. Spałek, *Acta. Phys. Pol. A*, in press.

[8] T. Nomura, K. Yamada, *J. Phys. Soc. Jpn.* **71**, 1993 (2002).

[9] P. Wróbel, Ph.D. Thesis, Jagiellonian University, Kraków, (2004), unpublished.

PHYSICAL REVIEW B **86**, 014505 (2012)

Coexistence of spin-triplet superconductivity with magnetic ordering in an orbitally degenerate system: Hartree-Fock-BCS approximation revisited

Michał Zegrodnik
AGH University of Science and Technology, Faculty of Physics and Applied Computer Science, Al. Mickiewicza 30, 30-059 Kraków, Poland

Jozef Spałek
Marian Smoluchowski Institute of Physics, Jagiellonian University, ul. Reymonta 4, 30-059 Kraków, Poland and AGH University of Science and Technology, Faculty of Physics and Applied Computer Science, Al. Mickiewicza 30, 30-059 Kraków, Poland

(Received 25 April 2012; revised manuscript received 12 June 2012; published 9 July 2012)

The Hund's-rule-exchange induced and coexisting spin-triplet paired and magnetic states are considered within the doubly degenerate Hubbard model with interband hybridization. The Hartree-Fock approximation combined with the Bardeen-Cooper-Schrieffer (BCS) approach is analyzed for the case of square lattice. The calculated phase diagram contains regions of stability of the spin-triplet superconducting phase coexisting with either ferromagnetism or antiferromagnetism, as well as a pure superconducting phase. The influence of the intersite hybridization on the stability of the considered phases, as well as the temperature dependence of both the magnetic moment and the superconducting gaps, are also discussed. Our approach supplements the well-known phase diagrams containing only magnetic phases with the paired triplet states treated on the same footing. We also discuss briefly how to include the spin fluctuations within this model with real-space pairing.

DOI: 10.1103/PhysRevB.86.014505 PACS number(s): 74.20.−z, 74.25.Dw, 75.10.Lp

I. INTRODUCTION

The spin-triplet superconducting phase is believed to appear in Sr_2RuO_4,[1] UGe_2,[2] and URhGe.[3] In the last two compounds, the considered type of superconducting phase occurs as coexisting with ferromagnetism. Additionally, even though U atoms in these compounds contain $5f$ electrons responsible for magnetism, this multiple-band system can be regarded as a weakly or moderately correlated electron system, particularly at higher pressure. Originally, it had been suggested via a proper quantitative analysis[4–6] that the the intra-atomic Hund's rule exchange can lead in a natural manner to the coexistence of superconductivity with magnetic ordering: ferromagnetism or antiferromagnetism.

The coexisting superconducting and magnetic phases are discussed in this work within an orbitally degenerate two-band Hubbard model using the Hartree-Fock approximation (HF), here combined with the Bardeen-Cooper-Schrieffer (BCS) approach, i.e., in the vicinity of the ferromagnetism disappearance, where also the superconductivity occurs. The particular emphasis is put on the appearance of superconductivity near the Stoner threshold, where the Hartree-Fock-BCS approximation can be regarded as realistic. This type of approach can be formulated also for other systems.[7]

The alternative suggested mechanism for appearance of superconductivity in those systems is the pairing mediated by ferromagnetic spin fluctuations, which can also appear in the paramagnetic or weakly ferromagnetic phase.[8] Here, the mean-field approximation provides not only the starting magnetic phase diagram, but also a related discussion of the superconducting states treated on equal footing. In this approach, the spin-fluctuation contribution appears as a next-order contribution. This is the reason for undertaking a revision of the standard Hartree-Fock approximation. Namely, we concentrate here on the spin-triplet states, pure and coexisting with either ferromagnetism or antiferromagnetism, depending on the relative magnitude of microscopic parameters: the Hubbard intraorbital and interorbital interactions U and U', respectively, the Hund's rule ferromagnetic exchange integral J, the relative magnitude of hybridization β_h, and the band filling n. The bare bandwidth W is taken as unit of energy. In the concluding section, we discuss briefly how to outline the approach to include also the quantum fluctuations around this HF-BCS (saddle-point) state as a higher-order contribution.

The role of exchange interactions is crucial in both the so-called t-J model of high-temperature superconductivity[9] and in the so-called Kondo-mediated pairing in heavy-fermion systems.[10] In this and the following papers, we discuss the idea of real-space pairing for the triplet-paired states in the regime of weakly correlated particles and include both the interband hybridization and the corresponding Coulomb interactions. We think that this relatively simple approach is relevant to the mentioned at the beginning ferromagnetic superconductors because of the following reasons. Although the effective exchange (Weiss-type) field acts only on the spin degrees of freedom, it is important in determining the second critical field of ferromagnetic superconductor in the so-called Pauli limit,[11] as the orbital effects in the Cooper-pair breaking process are then negligible. The appearance of a stable coexistent ferromagnetic-superconducting phase means that either Pauli limiting situation critical field has not been reached in the case of spin-singlet pairing or else the pairing has the spin-triplet nature, without the component with spin $S^z = 0$, and then the Pauli limit is not operative.

The present model with local spin-triplet pairing has its precedents of the same type in the case of spin-singlet pairing, i.e., the Hubbard model with $U < 0$,[12] which played the central role in singling out a nontrivial character of pairing in real space. Here, the same role is being played by the intra-atomic (but interorbital) ferromagnetic exchange. We believe that this area of research unexplored so far in detail opens up new

possibilities of studies of weakly and moderately correlated magnetic superconductors.[13]

The structure of this paper is as follows. In Sec. II, we define the model and the full Hartee-Fock-BCS approximation (i.e., mean-field approximation for magnetic ordering with the concomitant BCS-type decoupling) for the coexistent two-sublattice antiferromagnetic and spin-triplet superconducting phase (cf. also Appendix A for details). For completeness, in Appendix B, we include also the analysis of a simpler coexistent superconducting-ferromagnetic phase. In Sec. III, we provide a detailed numerical analysis and construct the full phase diagram on the Hund's rule coupling-band filling plane. We describe also the physical properties of the coexistent phases. In Appendix C, we sketch a systematic approach of going beyond Hartree-Fock approximation, i.e., including the spin fluctuations, starting from our Hartree-Fock-BCS state.

II. MODEL AND COEXISTENT ANTIFERROMAGNETIC-SPIN-TRIPLET SUPERCONDUCTING PHASE: MEAN-FIELD-BCS APPROXIMATION

We start with the extended orbitally degenerate Hubbard Hamiltonian, which has the form

$$\hat{H} = \sum_{ij(i\neq j)ll'\sigma} t_{ij}^{ll'} a_{il\sigma}^{\dagger} a_{jl'\sigma} + (U'+J)\sum_{i} \hat{n}_{i1}\hat{n}_{i2} + U\sum_{il} \hat{n}_{il\uparrow}\hat{n}_{il\downarrow} - J\sum_{ill'(l\neq l')} \left(\hat{\mathbf{S}}_{il}\cdot\hat{\mathbf{S}}_{il'} + \frac{3}{4}\hat{n}_{il}\hat{n}_{il'}\right), \tag{1}$$

where $l = 1,2$ label the orbitals and the first term describes electron hopping between atomic sites i and j. For $l \neq l'$, this term represents electron hopping with change of the orbital (intersite, interorbital hybridization). The next two terms describe the Coulomb interaction between electrons on the same atomic site. However, as one can see, the second term contains the contribution that originates from the exchange interaction (J). The last term expresses the (Hund's rule) ferromagnetic exchange between electrons localized on the same site, but on different orbitals. This term is regarded as responsible for the local spin-triplet pairing in the subsequent discussion. The components of the spin operator $\hat{\mathbf{S}}_{il} = (\hat{S}_{il}^{x}, \hat{S}_{il}^{y}, \hat{S}_{il}^{z})$ used in (1) acquire the form

$$\hat{S}_{il}^{x,y,z} = \tfrac{1}{2}\hat{\mathbf{h}}_{il}^{\dagger}\sigma_{x,y,z}\hat{\mathbf{h}}_{il}, \tag{2}$$

where $\sigma_{x,y,z}$ are the Pauli matrices and $\mathbf{h}_{il}^{\dagger} \equiv (a_{il\uparrow}^{\dagger}, a_{il\downarrow}^{\dagger})$. In our considerations, we neglect the interaction-induced intra-atomic singlet-pair hopping ($Ja_{i1\uparrow}^{\dagger}a_{i1\downarrow}^{\dagger}a_{i2\downarrow}a_{i2\uparrow}$ + H.c.) and the correlation-induced hopping $[Vn_{1\bar{\sigma}}(a_{1\bar{\sigma}}^{\dagger}a_{2\bar{\sigma}} + a_{2\bar{\sigma}}^{\dagger}a_{1\bar{\sigma}}) + 1 \leftrightarrow 2]$,[13] as they should not introduce any important new qualitative feature in the considered here spin-triplet paired states. What is more important, we assume that $t_{ij}^{12} = t_{ij}^{21}$ and $t_{ij}^{11} = t_{ij}^{22} \equiv t_{ij}$, i.e., the starting degenerate bands have the same width (*the extreme degeneracy limit*), as we are interested in establishing new qualitative features to the overall phase diagram, which are introduced by the magnetic pairing.

As has already been said, the aim of this work is to examine the spin-triplet superconductivity coexisting with ferromagnetism and antiferromagnetism as well as the pure spin-triplet superconducting phase and the pure magnetically ordered phases. Labels defining the spin-triplet paired phases (A and A1) that are going to be used in this work correspond to those defined for superfluid ^{3}He according to Refs. 14 and 8. Namely, in the A phase, the superconducting gaps that correspond to Cooper pairs with total spin up and down are equal ($\Delta_1 = \Delta_{-1} \neq 0$, $\Delta_0 = 0$), whereas in the A1 phase the only nonzero superconducting gap is the one that corresponds to the Cooper pair with total spin up ($\Delta_1 \neq 0$, $\Delta_{-1} = \Delta_0 = 0$). In this section, we show the method of calculations that is appropriate for the superconducting phase coexisting with antiferromagnetism, as well as pure superconducting phase of type A and pure antiferromagnetic phase. The corresponding considerations for the case of ferromagnetically ordered phases and superconducting phase A1 are deferred to the Appendix B.

From the start, we make use of the fact that the full exchange term can be represented by the real-space spin-triplet pairing operators, in the following manner:

$$J\sum_{ill'(l\neq l')}\left(\hat{\mathbf{S}}_{il}\cdot\hat{\mathbf{S}}_{il'} + \frac{3}{4}\hat{n}_{il}\hat{n}_{il'}\right) \equiv 2J\sum_{i,m}\hat{A}_{im}^{\dagger}\hat{A}_{im}, \tag{3}$$

which are of the form

$$\hat{A}_{i,m}^{\dagger} \equiv \begin{cases} a_{i1\uparrow}^{\dagger}a_{i2\uparrow}^{\dagger}, & m = 1 \\ a_{i1\downarrow}^{\dagger}a_{i2\downarrow}^{\dagger}, & m = -1 \\ \frac{1}{\sqrt{2}}(a_{i1\uparrow}^{\dagger}a_{i2\downarrow}^{\dagger} + a_{i1\downarrow}^{\dagger}a_{i2\uparrow}^{\dagger}), & m = 0. \end{cases} \tag{4}$$

Furthermore, the interorbital Coulomb repulsion term can be expressed with the use of spin-triplet pairing operators and the spin-singlet pairing operators in the following manner:

$$(U'+J)\sum_{i}\hat{n}_{i1}\hat{n}_{i2} = (U'+J)\left(\sum_{i}\hat{B}_{i}^{\dagger}\hat{B}_{i} + \sum_{im}\hat{A}_{im}^{\dagger}\hat{A}_{im}\right), \tag{5}$$

where

$$\hat{B}_{i}^{\dagger} = \frac{1}{\sqrt{2}}(a_{i1\uparrow}^{\dagger}a_{i2\downarrow}^{\dagger} - a_{i1\downarrow}^{\dagger}a_{i2\uparrow}^{\dagger}) \tag{6}$$

are the interorbital, intra-atomic spin-singlet pairing operators in real space. Using Eqs. (3) and (5), one can write our model Hamiltonian in the form

$$\hat{H} = \sum_{ij(i\neq j)ll'\sigma} t_{ij}^{ll'} a_{il\sigma}^{\dagger}a_{jl'\sigma} + U\sum_{il}\hat{n}_{il\uparrow}\hat{n}_{il\downarrow} + (U'+J)\sum_{i}\hat{B}_{i}^{\dagger}\hat{B}_{i} - (J-U')\sum_{im}\hat{A}_{im}^{\dagger}\hat{A}_{im}. \tag{7}$$

It should be noted here that for $J < U'$, the interorbital Coulomb repulsion suppresses the spin-triplet pairing mechanism and the superconducting phases will not appear in the system in the weak-coupling (Hartree-Fock) limit. For $3d$ electrons,[15] $U' = U - 2J$, thus the necessary condition for the pairing to occur in our model is $U < 3J$. Usually, for $3d$ metals, we have $U \sim 3J$, so it represents a rather stringent condition for the superconductivity to appear in that situation. We use this relation to fix the parameters for modeling purposes, not limited to $3d$ systems. This is also

because, e.g., $5f$ electrons in uranium compounds lead to a similar behavior as do $3d$ electrons. One should note that the considered here pairing is based on the intra-atomic interorbital ferromagnetic Hund's rule exchange. A simple extension to the situation with nonlocal J has been considered by Dai *et al.*[7] Also, as we consider only the weakly correlated regime, where the metallic state is stable, no orbital ordering is expected (cf. Klejnberg and Spałek in Ref. 5).

In our considerations, the antiferromagnetic state represents the simplest example of the spin-density-wave state. In this state, we can divide our system into two interpenetrating sublattices A and B. The average staggered magnetic moment of electrons on each of the $N/2$ sublattice A sites is equal, $\langle S_i^z\rangle = \langle S_A^z\rangle$, whereas on the remaining $N/2$ sublattice B sites, we have $\langle S_i^z\rangle = \langle S_B^z\rangle \equiv -\langle S_A^z\rangle$. In accordance with this division into two sublattices, we define different annihilation operators for each sublattice, namely,

$$a_{il\sigma} = \begin{cases} a_{il\sigma A} & \text{for i} \in A, \\ a_{il\sigma B} & \text{for i} \in B. \end{cases} \tag{8}$$

The same holds for the creation operators $a_{il\sigma}^\dagger$. We assume that the charge ordering is absent. In this situation, we can write that

$$\langle S_{i1A}^z\rangle = \langle S_{i2A}^z\rangle \equiv \bar{S}_s^z, \quad \langle S_{i1B}^z\rangle = \langle S_{i2B}^z\rangle \equiv -\bar{S}_s^z, \tag{9}$$

$$\langle n_{i1A}\rangle = \langle n_{i2A}\rangle = \langle n_{i1B}\rangle = \langle n_{i2B}\rangle \equiv n/2, \tag{10}$$

where n is the band filling. In what follows, we treat the pairing and the Hubbard parts in the combined mean-field BCS approximation. In effect, we can write the Hamiltonian transformed in reciprocal ($\mathbf{k}$) space in the form

$$\begin{aligned}
\hat{H}_{\mathrm{HF}} - \mu\hat{N} = {} & \sum_{\mathbf{k}l\sigma}[\epsilon_{\mathbf{k}}(a_{\mathbf{k}l\sigma A}^\dagger a_{\mathbf{k}l\sigma B} + a_{\mathbf{k}l\sigma B}^\dagger a_{\mathbf{k}l\sigma A}) - \sigma I\bar{S}_s^z(\hat{n}_{\mathbf{k}l\sigma A} - \hat{n}_{\mathbf{k}l\sigma B})] \\
& + \sum_{kll'(l\neq l'\sigma)} \epsilon_{\mathbf{k}12}(a_{\mathbf{k}l\sigma A}^\dagger a_{\mathbf{k}l'\sigma B} + a_{\mathbf{k}l\sigma B}^\dagger a_{\mathbf{k}l'\sigma A}) + \sum_{\mathbf{k}l\sigma}\left[\frac{n}{8}(U+2U'-J) - \mu\right](\hat{n}_{\mathbf{k}l\sigma A} + \hat{n}_{\mathbf{k}l\sigma B}) \\
& + \sum_{\mathbf{k},m=\pm1}(\Delta_{mA}^*\hat{A}_{\mathbf{k}mA} + \Delta_{mA}\hat{A}_{\mathbf{k}mA}^\dagger) + \sum_{\mathbf{k},m=\pm1}(\Delta_{mB}^*\hat{A}_{\mathbf{k}mB} + \Delta_{mB}\hat{A}_{\mathbf{k}mB}^\dagger) \\
& + \sqrt{2}\sum_{\mathbf{k}}(\Delta_{0A}^*\hat{A}_{\mathbf{k}0A} + \Delta_{0A}\hat{A}_{\mathbf{k}0A}^\dagger) + \sqrt{2}\sum_{\mathbf{k}}(\Delta_{0B}^*\hat{A}_{\mathbf{k}0B} + \Delta_{0B}\hat{A}_{\mathbf{k}0B}^\dagger) - N\frac{n^2}{16}(U+2U'-J) \\
& + 2NI\left(\bar{S}_s^z\right)^2 - \frac{N}{2(J-U')}(|\Delta_{1A}|^2 + |\Delta_{-1A}|^2 + |\Delta_{1B}|^2 + |\Delta_{-1B}|^2 + 2|\Delta_{0A}|^2 + 2|\Delta_{0B}|^2),
\end{aligned} \tag{11}$$

where $I \equiv U + J$ is the effective magnetic coupling constant and $\epsilon_{\mathbf{k}1} = \epsilon_{\mathbf{k}2} \equiv \epsilon_{\mathbf{k}}$ is the dispersion relation. The results presented in the next section have been carried out for square lattice with nonzero hopping t between nearest neighbors only. The corresponding bare dispersion relation in a nonhybridized band acquires the form

$$\epsilon_{\mathbf{k}} = -2t\cos k_x - 2t\cos k_y. \tag{12}$$

As we are considering the doubly degenerate band model situation, we make a simplifying assumption that the hybridization matrix element $\epsilon_{12\mathbf{k}} = \beta_h\epsilon_{\mathbf{k}}$, where $\beta_h \in [0,1]$ is the parameter, which specifies the hybridization strength (i.e., represents a second scale of electron energies, in addition to $\epsilon_{\mathbf{k}}$). This means that we have just one active atom per unit cell with a doubly degenerate orbital of the same kind (their spatial asymmetry is disregarded). One should note that the sums in (11) (and in all corresponding equations below) is taken over $N/2$ independent $\mathbf{k}$ states. In the Hamiltonian written above, we have also introduced the superconducting spin-triplet sublattice gap parameters

$$\begin{aligned}
\Delta_{\pm1A(B)} &\equiv -\frac{2(J-U')}{N}\sum_{\mathbf{k}}\langle\hat{A}_{\mathbf{k},\pm1A(B)}\rangle, \\
\Delta_{0A(B)} &\equiv -\frac{2(J-U')}{\sqrt{2}N}\sum_{\mathbf{k}}\langle\hat{A}_{\mathbf{k},0A(B)}\rangle.
\end{aligned} \tag{13}$$

The terms $N\frac{n^2}{16}(U+2U'-J)$ and $\frac{n}{8}(U+2U'-J)$ in (11) can be neglected, as they lead only to a shift of the reference point of the system energy. One should note that since the real-space pairing mechanism is of intra-atomic nature, there is no direct conflict with either ferromagnetic or antiferromagnetic ordering coexisting with it.

A. Antiferromagnetic (Slater) subbands

The diagonalization of the Hamiltonian (11) can be carried out in two steps. In the first step, we diagonalize the one-particle part of the Hartree-Fock Hamiltonian [the first two sums of (11)]. Note that we have to carry out this step first since we assume the bands are both hybridized and contain pairing part. By introducing the four-composite fermion operator $\mathbf{f}_{\mathbf{k}\sigma}^\dagger \equiv (a_{\mathbf{k}1\sigma A}^\dagger, a_{\mathbf{k}2\sigma A}^\dagger, a_{\mathbf{k}1\sigma B}^\dagger, a_{\mathbf{k}2\sigma B}^\dagger)$, we can express the one-particle Hamiltonian in the following form:

$$\hat{H}_{\mathrm{HF}}^0 = \sum_{\mathbf{k}\sigma}\mathbf{f}_{\mathbf{k}\sigma}^\dagger\mathbf{H}_{\mathbf{k}\sigma}^0\mathbf{f}_{\mathbf{k}\sigma}, \tag{14}$$

where $\mathbf{f}_{\mathbf{k}} \equiv (\mathbf{f}_{\mathbf{k}}^\dagger)^\dagger$, and

$$\mathbf{H}_{\mathbf{k}\sigma}^0 = \begin{pmatrix} -\sigma I\bar{S}_s^z & 0 & \epsilon_{\mathbf{k}} & \epsilon_{\mathbf{k}12} \\ 0 & -\sigma I\bar{S}_s^z & \epsilon_{\mathbf{k}12} & \epsilon_{\mathbf{k}} \\ \epsilon_{\mathbf{k}} & \epsilon_{\mathbf{k}12} & \sigma I\bar{S}_s^z & 0 \\ \epsilon_{\mathbf{k}12} & \epsilon_{\mathbf{k}} & 0 & \sigma I\bar{S}_s^z \end{pmatrix}. \tag{15}$$

To diagonalize this Hamiltonian, we introduce a generalized Bogoliubov transformation to new operators $\tilde{a}_{kl\sigma A}$ and $\tilde{a}_{kl\sigma B}$ in the following manner:

$$\begin{pmatrix} a_{\mathbf{k}1\sigma A} \\ a_{\mathbf{k}2\sigma A} \\ a_{\mathbf{k}1\sigma B} \\ a_{\mathbf{k}2\sigma B} \end{pmatrix} = \begin{pmatrix} -U^{+}_{\mathbf{k}\sigma} & U^{-}_{\mathbf{k}\sigma} & V^{+}_{\mathbf{k}\sigma} & -V^{-}_{\mathbf{k}\sigma} \\ -U^{+}_{\mathbf{k}\sigma} & -U^{-}_{\mathbf{k}\sigma} & V^{+}_{\mathbf{k}\sigma} & V^{-}_{\mathbf{k}\sigma} \\ V^{+}_{\mathbf{k}\sigma} & -V^{-}_{\mathbf{k}\sigma} & U^{+}_{\mathbf{k}\sigma} & -U^{-}_{\mathbf{k}\sigma} \\ V^{+}_{\mathbf{k}\sigma} & V^{-}_{\mathbf{k}\sigma} & U^{+}_{\mathbf{k}\sigma} & U^{-}_{\mathbf{k}\sigma} \end{pmatrix} \begin{pmatrix} \tilde{a}_{\mathbf{k}1\sigma A} \\ \tilde{a}_{\mathbf{k}2\sigma A} \\ \tilde{a}_{\mathbf{k}1\sigma B} \\ \tilde{a}_{\mathbf{k}2\sigma B} \end{pmatrix}, \tag{16}$$

where

$$\begin{aligned} U^{(\pm)}_{\mathbf{k}\sigma} &= \frac{1}{\sqrt{2}}\left(1 + \frac{\sigma I \hat{S}^{z}_{s}}{\sqrt{(\epsilon_{\mathbf{k}} \pm \epsilon_{\mathbf{k}12})^{2} + \left(I\bar{S}^{z}_{s}\right)^{2}}}\right)^{1/2}, \\ V^{(\pm)}_{\mathbf{k}\sigma} &= \frac{1}{\sqrt{2}}\left(1 - \frac{\sigma I \hat{S}^{z}_{s}}{\sqrt{(\epsilon_{\mathbf{k}} \pm \epsilon_{\mathbf{k}12})^{2} + \left(I\bar{S}^{z}_{s}\right)^{2}}}\right)^{1/2}. \end{aligned} \tag{17}$$

One should note that the symbols A and B that appear as indices of the new quasiparticle operators $\tilde{a}_{\mathbf{k}l\sigma A}$ and $\tilde{a}_{\mathbf{k}l\sigma B}$ single out the new, hybridized, quasiparticle subbands and do not correspond to the sublattices indices A and B as in the case of operators $a_{\mathbf{k}l\sigma A}$ and $a_{\mathbf{k}l\sigma B}$. The dispersion relations in the new quasiparticle representation acquire the form

$$\begin{aligned} \tilde{\epsilon}_{\mathbf{k}1A} &= -\sqrt{(\epsilon_{\mathbf{k}} + \epsilon_{\mathbf{k}12})^{2} + \left(I\bar{S}^{z}_{s}\right)^{2}}, \\ \tilde{\epsilon}_{\mathbf{k}1B} &= \sqrt{(\epsilon_{\mathbf{k}} + \epsilon_{\mathbf{k}12})^{2} + \left(I\bar{S}^{z}_{s}\right)^{2}}, \\ \tilde{\epsilon}_{\mathbf{k}2A} &= -\sqrt{(\epsilon_{\mathbf{k}} - \epsilon_{\mathbf{k}12})^{2} + \left(I\bar{S}^{z}_{s}\right)^{2}}, \\ \tilde{\epsilon}_{\mathbf{k}2B} &= \sqrt{(\epsilon_{\mathbf{k}} - \epsilon_{\mathbf{k}12})^{2} + \left(I\bar{S}^{z}_{s}\right)^{2}}. \end{aligned} \tag{18}$$

As one can see, the new dispersion relations do not depend on the spin quantum numbers of the quasiparticle. In general, if $\epsilon_{\mathbf{k}12}$ is not $\sim \epsilon_{\mathbf{k}}$, we may have four nondegenerate Slater subbands, which is not the case considered here. To express the pairing operators that are present in the Hamiltonian (11) in terms of the new quasiparticle operators, one can use relations (16) and the definitions (4). The explicit form of the original pairing operators in terms of the newly created quasiparticle operators is provided in Appendix A.

B. Quasiparticle states for the coexistent antiferromagnetic and superconducting phases

In the second step of the diagonalization of (11), a generalized Nambu–Bogoliubov–de Gennes scheme is introduced to write the complete HF Hamiltonian again in the matrix form, which allows for an easy determination of its eigenvalues. With the help of composite creation operator $\tilde{\mathbf{f}}^{\dagger}_{\mathbf{k}\sigma} \equiv (\tilde{a}^{\dagger}_{\mathbf{k}1\sigma A}, \tilde{a}_{-\mathbf{k}2\sigma A}, \tilde{a}^{\dagger}_{\mathbf{k}1\sigma B}, \tilde{a}_{-\mathbf{k}2\sigma B})$, we can construct this new 4×4 Hamiltonian matrix and write

$$\begin{aligned} \hat{H}_{\mathrm{HF}} - \mu\hat{N} = \sum_{\mathbf{k}\sigma} \tilde{\mathbf{f}}^{\dagger}_{\mathbf{k}\sigma} \mathbf{H}_{\mathbf{k}\sigma} \tilde{\mathbf{f}}_{\mathbf{k}\sigma} + 2\sum_{\mathbf{k}} (\tilde{\epsilon}_{\mathbf{k}2A} + \tilde{\epsilon}_{\mathbf{k}2B}) \\ - 2\mu N + C, \end{aligned} \tag{19}$$

with

$$\mathbf{H}_{\mathbf{k}\sigma} \equiv \begin{pmatrix} \tilde{\epsilon}_{\mathbf{k}1A} - \mu & \delta_{1\mathbf{k}\sigma} & 0 & \delta_{3\mathbf{k}\sigma} \\ \delta^{*}_{1\mathbf{k}\sigma} & -\tilde{\epsilon}_{\mathbf{k}2A} + \mu & \delta_{4\mathbf{k}\sigma} & 0 \\ 0 & \delta^{*}_{4\mathbf{k}\sigma} & \tilde{\epsilon}_{\mathbf{k}1B} - \mu & \delta_{2\mathbf{k}\sigma} \\ \delta^{*}_{3\mathbf{k}\sigma} & 0 & \delta^{*}_{2\mathbf{k}\sigma} & -\tilde{\epsilon}_{\mathbf{k}2B} + \mu \end{pmatrix} \tag{20}$$

and $\tilde{\mathbf{f}}_{\mathbf{k}} \equiv (\tilde{\mathbf{f}}^{\dagger}_{\mathbf{k}})^{\dagger}$. The parameters $\delta_{l\mathbf{k}\sigma}$ are defined as follows:

$$\begin{aligned} \delta_{1\mathbf{k}\sigma} &= \Delta_{\sigma A} U^{+}_{\mathbf{k}\sigma} U^{-}_{\mathbf{k}\sigma} + \Delta_{\sigma B} V^{+}_{\mathbf{k}\sigma} V^{-}_{\mathbf{k}\sigma}, \\ \delta_{2\mathbf{k}\sigma} &= \Delta_{\sigma A} V^{+}_{\mathbf{k}\sigma} V^{-}_{\mathbf{k}\sigma} + \Delta_{\sigma B} U^{-}_{\mathbf{k}\sigma} U^{+}_{\mathbf{k}\sigma}, \\ \delta_{3\mathbf{k}\sigma} &= -\Delta_{\sigma A} U^{+}_{\mathbf{k}\sigma} V^{-}_{\mathbf{k}\sigma} + \Delta_{\sigma B} U^{-}_{\mathbf{k}\sigma} V^{+}_{\mathbf{k}\sigma}, \\ \delta_{4\mathbf{k}\sigma} &= -\Delta_{\sigma A} V^{+}_{\mathbf{k}\sigma} U^{-}_{\mathbf{k}\sigma} + \Delta_{\sigma B} V^{-}_{\mathbf{k}\sigma} U^{+}_{\mathbf{k}\sigma}. \end{aligned} \tag{21}$$

Constant C contains the last two terms of the right-hand side of expression (11). Hamiltonian (19) and matrix (20) have been written under the assumption that $\Delta_{0A} = \Delta_{0B} \equiv 0$. Calculations for the more general case of nonzero gap parameters for $m = 0$ have been also done, but no stable coexisting superconducting and antiferromagnetic solutions have been found numerically. The only coexisting solutions that have been found fulfill the relation $\Delta_{0A} = \Delta_{0B} \equiv 0$. This fact can be understood by the following argument. As in the antiferromagnetic state, all lattice sites have nonzero magnetic moment, the Cooper pairs in the spin-triplet state for $m = 0$ (i.e., with the total spin $S^{z} = 0$, corresponding $\langle \hat{A}_{\mathbf{k}0} \rangle$) are not likely to appear. Nevertheless, we present the matrix form of the Hamiltonian (11) for the mentioned most general case in Appendix A. In our considerations here, we limit also to the situation with the real gap parameters $\Delta^{*}_{\pm 1A(B)} = \Delta_{\pm 1A(B)}$. Then, the straightforward diagonalization of (20) yields to the following Hamiltonian:

$$\begin{aligned} \hat{H}_{\mathrm{HF}} - \mu\hat{N} = \sum_{\mathbf{k}l\sigma} (-1)^{l+1} (\lambda_{\mathbf{k}l\sigma A} \alpha^{\dagger}_{\mathbf{k}l\sigma A} \alpha_{\mathbf{k}l\sigma A} \\ + \lambda_{\mathbf{k}l\sigma B} \alpha^{\dagger}_{\mathbf{k}l\sigma B} \alpha_{\mathbf{k}l\sigma B}) + 2\sum_{\mathbf{k}} (\tilde{\epsilon}_{\mathbf{k}2A} + \tilde{\epsilon}_{\mathbf{k}2B}) \\ + \sum_{\mathbf{k}\sigma} (\lambda_{\mathbf{k}2\sigma\mathbf{A}} + \lambda_{\mathbf{k}2\sigma\mathbf{B}}) - 2\mu N + C, \end{aligned} \tag{22}$$

where $\lambda_{\mathbf{k}l\sigma A(B)}$ are the eigenvalues of the matrix (20) and $\alpha_{\mathbf{k}l\sigma A(B)}$ ($\alpha^{\dagger}_{\mathbf{k}l\sigma A(B)}$) are the quasiparticle annihilation (creation) operators, related to the original annihilation and creation operators $\tilde{a}_{\mathbf{k}l\sigma}$, $\tilde{a}^{\dagger}_{\mathbf{k}l\sigma}$ from the first step of our diagonalization, via generalized Bogoliubov transformation of the form

$$\tilde{\mathbf{f}}_{\mathbf{k}\sigma} = \mathbf{U}^{\dagger}_{\mathbf{k}\sigma} \mathbf{g}_{\mathbf{k}\sigma}, \tag{23}$$

with $\mathbf{g}^{\dagger}_{\mathbf{k}\sigma} \equiv (\alpha^{\dagger}_{\mathbf{k}1\sigma A}, \alpha_{-\mathbf{k}2\sigma A}, \alpha^{\dagger}_{\mathbf{k}1\sigma B}, \alpha_{-\mathbf{k}2\sigma B})$. Eigenvectors of the Hamiltonian matrix (20) are the columns of the diagonalization matrix $\mathbf{U}^{\dagger}_{\mathbf{k}}$. Using the definitions of gap parameters $\Delta_{\pm 1A}$, $\Delta_{\pm 1B}$, the average number of particles per atomic site $n = \sum_{l} \langle \hat{n}_{il\uparrow A} + \hat{n}_{il\downarrow A} \rangle$, and the average magnetic moment per band per site $\bar{S}^{z} = \langle \hat{n}_{il\uparrow A} - \hat{n}_{il\downarrow A} \rangle / 2$, we can construct the set of self-consistent equations for the mean-field parameters

$(\Delta_{\pm 1A},\ \Delta_{\pm 1B},\ \bar{S}^z)$ and for the chemical potential. The averages that appear in the set of self-consistent equations $\langle \alpha^{\dagger}_{\mathbf{k}l\sigma A(B)} \alpha_{\mathbf{k}l\sigma A(B)} \rangle$ can be replaced by the corresponding Fermi distribution functions

$$f[(-1)^{l+1}\lambda_{\mathbf{k}l\sigma A(B)}] = 1/\{\exp[\beta(-1)^{l+1}\lambda_{\mathbf{k}l\sigma A(B)}] + 1\}, \quad (24)$$

where $\beta = 1/k_B T$. The eigenvalues and the eigenvectors of (20) are evaluated numerically while executing the numerical procedure of solving the set of self-consistent equations. For a given set of microscopic parameters n, J, U, U', and temperature T, the set of self-consistent equations has several solutions that correspond to different phases.[16–18] Free energy can be evaluated for each of the solutions that have been found, and the one that corresponds to the lowest value of the free energy is regarded as the stable phase. The expression for the free-energy functional in the considered case has the form

$$\begin{aligned} F = &-\frac{1}{\beta}\sum_{\mathbf{k}l\sigma}[\ln(1+\exp[-\beta(-1)^{l+1}\lambda_{\mathbf{k}l\sigma A}]) \\ &+ \ln(1+\exp[-\beta(-1)^{l+1}\lambda_{\mathbf{k}l\sigma B}])] \\ &+ 2\sum_{\mathbf{k}}(\tilde{\epsilon}_{\mathbf{k}2A} + \tilde{\epsilon}_{\mathbf{k}2B}) + \sum_{\mathbf{k}\sigma}(\lambda_{\mathbf{k}2\sigma A} \\ &+ \lambda_{\mathbf{k}2\sigma B}) - \mu(2-n)N + C. \end{aligned} \quad (25)$$

Numerical results are carried out for square lattice with nonzero hopping t between the nearest neighbors only. The described above numerical scheme is executed for the following selection of phases:

(i) normal state (NS): $\Delta_{\pm 1A(B)} = 0$, $\bar{S}^z_s = 0$,

(ii) pure superconducting phase type A (A): $\Delta_{\pm 1A(B)} \equiv \Delta \neq 0$, $\bar{S}^z_s = 0$,

(iii) pure antiferromagnetic phase (AF): $\Delta_{\pm 1A(B)} = 0$, $\bar{S}^z_s \neq 0$,

(iv) coexistent superconducting and antiferromagnetic phase (SC + AF): $\Delta_{\pm 1A(B)} \neq 0$, $\bar{S}^z_s \neq 0$.

The ferromagnetically ordered phases, which will also be included in our considerations in the following sections, are listed below:

(a) pure saturated ferromagnetic phase (SFM): $\Delta_{\pm 1A(B)} = 0$, $\bar{S}^z_u = \bar{S}^z_{u(\max)} \neq 0$,

(b) pure nonsaturated ferromagnetic phase (FM): $\Delta_{\pm 1A(B)} = 0$, $0 < \bar{S}^z_u < \bar{S}^z_{u(\max)}$,

(c) saturated ferromagnetic phase coexistent with superconductivity of type A1 (A1 + SFM): $\Delta_{1A(B)} \equiv \Delta_1 \neq 0$, $\Delta_{-1A(B)} = 0$, $\bar{S}^z_u = \bar{S}^z_{u(\max)} \neq 0$,

(d) nonsaturated ferromagnetic phase coexistent with superconductivity of type A1 (A1 + FM): $\Delta_{1A(B)} \equiv \Delta_1 \neq 0$, $\Delta_{-1A(B)} = 0$, $0 < \bar{S}^z_u < \bar{S}^z_{u(\max)}$.

It should be noted that $\bar{S}^z_u$ refers to the uniform magnetic moment per band per site in the ferromagnetically ordered phases, whereas $\bar{S}^z_s$ is the staggered magnetic moment that corresponds to the antiferromagnetic phases. One could also consider the so-called superconducting phase of type B for which all superconducting gaps (including $\Delta_{0A(B)}$) are equal and different from zero. However, this phase never coexists with magnetic ordering. What is more important in the absence of magnetic ordering the superconducting phase A has always lower free energy than the B phase. Therefore, the superconducting B phase is absent in the following discussion.

III. RESULTS AND DISCUSSION

We assume that $U' = U - 2J$ and $U = 2.2J$, so there are actually two independent parameters in the considered model: n and J. The energies have been normalized to the bare bandwidth $W = 8|t|$, and T expresses the reduced temperature $T \equiv k_B T/W$.

A. Overall phase diagram: Coexistent magnetic-paired states

In Figs. 1(a)–1(d), we present the complete phase diagrams in coordinates (n, J) for different values of the hybridization parameter β_h. They comprise sizable regions of stable spin-triplet superconducting phase coexisting with either ferromagnetism or antiferromagnetism, as well as pure superconducting phase A. In the phase SC + AF, the calculated gap parameters fulfill the relations

$$\begin{aligned} \Delta_{+1A} = \Delta_{-1B} \equiv \Delta_+, \\ \Delta_{-1A} = \Delta_{+1B} \equiv \Delta_-, \\ \Delta_+ > \Delta_-. \end{aligned} \quad (26)$$

For the singlet paired state, one would have $\Delta_{+1A} = -\Delta_{-1A}$, which is not the case here. For the case of half-filled band $n = 2$, the superconducting gaps Δ_+ and Δ_- vanish and only pure (Slater-type) AF survives. The appearance of the AF state for $n = 2$ corresponds to the fact that the bare Fermi-surface topology has a rectangular structure with $Q = (\pi, \pi)$ nesting. This feature survives also for $\beta_h \neq 0$. Also, the symmetry of the phase diagrams with respect to half-filled band situation is a manifestation of the particle-hole symmetry since the bare density of states is symmetric with respect to the middle point of the band. This feature of the problem provides an additional test for the correctness of the numerical results.

It is clearly seen from the presented figures that the influence of hybridization is significant quantitatively when it comes to the superconducting phase A, as the region of its stability narrows down rapidly with the increase of β_h. The stability areas of A1 + FM and NS phases expand on the expense of A and A1 + SFM phases. With the further increase of the hybridization, the stability of A phase is completely suppressed, as shown in Fig. 1(d). The regions of stable antiferromagnetically ordered phase do not alter significantly with the increasing hybridization. To relate the appearance of superconductivity with the onset of ferromagnetism, we have marked explicitly in Fig. 2 the Stoner threshold on the phase diagram. One sees clearly that only the A1 phase appearance is related to the onset of ferromagnetism. What is more important, the FM phase coexisting with the paired A1 phase becomes stable for slightly lower J values than the Stoner threshold for appearance of pure FM phase. The A1 + FM coexistence near the Stoner threshold can be analyzed by showing explicitly the magnetization and superconducting gap evolution with increasing J. This is shown in Figs. 3 and 4. One sees explicitly that the nonzero magnetization appears slightly below the Stoner threshold and is thus induced by the onset of

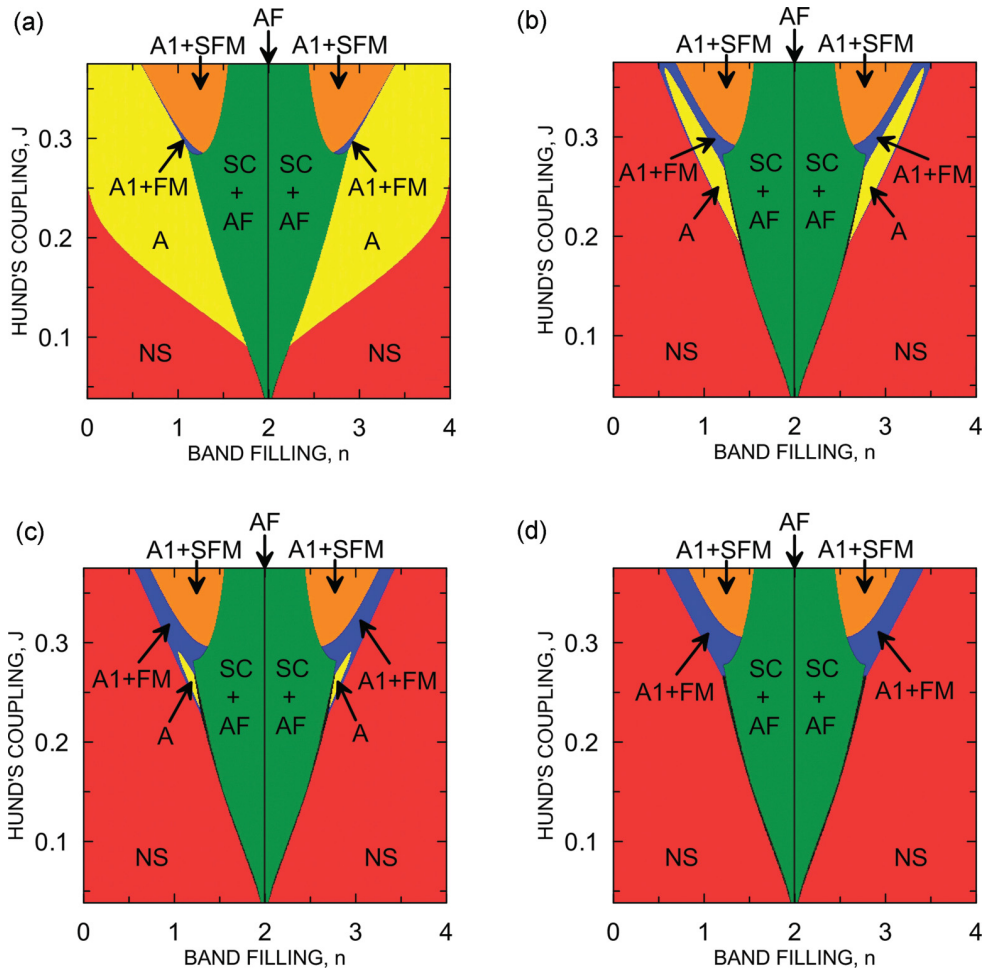

FIG. 1. (Color online) Phase diagrams in space (n, J) for $T = 10^{-4}$ and for different values of the β_h parameter: (a) $\beta_h = 0.00$, (b) $\beta_h = 0.04$, (c) $\beta_h = 0.06$, (d) $\beta_h = 0.11$. Labels representing different phases are described in the main text. One sees that practically all magnetic phases here are in fact the coexistent phases with superconductivity except the half-filled situation where we have pure AF phase.

A1 paired state. In other words, superconductivity enhances magnetism. But the opposite is also true, i.e., the gap increases rapidly in this regime, where magnetization changes. The situation is preserved for nonzero hybridization. The transition A$\rightarrow$A1 + FM is sharp, as detailed free-energy plot shows. For $\beta_h = 0.11$ in a certain range of J, the superconducting solutions A1 + FM and A can not be found by the numerical procedure. That is why the curves representing the gap parameters Δ and free energy suddenly break. The most important and surprising conclusion is that in the A1 + FM phase, only the electrons in spin-majority subband are paired. This conclusion may have important practical consequences for spin filtering across NS/A1 + FM interface, as discussed at the end. Nevertheless, one should note that the partially polarized (FM) state appears only in a narrow window of J values near the Stoner threshold, at least for the selected density of states.

Summarizing, we have supplemented the well-known magnetic phase diagrams with the appropriate stable and spin-triplet paired states. A relatively weak hybridization of band states destabilizes pure paired states but stabilizes coexistent superconducting-magnetic phases except for the half-filled band case, when the appearance of the Slater gap at the Fermi level excludes any superconducting state. A very interesting phenomenon of pairing for one-spin (majority) electrons occurs near the Stoner threshold for the onset of FM phase and extends to the regime slightly below threshold.

B. Detailed physical properties

In Figs. 5 and 6, we show the low-temperature values of superconducting gaps and the staggered magnetic moment as a function of band filling. In the SC + AF phase, both gap parameters Δ_+ and Δ_- decrease continuously to zero as the system approaches the half-filling. On the contrary, the staggered magnetic moment $\bar{S}_s^z$ reaches then the maximum. For the case of $\beta_h = 0.0$, below the critical value of band filling $n_c \approx 1.45$, the gap parameters Δ_+ and Δ_- are equal and the staggered magnetic moment vanishes. In this regime, the superconducting phase of type A is the stable one. For the A phase, the superconducting gap decreases with the band-filling

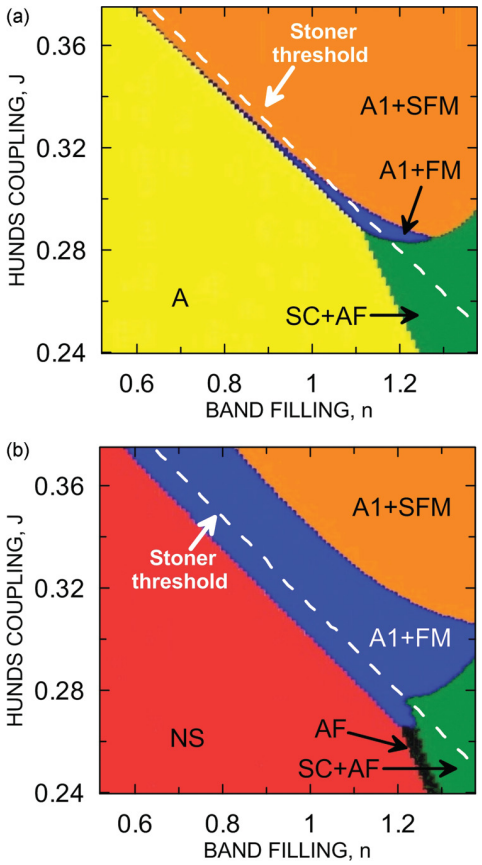

FIG. 2. (Color online) Phase diagrams zoomed in space (n, J) with the dashed line marking the Stoner threshold for the onset of pure ferromagnetism. The values of the hybridization parameter are β_h: (a) $\beta_h = 0.00$, (b) $\beta_h = 0.11$, while the temperature is $T = 10^{-4}$.

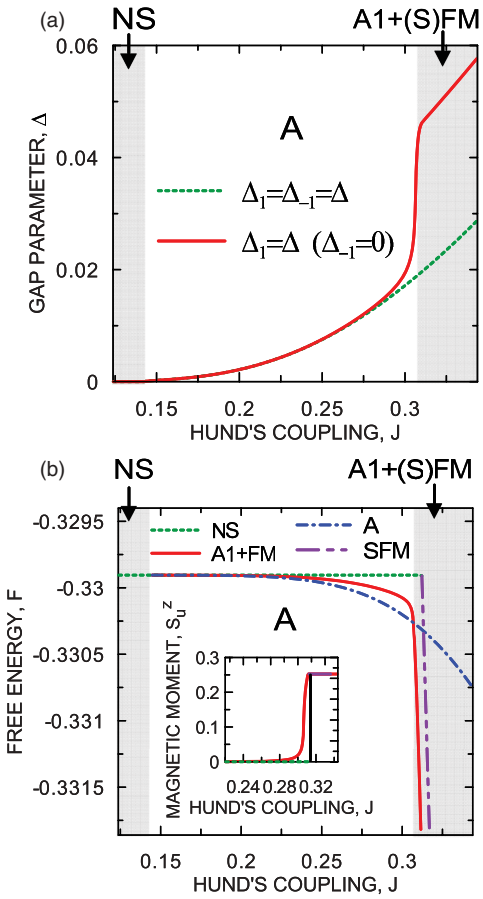

FIG. 3. (Color online) Magnetic moment (per orbital per site), ground-state energy, and superconducting gap as a function of J near the Stoner threshold for $n = 1$ and $\beta_h = 0.0$. Black vertical line in the inset marks the onset of saturated magnetism at the Stoner threshold.

decrease and becomes zero for some particular value of n. Below that value, the NS (paramagnetic state) is stable. It is clearly seen that the appearance of two gap parameters above n_c is connected with the onset of the staggered-moment structure, as above n_c we have $S_s^z \neq 0$ [cf. Fig. 5(b)]. For comparison, we also show the staggered moment for pure AF in Figs. 5(b) and 6(b) (dashed line). As one can see, the appearance of SC increases slightly the staggered moment in SC + AF phase. For $\beta_h = 0.11$ below some critical value of band filling $n_c \approx 1.473$ in a very narrow range of n, a pure AF phase is stable. The inset in Fig. 6(a) shows that there is a weak first-order transition between the AF + SC and SC phases as a function of doping. The A phase is not stable in this case.

One should mention that the easiness with which the superconducting triplet state is accommodated within the antiferromagnetic phase stems from the fact that the SC gaps have an intra-atomic origin and the corresponding spins have then the tendency to be parallel. Therefore, the pairs respect the Hund's rule and do not disturb largely the staggered-moment structure, which is of interatomic character.

In Fig. 7,we show temperature dependence of the free energy for the six considered phases for the set of microscopic parameters selected to make the SC + AF phase stable at $T = 0$ and for $\beta_h = 0$. Because the free-energy values of the A and NS phases are very close, we exhibit their temperature dependencies zoomed in Fig. 7(b). The same is done for the free energy of phases A1 + FM and FM. For the same values of n, J, U, and U', the temperature dependence of the superconducting gaps and the staggered magnetic moment in SC + AF phase are shown in Fig. 8 for selected β_h values. For given β_h below the superconducting critical temperature T_S, the staggered magnetic moment and the superconducting gaps have all nonzero values, which means that we are dealing with the coexistence of superconductivity and antiferromagnetism in this range of temperatures. Both Δ_+ and Δ_- vanish at T_S, while the staggered magnetic moment vanishes at the Néel temperature $T_N \gg T_S$. In Fig. 9, one can observe that there are two typical mean-field discontinuities in the specific heat at T_S and T_N for a given β_h. The first of them, at T_S, corresponds to the phase transition from the SC + AF phase to the pure AF phase, while the second, at T_N, corresponds to the transition from the AF phase to the NS phase. The values of the ratios of the specific heat jump $(\Delta c/c_N)$ at T_C that correspond to $\beta_h = 0.0, 0.4, 0.6$ are 15.075, 16.298, 17.375, respectively. No antiferromagnetic gap is created since we have

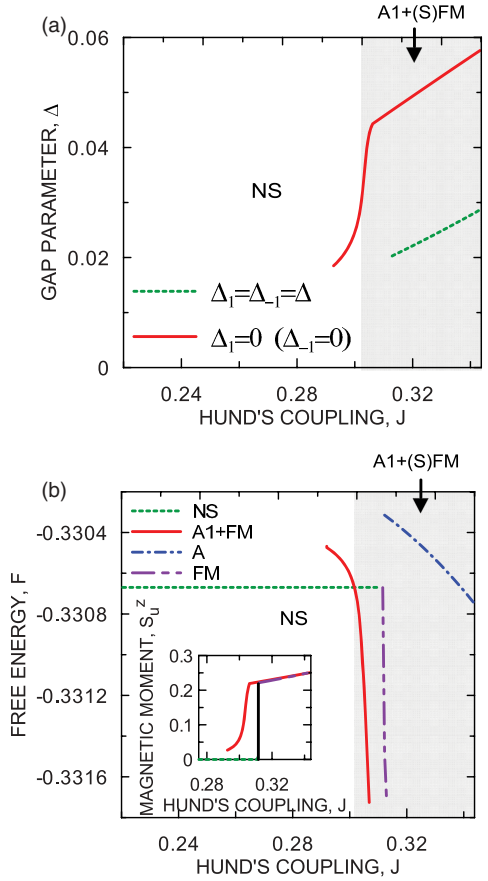

FIG. 4. (Color online) Magnetic moment (per orbital per site), ground-state energy, and superconducting gap as a function of J near the Stoner threshold for $n = 1$ and $\beta_h = 0.11$. Black vertical line in the inset marks the onset of magnetism at the Stoner threshold.

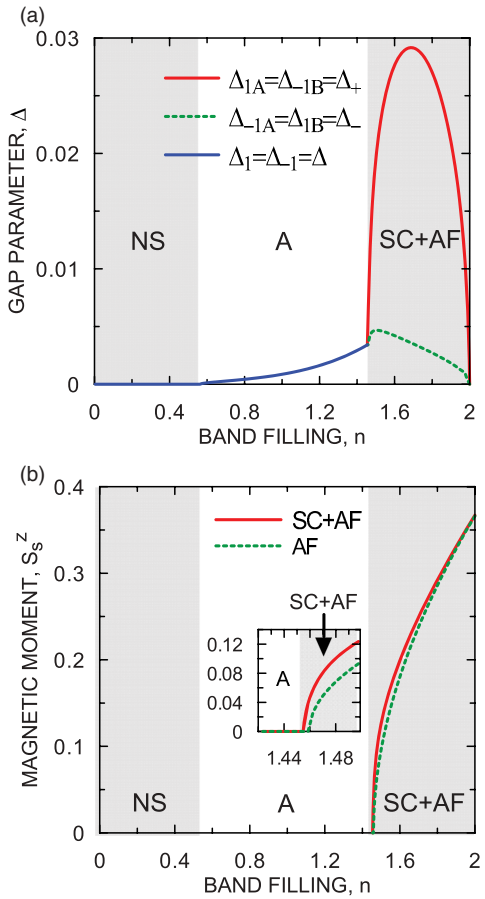

FIG. 5. (Color online) Low-temperature values of the superconducting gaps and the staggered magnetic moment both as a function of band filling for $\beta_h = 0$ and $J = 0.175$. The stable phases are appropriately labeled in the regimes of their stability. Note that $\Delta_- \ll \Delta_+$, i.e., the paired state is closer to A1 state than to A state in the coexistent regime.

number of electrons $n < 2$. The specific-heat discontinuity at the AF transition is due to the change of spin entropy near T_N. For $n = 2$, the formation of the Slater gap at T_N makes the superconducting transition to disappear. As one can see form Figs. 8 and 9, with the increase of β_h, the critical temperature T_S is decreasing slightly, while the Néel temperature increases, but the ratio remains almost fixed, $T_N/T_C \approx 10$.

Temperature dependence of free energies of relevant phases are presented in Fig. 10 ($\beta_h = 0$) for the microscopic parameters selected to make the A1 + FM phase stable at $T = 0$. Free energies for A and A1 + FM phases are drawn only in the low-T regime [Fig. 10(b)] for the sake of clarity. The corresponding temperature dependence of the superconducting gaps, magnetic moment, and specific heat in A1 + FM phase for three selected values of β_h are shown in Fig. 11. Analogously as in the SC + AF case, the system undergoes two phase transitions. The influence of hybridization on the temperature dependencies is also similar to that in the case of coexistence of superconductivity with antiferromagnetism. With the increasing β_h, the critical temperature T_S is decreasing slightly, whereas the Curie temperature T_C is slightly increasing, but still $T_C/T_S \approx 5$. The values of the ratios of the specific heat jump $(\Delta c/c_N)$ at T_C that correspond to $\beta_h = 0.0$, 0.2, 0.4 are 1.329, 1.421, 0.793, respectively.

For the sake of completeness, in Fig. 12 we provide the temperature dependence of superconducting gap for the values of parameters that correspond to stable pure superconducting phase of type A at $T = 0$ and for three different values of β_h. In this case, neither the antiferromagnetically ordered nor the pure ferromagnetic phases exist. As in previous cases, the increasing hybridization decreases T_S. It should be noted that the values of β_h are very close to zero. This is necessary to assume for the A phase to appear. The values of the ratios of the specific heat jump $(\Delta c/c_N)$ at T_C that correspond to $\beta_h = 0.0$, 0.035, 0.006 are 1.382, 1.326, 1.202, respectively.

In Table I we have assembled the exemplary values of mean-field parameters, chemical potential, as well as free energy for two different sets of values of microscopic parameters corresponding to the low-temperature stability of two considered here superconducting phases: SC + AF and A1 + FM. For the two sets of values of n and J, the free-energy

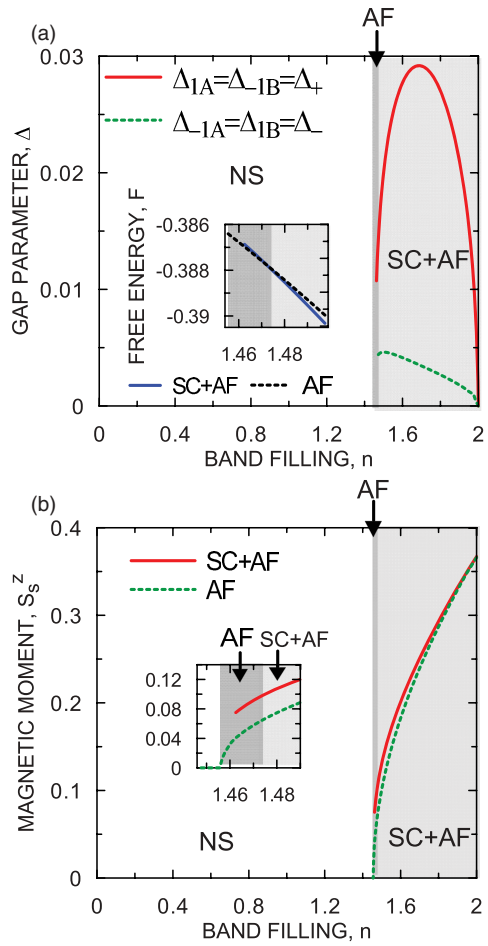

FIG. 6. (Color online) Low-temperature values of the superconducting gaps and the staggered magnetic moment as a function of band filling for $\beta_h = 0.11$ and $J = 0.175$. Note the disappearance of the pure A phase and that again $\Delta_- \ll \Delta_+$. The inset in (b) illustrates the fact that a pure AF phase appears in a very narrow regime of n before the SC + AF phase becomes stable, whereas the inset in (a) shows the free energy of those two phases for n close to n_C when a weak first-order transition occurs.

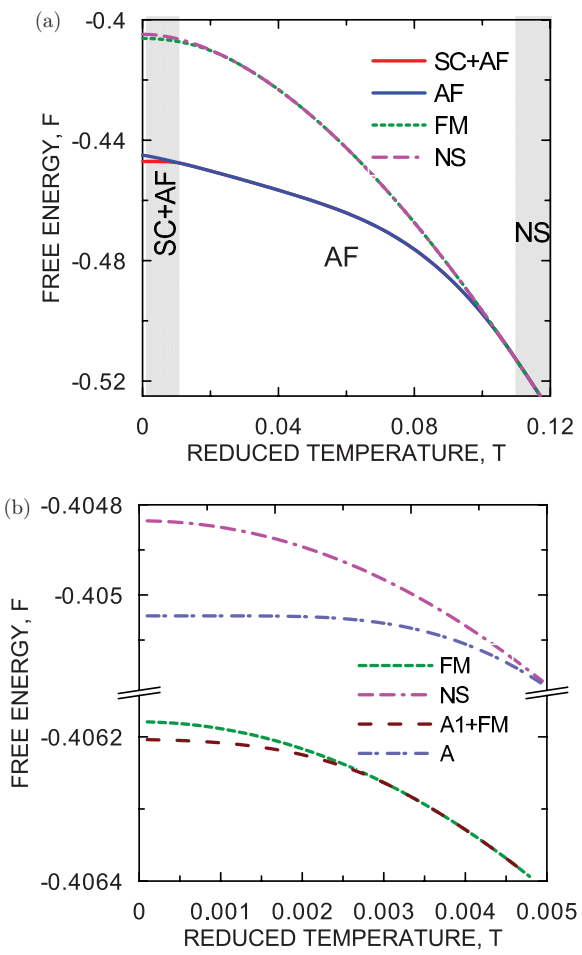

FIG. 7. (Color online) (a) Temperature dependence of the free energy for considered phases for $n = 1.9$ and $J = 0.175$ when the SC + AF phase is stable at $T = 0$. The free-energy values of A and NS phases are very close, so we exhibit their temperature dependence blown up in part (b).

difference between the stable and first unstable phases is of order 10^{-3}. The values for the stable phases are underlined.

IV. CONCLUSIONS AND OUTLOOK

We have carried out the Hartree-Fock-BCS analysis of the hybridized two-band Hubbard model with the Hund's-rule induced magnetism and spin-triplet pairing. We have determined the regions of stability of the spin-triplet paired phases with $\Delta_0 \equiv 0$, coexisting with either ferromagnetism (A1 + FM) or antiferromagnetism (SC + AF), as well as pure paired phase (A). We have analyzed in detail the effect of interband hybridization on stability of the those phases. The hybridization reduces significantly the stability regime of the superconducting phase A, mainly in favor of the paramagnetic (normal) phase NS. For a large enough value of β_h ($\beta_h >$ 0.08), the A phase disappears altogether. When it comes to magnetism, with the increase of β_h, the stability regime of the saturated ferromagnetically ordered phase is reduced in favor of the nonsaturated. The influence of the hybridization on the low-temperature stability of the SC + AF phase is not significant. When the system is close to the half-filling, the SC + AF phase is the stable one. However, for the half-filled band case ($n = 2$), the superconductivity disappears and only pure antiferromagnetic state survives since the nesting effect of the two-dimensional band structure prevails then.

We have also examined the temperature dependence of the order parameters and the specific heat. For both coexistent superconducting and magnetically ordered phases (SC + AF and A1 + FM), one observes two separate phase transitions with the increasing temperature. The first of them, at substantially lower temperature (T_S), is the transition from the superconducting-magnetic coexistent phase to the pure magnetic phase and the second, occurring at much higher temperature (T_N or T_C), is from the magnetic to the paramagnetic phase (NS). The hybridization has a negative influence on the spin-triplet superconductivity since it reduces the critical temperature for each type of the spin-triplet superconducting phase considered here. On the other hand, the Curie (T_C) and

the Néel (T_N) temperatures are increasing with the increase of the β_h parameter, as it generally increases the density of states at the Fermi level (for appropriate band fillings).

One should note that since the pairing is intra-atomic in nature, the spin-triplet gaps Δ_m are of the s type. This constitutes one of the differences with the corresponding situation for superfluid ^{3}He, where they are of p type.[8]

It is also important to note that the paired state appears both below and above the Stoner threshold for the onset of ferromagnetism (cf. Fig. 2), although its nature changes (A and A1 states, respectively). In the ferromagnetically ordered phase, only the spin-majority carriers are paired. This is not the case for the AF + SC phase. It would be very interesting to try to detect such highly unconventional SC phase. In particular, the Andreev reflection and, in general, the NS/SC conductance spectroscopy will have an unusual character. We should see progress along this line of research soon.

As mentioned before, all the results presented in the previous section have been obtained assuming that $U = 2.2J$ and $U' = U - 2J$. Having said that, the value of $J^H = J - U'$ determines the strength of the pairing mechanism, while $I = U + J$ is the effective magnetic coupling constant, one

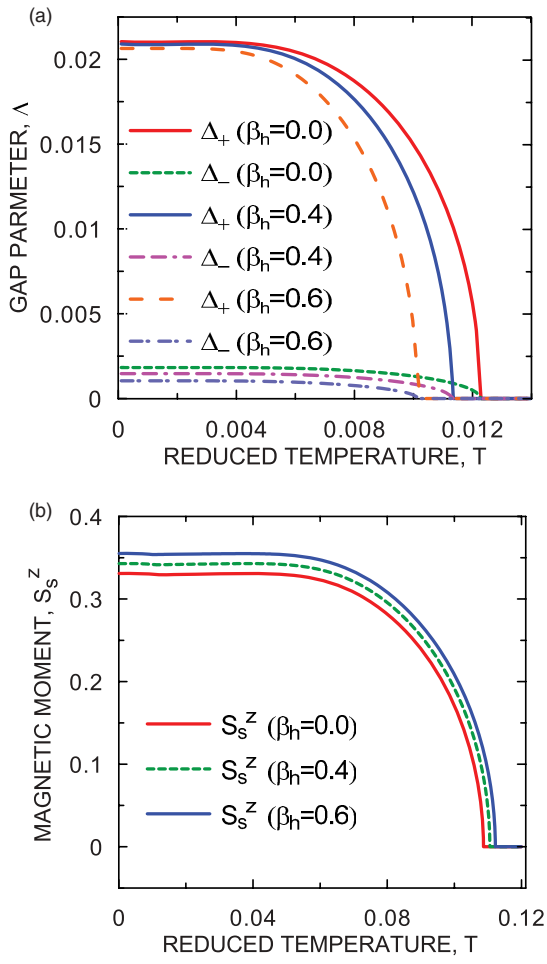

FIG. 8. (Color online) Temperature dependencies of the superconducting gaps Δ_+, Δ_- and of the staggered magnetic moment for $n = 1.9$, $J = 0.175$ and for selected values of the β_h parameter. Note that $T_S \ll T_N$.

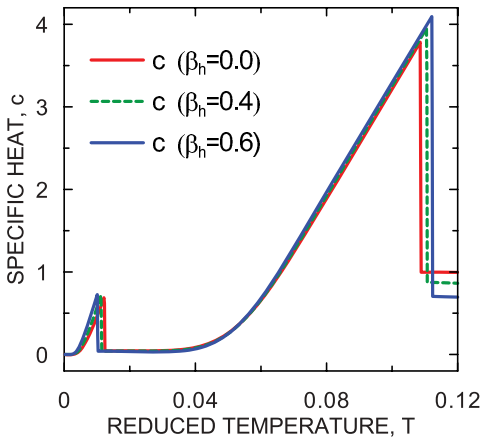

FIG. 9. (Color online) Temperature dependence of the specific heat for $n = 1.9$, $J = 0.175$, and for selected values of β_h parameter. The behavior is almost independent of β_h value and the ratio $T_N/T_S \approx 10$.

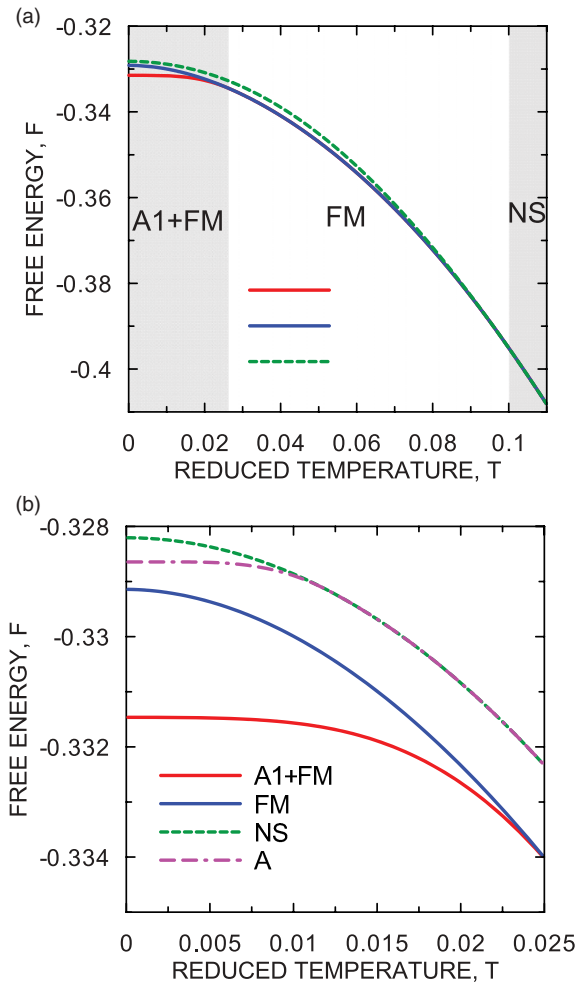

FIG. 10. (Color online) Temperature dependence of the free energy for $n = 1.0$ and $J = 0.31625$ when the A1 + FM phase is stable at $T = 0$. AF phases do not appear in this case. Free energies for A and A1 + FM phases are shown in the low-T regime (b) for the sake of clarity.

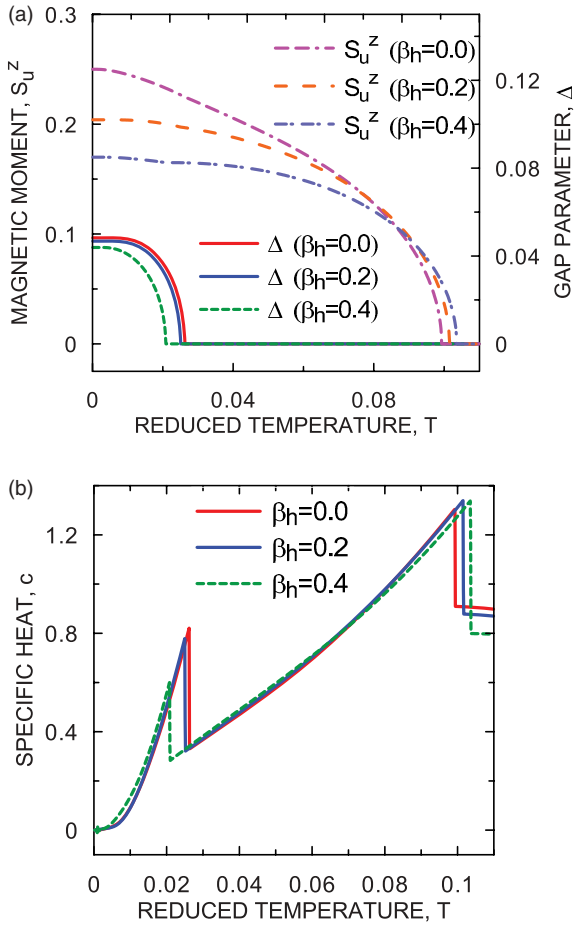

FIG. 11. (Color online) Temperature dependence of the superconducting gaps Δ_+, Δ_-, magnetic moment (a), and specific heat (b) for $n = 1.0$, $J = 0.31625$, and for selected values of β_h. Qualitative features do not alter appreciably even for $\beta_h = 0.4$. The ratio $T_C/T_S \approx 5$.

can roughly predict how will the change in the relations between U, U', and J result. It seems reasonable to say that the larger J is with respect to U', the stronger the superconducting gap in the paired phases. This would also result in the increase of T_C and a corresponding enlargement of the area occupied by the superconducting phases on the diagrams. Furthermore, the increase of U with respect to J should result in the increase of the ratios T_C/T_S and T_N/T_S. This is because in that manner we make the magnetic coupling stronger with respect to the pairing. If we, however, increase U but do not change J^H, then the strength of the pairing would be the same but the magnetic coupling constant would be stronger so this would favor the coexistent magnetic and superconducting phases with respect to the pure superconducting phase. Quite a stringent necessary condition for the pairing to appear $J > U'$ (equivalent to $3J > U$ if we assume $U' = U - 2J$, as has been done here) indicates that only in specific materials one would expect for the Hund's rule to create the superconducting phase. This may explain why only in very few compounds the coexistent ferromagnetic and superconducting phase has been indeed observed. Obviously, one still has to add the paramagnon pairing (cf. Appendix C).

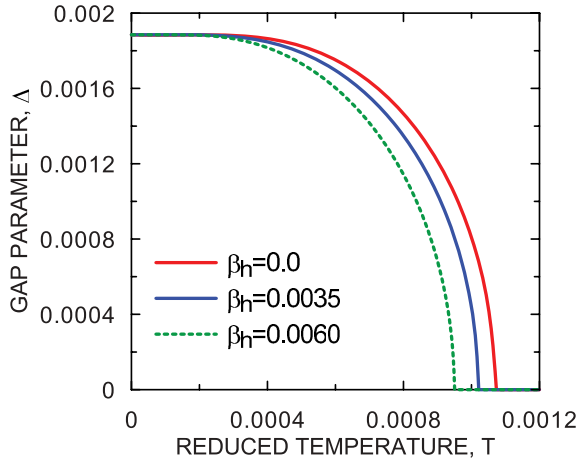

FIG. 12. (Color online) Temperature dependencies of the superconducting gaps Δ_+, Δ_- (a), and the specific heat (b) for $n = 1.25$, $J = 0.175$, and for selected values of β_h parameter.

It should be noted that more exotic magnetic phases may appear in the two-band model.[19] Here, we neglect those phases because of two reasons. First the lattice selected for analysis is bipartite, with strong nesting (AF tendency). Second the additional ferrimagnetic, spiral, etc., phase might appear if we assumed that the second hopping integral $t' \neq 0$. Inclusion of t' would require a separate analysis, as the lattice becomes frustrated then.

TABLE I. Exemplary values of the mean-field parameters, the chemical potential, and the free energy of the considered phases at $T = 10^{-4}$ for two different sets of values of microscopic parameters: n, J. The underlined values correspond the stable phases. The numerical accuracy is better than the last digit.

Parameter	Phase	$n = 1.9$ $J = 0.175$	$n = 1.0$ $J = 0.31625$
Δ	A	0.0097911	0.0208481
Δ	A1 + FM	0.0056821	<u>0.0482677</u>
Δ_+	SC + AF	<u>0.0210081</u>	
Δ_-	SC + AF	<u>0.0017366</u>	
S_u^z	A1 + (S)FM	0.1134254	<u>0.2500000</u>
S_u^z	(S)FM	0.1144301	0.2500000
S_s^z	SC + AF	<u>0.3340563</u>	
S_s^z	AF	0.3314687	
μ	A	−0.0107669	−0.1815757
μ	NS	−0.0094009	−0.1799612
μ	A1 + (S)FM	−0.0175982	<u>−0.2530000</u>
μ	(S)FM	−0.0178066	−0.253000
μ	SC + AF	<u>−0.1708890</u>	
μ	AF	−0.1859011	
F	A	−0.4050464	−0.3286443
F	NS	−0.4048522	−0.3282064
F	A1 + (S)FM	−0.4062039	<u>−0.3314652</u>
F	(S)FM	−0.4061793	−0.3291425
F	SC + AF	<u>−0.4489338</u>	
F	AF	−0.4469097	

ACKNOWLEDGMENTS

M.Z. has been partly supported by the EU Human Capital Operation Program, Polish Project No. POKL.04.0101-00-434/08-00. J.S. acknowledges the financial support from the Foundation for Polish Science (FNP) within project TEAM and, also, the support from the Ministry of Science and Higher Education, through Grant No. N N 202 128 736.

APPENDIX A: HAMILTONIAN MATRIX FORM IN THE COEXISTENT SC + AF PHASE AND QUASIPARTICLE OPERATORS

In this appendix, we show the general form of the Hamiltonian matrix $\mathbf{H_k}$ and the pairing operators expressed in terms of the quasiparticle creation operators from the first step of the diagonalization procedure discussed in Sec. II.

For the case of nonzero gap parameters $\Delta_{0A(B)}$, we have to use eight element composite creation operator

$$\tilde{\mathbf{f}}_{\mathbf{k}}^{\dagger} \equiv (\tilde{a}_{\mathbf{k}1\uparrow A}^{\dagger}, \tilde{a}_{\mathbf{k}1\downarrow A}^{\dagger}, \tilde{a}_{-\mathbf{k}2\uparrow A}, \tilde{a}_{-\mathbf{k}2\downarrow A}, \tilde{a}_{\mathbf{k}1\uparrow B}^{\dagger}, \tilde{a}_{\mathbf{k}1\downarrow B}^{\dagger}, \tilde{a}_{-\mathbf{k}2\uparrow B}, \tilde{a}_{-\mathbf{k}2\downarrow B}),$$

to write the Hamiltonian (11) in the matrix form

$$\hat{H}_{\mathrm{HF}} - \mu\hat{N} = \sum_{\mathbf{k}} \tilde{\mathbf{f}}_{\mathbf{k}}^{\dagger} \mathbf{H}_{\mathbf{k}} \tilde{\mathbf{f}}_{\mathbf{k}} + 2\sum_{\mathbf{k}} (\tilde{\epsilon}_{\mathbf{k}2A} + \tilde{\epsilon}_{\mathbf{k}2B}) - 2\mu N + C, \tag{A1}$$

where $\tilde{\mathbf{f}}_{\mathbf{k}} \equiv (\tilde{\mathbf{f}}_{\mathbf{k}}^{\dagger})^{\dagger}$, and

$$\mathbf{H_k} = \begin{pmatrix}
\tilde{\epsilon}_{\mathbf{k}1A} - \mu & 0 & \delta_{1\mathbf{k}\uparrow\uparrow} & \delta_{1\mathbf{k}\uparrow\downarrow} & 0 & 0 & \delta_{3\mathbf{k}\uparrow\uparrow} & \delta_{3\mathbf{k}\uparrow\downarrow} \\
0 & \tilde{\epsilon}_{\mathbf{k}1A} - \mu & \delta_{1\mathbf{k}\downarrow\uparrow} & \delta_{1\mathbf{k}\downarrow\downarrow} & 0 & 0 & \delta_{3\mathbf{k}\downarrow\uparrow} & \delta_{3\mathbf{k}\downarrow\downarrow} \\
\delta_{1\mathbf{k}\uparrow\uparrow}^{*} & \delta_{1\mathbf{k}\downarrow\uparrow}^{*} & -\tilde{\epsilon}_{\mathbf{k}2A} + \mu & 0 & \delta_{4\mathbf{k}\uparrow\uparrow} & \delta_{4\mathbf{k}\downarrow\uparrow} & 0 & 0 \\
\delta_{1\mathbf{k}\uparrow\downarrow}^{*} & \delta_{1\mathbf{k}\downarrow\downarrow}^{*} & 0 & -\tilde{\epsilon}_{\mathbf{k}2A} + \mu & \delta_{4\mathbf{k}\uparrow\downarrow} & \delta_{4\mathbf{k}\downarrow\downarrow} & 0 & 0 \\
0 & 0 & \delta_{4\mathbf{k}\uparrow\uparrow}^{*} & \delta_{4\mathbf{k}\uparrow\downarrow}^{*} & \tilde{\epsilon}_{\mathbf{k}1B} - \mu & 0 & \delta_{2\mathbf{k}\uparrow\uparrow} & \delta_{2\mathbf{k}\uparrow\downarrow} \\
0 & 0 & \delta_{4\mathbf{k}\downarrow\uparrow}^{*} & \delta_{4\mathbf{k}\downarrow\downarrow}^{*} & 0 & \tilde{\epsilon}_{\mathbf{k}1B} - \mu & \delta_{2\mathbf{k}\downarrow\uparrow} & \delta_{2\mathbf{k}\downarrow\downarrow} \\
\delta_{3\mathbf{k}\uparrow\uparrow}^{*} & \delta_{3\mathbf{k}\downarrow\uparrow}^{*} & 0 & 0 & \delta_{2\mathbf{k}\uparrow\uparrow}^{*} & \delta_{2\mathbf{k}\downarrow\uparrow}^{*} & -\tilde{\epsilon}_{\mathbf{k}2B} + \mu & 0 \\
\delta_{3\mathbf{k}\uparrow\downarrow}^{*} & \delta_{3\mathbf{k}\downarrow\downarrow}^{*} & 0 & 0 & \delta_{2\mathbf{k}\uparrow\downarrow}^{*} & \delta_{2\mathbf{k}\downarrow\downarrow}^{*} & 0 & -\tilde{\epsilon}_{\mathbf{k}2B} + \mu
\end{pmatrix}. \tag{A2}$$

The $\delta_{l\mathbf{k}\sigma\sigma'}$ are the generalization of parameters introduced earlier in Eq. (16):

$$\begin{aligned}
\delta_{1\mathbf{k}\sigma\sigma'} &= \Delta_{\sigma\sigma' A} U_{\mathbf{k}\sigma}^{+} U_{\mathbf{k}\sigma'}^{-} + \Delta_{\sigma\sigma' B} V_{\mathbf{k}\sigma}^{+} V_{\mathbf{k}\sigma'}^{-}, \\
\delta_{2\mathbf{k}\sigma\sigma'} &= \Delta_{\sigma\sigma' A} V_{\mathbf{k}\sigma}^{+} V_{\mathbf{k}\sigma'}^{-} + \Delta_{\sigma\sigma' B} U_{\mathbf{k}\sigma}^{+} U_{\mathbf{k}\sigma'}^{-}, \\
\delta_{3\mathbf{k}\sigma\sigma'} &= -\Delta_{\sigma\sigma' A} U_{\mathbf{k}\sigma}^{+} V_{\mathbf{k}\sigma'}^{-} + \Delta_{\sigma\sigma' B} V_{\mathbf{k}\sigma}^{+} U_{\mathbf{k}\sigma'}^{-}, \\
\delta_{4\mathbf{k}\sigma\sigma'} &= -\Delta_{\sigma\sigma' A} V_{\mathbf{k}\sigma}^{+} U_{\mathbf{k}\sigma'}^{-} + \Delta_{\sigma\sigma' B} U_{\mathbf{k}\sigma}^{+} V_{\mathbf{k}\sigma'}^{-},
\end{aligned} \tag{A3}$$

where $\Delta_{\uparrow\uparrow A(B)} = \Delta_{+1A(B)}$, $\Delta_{\downarrow\downarrow A(B)} = \Delta_{-1A(B)}$, $\Delta_{\downarrow\uparrow A(B)} = \Delta_{\uparrow\downarrow A(B)} = \Delta_{0A(B)}$.

In the following, we present the pairing operators expressed in terms of the quasiparticle creation operators that we have introduced during the first step of the diagonalization procedure of the Hamiltonian (11):

$$\begin{aligned}
\hat{A}_{\mathbf{k}\sigma A}^{\dagger} &= U_{\mathbf{k}\sigma}^{+} U_{\mathbf{k}\sigma}^{-} \tilde{a}_{\mathbf{k}1\sigma A}^{\dagger} \tilde{a}_{-\mathbf{k}2\sigma A}^{\dagger} + V_{\mathbf{k}\sigma}^{+} V_{\mathbf{k}\sigma}^{-} \tilde{a}_{\mathbf{k}1\sigma B}^{\dagger} \tilde{a}_{-\mathbf{k}2\sigma B}^{\dagger} \\
&\quad - U_{\mathbf{k}\sigma}^{+} V_{\mathbf{k}\sigma}^{-} \tilde{a}_{\mathbf{k}1\sigma A}^{\dagger} \tilde{a}_{-\mathbf{k}2\sigma B}^{\dagger} - V_{\mathbf{k}\sigma}^{+} U_{\mathbf{k}\sigma}^{-} \tilde{a}_{\mathbf{k}1\sigma B}^{\dagger} \tilde{a}_{-\mathbf{k}2\sigma A}^{\dagger}, \\
\hat{A}_{\mathbf{k}\sigma B}^{\dagger} &= U_{\mathbf{k}\sigma}^{+} U_{\mathbf{k}\sigma}^{-} \tilde{a}_{\mathbf{k}1\sigma B}^{\dagger} \tilde{a}_{-\mathbf{k}2\sigma B}^{\dagger} + V_{\mathbf{k}\sigma}^{+} V_{\mathbf{k}\sigma}^{-} \tilde{a}_{\mathbf{k}1\sigma A}^{\dagger} \tilde{a}_{-\mathbf{k}2\sigma A}^{\dagger} \\
&\quad + U_{\mathbf{k}\sigma}^{+} V_{\mathbf{k}\sigma}^{-} \tilde{a}_{\mathbf{k}1\sigma B}^{\dagger} \tilde{a}_{-\mathbf{k}2\sigma A}^{\dagger} + V_{\mathbf{k}\sigma}^{+} U_{\mathbf{k}\sigma}^{-} \tilde{a}_{\mathbf{k}1\sigma A}^{\dagger} \tilde{a}_{-\mathbf{k}2\sigma B}^{\dagger},
\end{aligned} \tag{A4}$$

$$\begin{aligned}
\hat{A}_{\mathbf{k}0A}^{\dagger} &= \frac{1}{\sqrt{2}} \sum_{\sigma} (U_{\mathbf{k}\sigma}^{+} U_{\mathbf{k}\bar{\sigma}}^{-} \tilde{a}_{\mathbf{k}1\sigma A}^{\dagger} \tilde{a}_{-\mathbf{k}2\bar{\sigma} A}^{\dagger} \\
&\quad + V_{\mathbf{k}\sigma}^{+} V_{\mathbf{k}\bar{\sigma}}^{-} \tilde{a}_{\mathbf{k}1\sigma B}^{\dagger} \tilde{a}_{-\mathbf{k}2\bar{\sigma} B}^{\dagger} - V_{\mathbf{k}\sigma}^{-} U_{\mathbf{k}\bar{\sigma}}^{+} \tilde{a}_{\mathbf{k}1\sigma B}^{\dagger} \tilde{a}_{-\mathbf{k}2\bar{\sigma} A}^{\dagger} \\
&\quad - U_{\mathbf{k}\sigma}^{+} V_{\mathbf{k}\bar{\sigma}}^{-} \tilde{a}_{\mathbf{k}1\sigma A}^{\dagger} \tilde{a}_{-\mathbf{k}2\bar{\sigma} B}^{\dagger}), \\
\hat{A}_{\mathbf{k}0B}^{\dagger} &= \frac{1}{\sqrt{2}} \sum_{\sigma} (V_{\mathbf{k}\sigma}^{+} V_{\mathbf{k}\bar{\sigma}}^{-} \tilde{a}_{\mathbf{k}1\sigma A}^{\dagger} \tilde{a}_{-\mathbf{k}2\bar{\sigma} A}^{\dagger} \\
&\quad + U_{\mathbf{k}\sigma}^{+} U_{\mathbf{k}\bar{\sigma}}^{-} \tilde{a}_{\mathbf{k}1\sigma B}^{\dagger} \tilde{a}_{-\mathbf{k}2\bar{\sigma} B}^{\dagger} + U_{\mathbf{k}\sigma}^{-} V_{\mathbf{k}\bar{\sigma}}^{+} \tilde{a}_{\mathbf{k}1\sigma B}^{\dagger} \tilde{a}_{-\mathbf{k}2\bar{\sigma} A}^{\dagger} \\
&\quad + V_{\mathbf{k}\sigma}^{+} U_{\mathbf{k}\bar{\sigma}}^{-} \tilde{a}_{\mathbf{k}1\sigma A}^{\dagger} \tilde{a}_{-\mathbf{k}2\bar{\sigma} B}^{\dagger}).
\end{aligned} \tag{A5}$$

APPENDIX B: HAMILTONIAN MATRIX AND QUASIPARTICLE STATES FOR THE COEXISTENT FERROMAGNETIC-SPIN-TRIPLET SUPERCONDUCTING PHASE

In this appendix, we show briefly the approach to the coexistent ferromagnetic-spin-triplet superconducting phase within the mean-field-BCS approximation. In analogy to the situation considered in Sec. II, we make use of relations (3) and (5) and transform our Hamiltonian into the reciprocal space to get

$$\begin{aligned}
\hat{H}_{\mathrm{HF}} - \mu\hat{N} &= \sum_{\underline{\mathbf{k}}l\sigma} (\epsilon_{\mathbf{k}} - \mu - \sigma I S_u^z) \hat{n}_{\mathbf{k}l\sigma} \\
&\quad + \sum_{\mathbf{k}ll'(l\neq l')\sigma} \epsilon_{12\mathbf{k}} a_{\mathbf{k}l\sigma}^{\dagger} a_{\mathbf{k}l'\sigma} \\
&\quad + \sum_{\mathbf{k},m=\pm 1} (\Delta_m^{*} \hat{A}_{\mathbf{k},m} + \Delta_m \hat{A}_{\mathbf{k},m}^{\dagger}) \\
&\quad + \sqrt{2} \sum_{\mathbf{k}} (\Delta_0^{*} \hat{A}_{\mathbf{k},0} + \Delta_0 \hat{A}_{\mathbf{k},0}^{\dagger}) \\
&\quad + N \left\{ \frac{|\Delta_1|^2 + |\Delta_{-1}|^2 + 2|\Delta_0|^2}{J - U'} + 2I \left(S_u^z\right)^2 \right\},
\end{aligned} \tag{B1}$$

where S_u^z is the uniform average magnetic moment and this time the sums are taken over all N independent $\mathbf{k}$ points, as here we do not need to perform the division into two sublattices. In the equation above, we have omitted the terms that only lead to the shift of the reference energy. Next, we diagonalize the one-particle part of the HF Hamiltonian by introducing quasiparticle operators

$$\begin{aligned}\tilde{a}_{\mathbf{k}1\sigma} &= \frac{1}{\sqrt{2}}(a_{\mathbf{k}1\sigma} + a_{\mathbf{k}2\sigma}),\\ \tilde{a}_{\mathbf{k}2\sigma} &= \frac{1}{\sqrt{2}}(-a_{\mathbf{k}1\sigma} + a_{\mathbf{k}2\sigma}),\end{aligned} \tag{B2}$$

with dispersion relations

$$\begin{aligned}\tilde{\epsilon}_{\mathbf{k}1\sigma} &= \epsilon_{\mathbf{k}} - \mu - \sigma I S^z + |\epsilon_{12\mathbf{k}}|,\\ \tilde{\epsilon}_{\mathbf{k}2\sigma} &= \epsilon_{\mathbf{k}} - \mu - \sigma I S^z - |\epsilon_{12\mathbf{k}}|.\end{aligned} \tag{B3}$$

Using the four-component composite creation operator $\tilde{\mathbf{f}}_{\mathbf{k}}^{\dagger} \equiv (\tilde{a}_{\mathbf{k}1\uparrow}^{\dagger}, \tilde{a}_{\mathbf{k}1\downarrow}^{\dagger}, \tilde{a}_{-\mathbf{k}2\uparrow}, \tilde{a}_{-\mathbf{k}2\downarrow})$, we can construct the 4×4 Hamiltonian matrix and write it in the following form:

$$\hat{H}_{\mathrm{HF}} - \mu\hat{N} = \sum_{\mathbf{k}} \tilde{\mathbf{f}}_{\mathbf{k}}^{\dagger} \tilde{\mathbf{H}}_{\mathbf{k}} \tilde{\mathbf{f}}_{\mathbf{k}} + \sum_{\mathbf{k}\sigma} \tilde{\epsilon}_{\mathbf{k}2\sigma} + C, \tag{B4}$$

where

$$\tilde{\mathbf{H}}_{\mathbf{k}} = \begin{pmatrix} \tilde{\epsilon}_{\mathbf{k}1\uparrow} & 0 & \Delta_1 & \Delta_0 \\ 0 & \tilde{\epsilon}_{\mathbf{k}1\downarrow} & \Delta_0 & \Delta_{-1} \\ \Delta_1^* & \Delta_0^* & -\tilde{\epsilon}_{\mathbf{k}2\uparrow} & 0 \\ \Delta_0^* & \Delta_{-1}^* & 0 & -\tilde{\epsilon}_{\mathbf{k}2\downarrow} \end{pmatrix}, \tag{B5}$$

with $\tilde{\mathbf{f}}_{\mathbf{k}} \equiv (\tilde{\mathbf{f}}_{\mathbf{k}}^{\dagger})^{\dagger}$. Symbol C refers to the last two terms of the right-hand side of expression (B1). After making the diagonalization transformation of (B5), we can write the HF Hamiltonian as

$$\hat{H}_{\mathrm{HF}} - \mu\hat{N} = \sum_{\mathbf{k}l\sigma} \lambda_{\mathbf{k}l\sigma} \alpha_{\mathbf{k}l\sigma}^{\dagger} \alpha_{\mathbf{k}l\sigma} + \sum_{\mathbf{k}\sigma} (\tilde{\epsilon}_{\mathbf{k}2\sigma} - \lambda_{\mathbf{k}2\sigma}) + C, \tag{B6}$$

where we have again introduced the quasiparticle operators $\alpha_{\mathbf{k}l\sigma}$ and $\alpha_{\mathbf{k}l\sigma}^{\dagger}$. Assuming that $\Delta_0 = 0$ and that the remaining gap parameters are real, we can write the dispersion relations for the quasiparticles $\lambda_{\underline{\mathbf{k}}l\sigma}$ in the following way:

$$\begin{aligned}\lambda_{\mathbf{k}1\uparrow} &= \sqrt{(\epsilon_{\mathbf{k}} - \mu - IS^z)^2 + \Delta_1^2} + \beta_h|\epsilon_{\mathbf{k}}|,\\ \lambda_{\mathbf{k}1\downarrow} &= \sqrt{(\epsilon_{\mathbf{k}} - \mu + IS^z)^2 + \Delta_{-1}^2} + \beta_h|\epsilon_{\mathbf{k}}|,\\ \lambda_{\mathbf{k}2\uparrow} &= \sqrt{(\epsilon_{\mathbf{k}} - \mu - IS^z)^2 + \Delta_1^2} - \beta_h|\epsilon_{\mathbf{k}}|,\\ \lambda_{\mathbf{k}2\downarrow} &= \sqrt{(\epsilon_{\mathbf{k}} - \mu + IS^z)^2 + \Delta_{-1}^2} - \beta_h|\epsilon_{\mathbf{k}}|.\end{aligned} \tag{B7}$$

In this manner, we have obtained the fully diagonalized Hamiltonian analytically for the case of superconductivity coexisting with ferromagnetism. Next, in the similar way as for the antiferromagnetically ordered phases, we can construct the set of self-consistent equations for the mean-field parameters $\Delta_{\pm 1}$, S_u^z and for the chemical potential, as well as construct the expression for the free energy.

APPENDIX C: BEYOND THE HARTREE-FOCK APPROXIMATION: HUBBARD-STRATONOVICH TRANSFORMATION

In outlining the systematic approach going beyond the Hartree-Fock approximation, we start with Hamiltonian (7) with the singlet pairing part $\sim (U' + J)\sum_i B_i^{\dagger} B_i$ neglected, i.e.,

$$\hat{H} = \hat{H}_0 + U \sum_{il} \hat{n}_{il\uparrow}\hat{n}_{il\downarrow} - J^H \sum_{im} \hat{A}_{im}^{\dagger}\hat{A}_{im}, \tag{C1}$$

where $\hat{H}_0$ contains the hopping term, and $J^H \equiv J - U'$. We use the spin-rotationally invariant form of the Hubbard term

$$\hat{n}_{il\uparrow}\hat{n}_{il\downarrow} = \frac{\hat{n}_{il}^2}{4} - (\vec{\mu}_{il} \cdot \hat{\mathbf{S}}_{il})^2, \tag{C2}$$

where $\hat{n}_{il} = \sum_{\sigma} \hat{n}_{il\sigma}$ and $\vec{\mu}_i$ is an arbitrary unit vector establishing local spin quantization axis. One should note that, strictly speaking, we have to make the Hubbard-Stratonovich transformation twice for each of the last two terms in (C2) separately. The last term will be effectively transformed in the following manner:

$$\begin{aligned}&-J^H \sum_{im} \hat{A}_{im}^{\dagger}\hat{A}_{im}\\ &\quad\rightarrow -\sum_{im} (\hat{A}_{im}^{\dagger}\Delta_{im} + \hat{A}_{im}\Delta_{im}^* - |\Delta_{im}|^2/J^H),\end{aligned} \tag{C3}$$

where Δ_{im} is the classical (Bose) field in the coherent-state representation. The term (C2) can be represented in the standard form through the Poisson integral

$$\exp\left(\frac{\hat{\alpha}_i^2}{2}\right) = \frac{1}{\sqrt{2\pi}} \int_{-\infty}^{\infty} dx_i \left(-\frac{x_i^2}{2} + \hat{\alpha}_i x_i\right). \tag{C4}$$

In effect, the partition function for the Hamiltonian (C1) will have the form in the coherent-state representation

$$\begin{aligned}\mathcal{Z} = \int &\mathcal{D}[a_{il\sigma}, a_{il\sigma}^{\dagger}, \Delta_{im}, \Delta_{im}^*, \lambda_{il}]\\ &\times \exp\left(-\int_0^{\beta} d\tau \left\{\sum_{ijll'\sigma} a_{il\sigma}^{\dagger}\left[t_{ij}^{ll'} + \left(\frac{\partial}{\partial\tau} - \mu\right)\delta_{ij}\delta_{ll'}\right]a_{jl'\sigma}\right.\right.\\ &- \sum_{im}\left[\Delta_{im}(\tau)\hat{A}_{im}^{\dagger}(\tau) + \Delta_{im}^*(\tau)\hat{A}_{im}(\tau) - \frac{|\Delta_{im}(\tau)|^2}{J^H}\right]\\ &\left.\left. - \sum_{il} \sqrt{2}\lambda_{il}\vec{\mu}_{il} \cdot \hat{\mathbf{S}}_{il} + \lambda_{il}^2\right\}\right),\end{aligned} \tag{C5}$$

where we have included only the spin and the pairing fluctuations. In this paper, $t_{ij}^{ll'} = t_{ij}\delta_{ll'} + (1 - \delta_{ll'})t_{ij}^{12}$. Also, the integration takes place in imaginary-time domain and the creation and annihilation operators are now Grassman variables.[20] In this formulation, Δ_{im} and λ_i represent local fields which can be regarded as mean (Hartree-Fock) fields with Gaussian fluctuations.

With the help of (C5), we can define "time-dependent" effective Hamiltonian

$$\hat{H}(\tau) \equiv \sum_{ijll'\sigma} t_{ij}^{ll'} a_{il\sigma}^{\dagger}(\tau) a_{jl'\sigma}(\tau) - J^H \sum_{im} \Big[\Delta_{im}(\tau) \hat{A}_{im}^{\dagger}(\tau) + \Delta_{im}^{*}(\tau) \hat{A}_{im}(\tau) - |\Delta_{im}(\tau)|^2 \Big] - U \sum_{i} \Big[\vec{\lambda}_{il}(\tau) \cdot \hat{\mathbf{S}}_{il}(\tau) + \frac{\vec{\lambda}_{il}^{2}(\tau)}{2} \Big], \tag{C6}$$

where now the fluctuating dimensionless fields are defined as

$$\vec{\lambda}_{il}(\tau) \equiv \frac{\sqrt{2}\vec{\mu}_{il}\lambda_{il}(\tau)}{U}, \quad \Delta_{im}(\tau) \equiv \frac{\Delta_{im}(\tau)}{J^H}. \tag{C7}$$

Note that the magnetic molecular field $\sim U\vec{\lambda}_{il}(\tau)$ is substantially stronger than the pairing field $\sim J^H \Delta_{im}(\tau)$. In the saddle-point approximation $\vec{\lambda}_{il}(\tau) \equiv \lambda_{il}\mathbf{e}_z$, $\Delta_{im}(\tau) = \Delta_{im}^{*}(\tau) \equiv \Delta$, and we obtain the Hartree-Fock-type approximation. Therefore, the quantum fluctuations are described by the terms

$$-U \sum_{il} \delta\vec{\lambda}_{il}(\tau) \cdot \hat{\mathbf{S}}_{il}(\tau) - J^H \sum_{im} [\delta\Delta_{im}(\tau) \hat{A}_{im}^{\dagger}(\tau) + \delta\Delta_{im}^{*}(\tau) \hat{A}_{im}(\tau)]. \tag{C8}$$

The first term represents the quantum spin fluctuations of the amplitude $\delta\vec{\lambda}_{il}(\tau) \equiv \vec{\lambda}_{il}(\tau) - \lambda\mathbf{e}_z$, and the second describes pairing fluctuations. Both fluctuations are Gaussian due to the presence of the terms $\sim \delta\vec{\lambda}_{il}^{2}(\tau)$ and $|\delta\Delta_{im}(\tau)|^2$. In other words, they represent the higher-order contributions and will be treated in detail elsewhere. In such manner, the mean-field part (real-space pairing) and the fluctuation part (pairing in $\mathbf{k}$ space) can be incorporated thus into a single scheme.

[1] Y. Maeno, H. Hashimoto, K. Yoshida, S. Nishizaki, T. Fujita, J. G. Bednorz, and F. Lichtenberg, Nature (London) **372**, 532 (1994).

[2] S. S. Saxena, P. Agarwal, K. Ahilan, F. M. Grosche, R. K. W. Haselwimmer, M. J. Steiner, E. Pugh, I. R. Walker, S. R. Julian, P. Monthoux, G. G. Lonzarich, A. Huxley, I. Sheikin, D. Braithwaite, and J. Flouquet, Nature (London) **406**, 587 (2000); A. Huxley, I. Sheikin, E. Ressouche, N. Kernavanois, D. Braithwaite, R. Calemczuk, and J. Flouquet, Phys. Rev. B **63**, 144519 (2001).

[3] N. Tateiwa, T. C. Kobayashi, K. Hanazono, K. Amaya, Y. Haga, R. Settai, and Y. Onuki, J. Phys.: Condens. Matter **13**, 117 (2001).

[4] K. Klejnberg and J. Spałek, J. Phys.: Condens. Matter **11**, 6553 (1999).

[5] J. Spałek, Phys. Rev. B **63**, 104513 (2001); J. Spałek, P. Wróbel, and W. Wójcik, Phys. C (Amsterdam) **387**, 1 (2003); A. Klejnberg and J. Spałek, Phys. Rev. B **61**, 15542 (2000).

[6] M. Zegrodnik and J. Spałek (unpublished); previous brief and qualitative speculation about ferromagnetism and spin-triplet superconductivity coexistence has been raised in S.-Q. Shen, Phys. Rev. **57**, 6474 (1998).

[7] C. M. Puetter, Ph.D. thesis, University of Toronto, 2012; K. Sano and Y. Ōno, J. Magn. Magn. Mater. **310**, 319 (2007); J. Phys. Soc. Jpn. **72**, 1847 (2003); J. E. Han, Phys. Rev. B **70**, 054513 (2004); T. Hotta and K. Ueda, Phys. Rev. Lett. **92**, 107007 (2004); X. Dai, Z. Fang, Y. Zhou, and F-C. Zhang, *ibid.* **101**, 057008 (2008); P. A. Lee and X-G. Wen, Phys. Rev. B **78**, 144517 (2008).

[8] P. W. Anderson and W. F. Brinkman, *The Helium Liquids*, edited by J. G. M. Armitage and I. E. Farqutar (Academic, New York, 1975), pp. 315–416. For discussion in the context of two-dimensional metals, P. Monthoux and G. G. Lonzarich, Phys. Rev. B **59**, 14598 (1999); **63**, 054529 (2001).

[9] J. Spałek, Phys. Rev. B **37**, 533 (1988); J. Kaczmarczyk and J. Spałek, *ibid.* **84**, 125140 (2011); for recent review, see e.g. P. A. Lee, N. G. Nagaosa, and X.-G. Wen, Rev. Mod. Phys. **78**, 17 (2006).

[10] J. Spałek, Phys. Rev. B **38**, 208 (1988).

[11] A. M. Clogston, Phys. Rev. Lett. **9**, 266 (1962); L. W. Gruenberg and L. Gunther, *ibid.* **16**, 996 (1966); K. Maki and T. Tsuento, Prog. Theor. Phys. **31**, 945 (1964).

[12] R. Micnas, J. Ranninger, and S. Robaszkiewicz, Rev. Mod. Phys. **62**, 113 (1990).

[13] T. Nomura and K. Yamada, J. Phys. Soc. Jpn. **71**, 1993 (2002); C. Noce, G. Busiello, and M. Cuocco, Europhys. Lett. **51**, 195 (2000); weak-coupling limit for triplet superconductors was also studied in J. Linder, I. B. Sperstad, A. H. Nievidomsky, M. Cuocco, and A. Sudbø, J. Phys. A: Math. Gen. **36**, 9289 (2003); B. J. Powell, J. F. Annett, B. L. Györffy, and K. I. Wysokiński, New J. Phys. **11**, 055063 (2009). Here, we make a full analysis of coexistent phases and ascribe the main role to the Hund's rule coupling in the pairing.

[14] D. Vollhardt and P. Wölfle, *The Superfluid Phases of Helium 3* (Taylor & Francis, London, 1990).

[15] S. Sugano, Y. Tanabe, and H. Kamimura, *Multiplets of Transition Metal Ions in Crystals* (Academic, New York, 1970).

[16] J. Spałek, P. Wróbel, and W. Wójcik, Phys. C (Amsterdam) **387**, 1 (2003).

[17] P. Wróbel, Ph.D. thesis, Jagiellonian University, Kraków, 2004.

[18] J. Dukelsky, C. Esebbag, and S. Pittel, Phys. Rev. Lett. **88**, 062501 (2002).

[19] S. Inagaki and R. Kubo, Int. J. Magn. **4**, 139 (1973).

[20] J. W. Negele and H. Orland, *Quantum Many-Particle Systems* (Addison-Wesley, RedWood City, 1988), Chap. 8.

Hund's rule induced spin-triplet superconductivity coexisting with magnetic ordering in the degenerate band Hubbard model

Michał Zegrodnik

Faculty of Physics and Applied Computer Science, AGH University of Science and Technology, al. Mickiewicza 30, 30-059 Kraków, Poland

Supervisor: Jozef Spałek

The Hartree-Fock approximation combined with the Bardeen-Cooper-Schrieffer (BCS) method is applied for the degenerate band Hubbard model to analyze the coexistence of spin-triplet superconductivity with ferromagnetism and antiferromagnetism. In the presented approach the Hund's rule exchange term is responsible for both pairing mechanism and magnetic ordering. The proper phase diagrams are presented and the influence of the intersite hybridization on the stability of considered phases is discussed. Additionally, the calculated temperature dependences of superconducting gaps and magnetic moment are shown.

It is believed that Sr_2RuO_4 [1], UGe_2 [2], and URhGe [3] are the candidates for the spin-triplet superconductors. The last two are particularly interesting as the paired state appears inside the ferromagnetic phase. It has been suggested by a proper qualitative analysis [4–6] that the intra-atomic Hund's rule can lead to the coexisting superconducting and magnetically ordered phases. In this letter we further discuss the idea of real-space spin-triplet pairing in the regime of weakly correlated particles and include both inter-band hybridization and corresponding Coulomb interactions. We think that this relatively simple approach is relevant to the mentioned at the beginning ferromagnetic superconductors because of the following reasons. Even though the effective exchange (Weiss-type) field acts only on the spin degrees of freedom, it is important in determining the second critical field of ferromagnetic superconductor in the so-called Pauli limit [7–9], as the orbital effects in the Cooper-pair breaking process are then negligible. The appearance of a stable coexistent ferromagnetic-superconducting phase means, that either Pauli limiting situation critical field has not been reached in the case of spin-singlet pairing or else, the pairing has the spin-triplet nature, without the component with spin $S^z = 0$, and then the Pauli limit is not operative.

We begin with the extended orbitally degenerate Hubbard Hamiltonian which has the following form

$$\begin{aligned}\hat{H} = &\sum_{ij(i\neq j)ll'\sigma} t_{ij}^{ll'} a_{il\sigma}^{\dagger} a_{jl'\sigma} + U\sum_{il} \hat{n}_{il\uparrow}\hat{n}_{il\downarrow} \\ &+ (U'+J)\sum_{i} \hat{n}_{i1}\hat{n}_{i2} \\ &- J\sum_{ill'(l\neq l')} \left(\hat{\mathbf{S}}_{il}\cdot\hat{\mathbf{S}}_{il'} + \frac{3}{4}\hat{n}_{il}\hat{n}_{il'}\right),\end{aligned} \tag{1}$$

where $l = 1,2$ label the orbitals. The first term describes electron hopping between atomic sites i and j. For $l \neq l'$ this term corresponds to inter-site, inter-orbital hybridization. Next two terms describe the Coulomb repulsion between electrons on the same atomic site. As one can see the third term contains the contribution that originates from the exchange interaction (J). The last term expresses the (Hund's rule) ferromagnetic exchange and is going to be regarded as responsible for the spin-triplet pairing mechanism. It can be expressed in terms of the spin-triplet pairing operators

$$\hat{A}_{i,m}^{\dagger} \equiv \begin{cases} a_{i1\uparrow}^{\dagger} a_{i2\uparrow}^{\dagger} & m = 1, \\ a_{i1\downarrow}^{\dagger} a_{i2\downarrow}^{\dagger} & m = -1, \\ \frac{1}{\sqrt{2}}(a_{i1\uparrow}^{\dagger} a_{i2\downarrow}^{\dagger} + a_{i1\downarrow}^{\dagger} a_{i2\uparrow}^{\dagger}) & m = 0. \end{cases} \tag{2}$$

The results presented here have been carried out for the case of square lattice with nonzero hopping t between nearest neighbors only. As we are considering the doubly degenerate band model, we make a simplifying assumption that the hybridization matrix element $\epsilon_{\mathbf{k}12} = \beta_h \epsilon_{\mathbf{k}}$, where $\beta_h \in [0,1]$ is the parameter, which specifies the hybridization strength. After applying the Hartree-Fock approximation to (1) and performing the transformation to the reciprocal space, one gets the following mean-field parameters in the resulting Hamiltonian

$$\begin{aligned} \Delta_{\pm 1} &\equiv -\frac{(J-U')}{WN}\sum_{\mathbf{k}}\langle \hat{A}_{\mathbf{k},\pm 1}\rangle, \\ \Delta_{0} &\equiv -\frac{(J-U')}{\sqrt{2}WN}\sum_{\mathbf{k}}\langle \hat{A}_{\mathbf{k},0}\rangle, \end{aligned} \tag{3}$$

$$S_l^z \equiv \frac{1}{2N}\sum_{\mathbf{k}}\left(\langle \hat{n}_{\mathbf{k}l\uparrow}\rangle - \langle \hat{n}_{\mathbf{k}l\downarrow}\rangle\right), \tag{4}$$

where N is the number of atomic sites and W is the bare band width. The Δ_m parameters have the interpretation of spin-triplet superconducting gaps, while S_l^z is the expectation value of the magnetic moment per site, per band. Because the considered bands are equivalent the magnetic moment fulfills the relation $S_1^z = S_2^z \equiv S^z$. Mean field parameters (3) and (4) are used to define the following phases

- normal state (**NS**): $\Delta_{\pm 1}=0$, $S^z=0$
- pure superconducting phase type A (**A**): $\Delta_{\pm 1}\equiv\Delta\neq 0$, $S^z=0$
- pure saturated ferromagnetic phase (**SFM**): $\Delta_{\pm 1}=0$, $S^z=S^z_{\max}\neq 0$
- pure nonsaturated ferromagnetic phase (**FM**): $\Delta_{\pm 1}=0$, $0<S^z<S^z_{\max}$
- saturated ferromagnetic phase coexistent with superconductivity of type A1 (**A1**+**SFM**): $\Delta_1\neq 0$, $\Delta_{-1}=0$, $S^z=S^z_{\max}\neq 0$
- nonsaturated ferromagnetic phase coexistent with superconductivity of type A1 (**A1**+**FM**): $\Delta_1\neq 0$, $\Delta_{-1}=0$, $0<S^z<S^z_{\max}$

One could also consider the so called superconducting phase of type B for which $\Delta_0 = \Delta_{\pm 1}\neq 0$. However this phase never coexists with magnetic ordering. Moreover in the absence of magnetic ordering the A phase has always lower free energy than the B phase. Therefore the superconducting B phase is absent in the following discussion.

In the case of antiferromagnetic ordering one has to divide the system into two interpenetrating sublattices A and B. The average staggered magnetic moment of electrons on each of the $N/2$ sublattice A sites is equal, $\langle S_i^z\rangle = \langle S_A^z\rangle$, whereas on the remaining $N/2$ sublattice B sites we have $\langle S_i^z\rangle = \langle S_B^z\rangle \equiv -\langle S_A^z\rangle$. Following this division one has to introduce the sublattice gap parameters $\Delta_{\pm 1A}$ and $\Delta_{\pm 1B}$ which are defined analogically as (3) but with regard to each of the sublattices separately. The sublattice gap parameters fulfill the relations

$$\begin{aligned} \Delta_{+1A} &= \Delta_{-1B} \equiv \Delta_{+}, \\ \Delta_{-1A} &= \Delta_{+1B} \equiv \Delta_{-}, \end{aligned} \tag{5}$$

The considered here antiferromagnetically ordered phases are defined as follows

- pure antiferromagnetic phase (**AF**): $\Delta_{\pm 1A(B)}=0$, $S_s^z\neq 0$
- coexistent superconducting and antiferromagnetic phase (**SC**+**AF**): $\Delta_{\pm 1A(B)}\neq 0$, $S_s^z\neq 0$

where the S_s^z is the so-called staggered magnetic moment. By using the Bogolubov-Nambu-de Gennes scheme one can diagonalize the Hartree-Fock Hamiltonian and construct the set of self consistent equations for all the mean field parameters and chemical potential. For given values of the microscopic parameters U, U', J, β_h, n, the set of self-consistent equations has several solutions that correspond to different phases. The free energy can be evaluated for each of the solutions and the one that corresponds to the lowest free energy is regarded as the stable phase.

The numerical calculations have been carried out for U'=U−2J, which is usual for $3d$ electrons. For U'>J the interorbital Coulomb

repulsion suppresses the pairing mechanism, so the necessary condition for the spin-triplet paired phases to appear in our model is $U < 3J$. It represents a rather stringent condition as usually for $3d$ metals we have $U \sim 3J$. This may explain why only in few compounds the coexistent superconducting and ferromagnetic phase has been indeed observed.

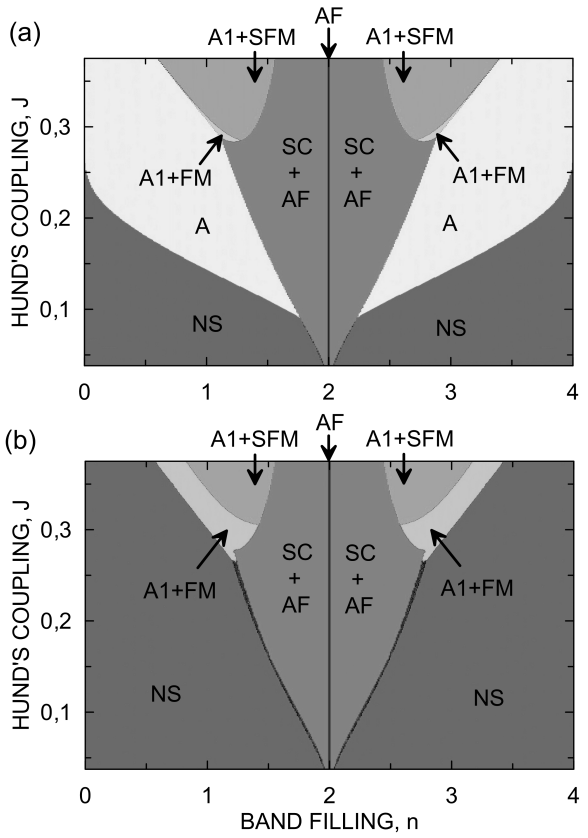

Figure 1: Phase diagrams in (n, J) space for $k_B T/W = 10^{-4}$; $\beta_h = 0{,}0$ (a) and $\beta_h = 0{,}11$ (b).

In Fig. 1 we present the phase diagrams in (n, J) space for two different values of the β_h parameter. It can be seen that they contain regions of stability of pure spin-triplet superconducting phase as well as superconducting phase coexisting with either ferromagnetism or antiferromagnetism. The appearance of the AF state for half filling ($n = 2$) corresponds to the fact that the bare Fermi-surface topology has a rectangular structure with $Q = (\pi, \pi)$ nesting. The symmetry of the phase diagrams with respect to half-filled band situation is a manifestation of the particle-hole symmetry, since the bare density of states is symmetric with respect to the middle point of the band. One can see from the presented diagrams that the influence of hybridization is significant quantitatively when it comes to the superconducting phase A, as for $\beta_h = 0{,}11$ the region of stability of this phase has disappeared completely from the diagram mainly in favor of the NS phase. Moreover due to hybridization the region of stability of the A1+SFM phase narrows down in favor of the A1+FM phase. Antiferromagnetically ordered phase is not affected much by the rise of the β_h parameter. The diagram in (n, T) space (Fig. 2) shows how the critical temperature corresponding to A and SC+AF phases depends on the band filling.

The temperature dependences of the gap parameters and staggered magnetic moment in the SC+AF phase for selected values of n and J are shown in Fig. 3. It is clearly seen from the plots that while the temperature is being raised the system undergoes two phase transitions. The first one is the transition from SC+AF to AF, when the superconducting gaps Δ_+ and Δ_- close in the critical temperature T_S. The second one is the transition from AF to NS, when the staggered structure of the system is destroyed in the Néel temperature T_N. With the increase of the hybridization strength the critical temperature T_S decreases slightly, while the Néel temperature increases. The transition temperature ratio $T_N/T_S \approx 10$. In Fig. 4 we show similar plots but for the case of superconductivity coexisting with ferromagnetism.

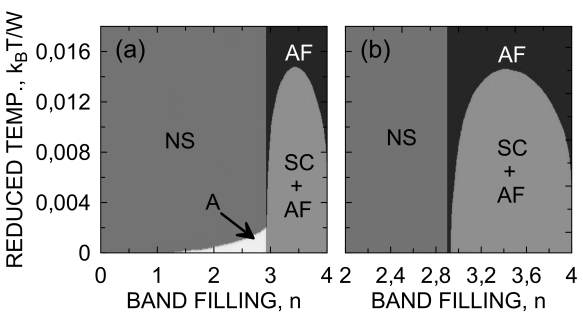

Figure 2: Phase diagrams in (n, T) space for $J = 0{,}175$; $\beta_h = 0{,}0$ (a) and $\beta_h = 0{,}11$ (b).

Analogously as in the case of SC+AF, the system undergoes two phase transitions. The influence of hybridization on the temperature dependences is also similar as in the case of SC+AF phase. This time the transition temperature ratio $T_C/T_S \approx 5$.

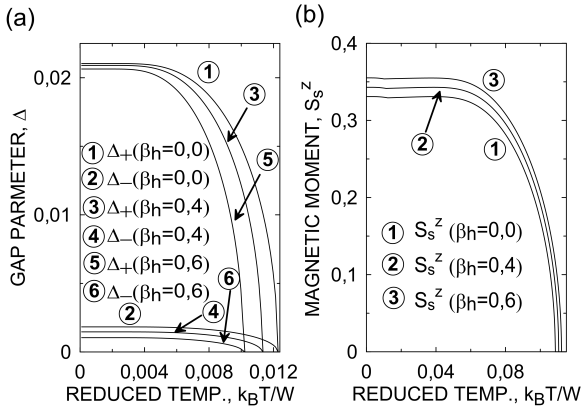

Figure 3: The temperature dependences of superconducting gaps (a) and magnetic moment (b) corresponding to the SC+AF phase for $n = 1{,}9$; $J = 0{,}175$.

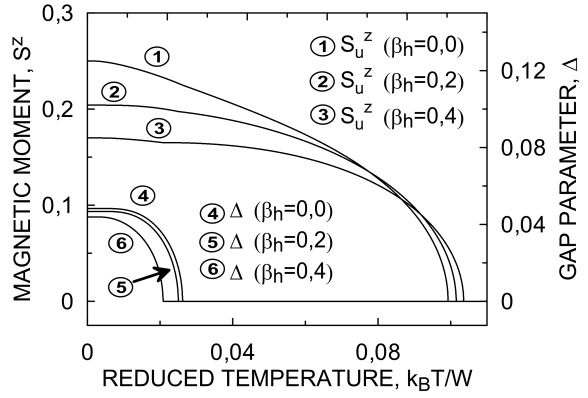

Figure 4: The temperature dependences of the superconducting gap and magnetic moment corresponding to A1+FM phase for $n = 1{,}0$; $J = 0{,}31625$.

In this letter we have carried out the Hartree-Fock analysis of the hybridized degenerate band Hubbard model with both spin-triplet pairing and magnetism induced by the Hund's rule. We have determined the regions of stability of the pure paired phase as well as paired phase coexisting with magnetic ordering. We have discussed the effect of hybridization which reduces significantly the stability regime of the A phase as well as decreases the critical temperature of all the superconducting phases considered. The influence of hybridization on the region of stability of SC+AF phase is not significant. It should be mentioned that the easiness with which the superconducting phase is accommodated within the antiferromagnetic phase is the result of the fact that the SC gaps have a intraatomic origin and the corresponding spins have then the tendency to be parallel. Therefore the spins do not disturb largely the staggered structure, which is of interatomic character.

M.Z. has been partly supported by the EU Human Capital Operation Program, Polish Project No. POKL.04.0101-00-434/08-00. J.S. acknowledges the financial support from the Foundation for Polish Science (FNP) within project TEAM.

⋆ ⋆ ⋆

[1] Y. Maeno, H. Hashimoto, K. Yoshida, S. Nishizaki, T. Fujita, J, G. Bednorz, F. Lichtenberg, *Nature* **372**, 532 (1994).

[2] S. S. Saxena, P. Agarwal, K. Ahilan, F. M. Grosche, R. K. W. Haselwimmer, M. J. Steiner, E. Pugh, I. R. Walker, S. R. Julian, P. Monthoux, G. G. Lonzarich, A. Huxley, I. Sheikin, D. Braithwaite, J. Flouquet, *Nature* **406**, 587 (2000)

[3] N. Tateiwa, T. C. Kobayashi, K. Hanazono, K. Amaya, Y. Haga, R. Settai, Y. Onuki, *J. Phys.: Condens. Matter* **13**, 117 (2001).

[4] K. Klejnberg, J. Spałek, *J. Phys.: Condens. Matter* **11**, 6553 (1999).

[5] J. Spałek, *Phys. Rev.* B **63**, 104513 (2001).

[6] J. Spałek, P. Wróbel, W. Wójcik, *Physica C* **387**, 1 (2003).

[7] A. M. Clogston, *Phys. Rev. Lett.* **9**, 266 (1962).

[8] L. W. Gruenberg, L. Gunther, *Phys. Rev. Lett.* **16**, 996 (1966).

[9] K. Maki, T. Tsuento, *Prog. Theor. Phys.* **31**, 945 (1964).

Coexistence of spin-triplet superconductivity with magnetism within a single mechanism for orbitally degenerate correlated electrons: Statistically-consistent Gutzwiller approximation.

M Zegrodnik[1], J Spałek[1,2], and J Bünemann[3]

[1]AGH University of Science and Technology, Faculty of Physics and Applied Computer Science, Al. Mickiewicza 30, PL-30-059 Kraków, Poland
[2]Marian Smoluchowski Institute of Physics, Jagiellonian University, ul. Reymonta 4, PL-30-059 Kraków, Poland
[3]Max-Planck Institute for Solid State Research, Heisenbergstr. 1, D-70569 Stuttgart, Germany

E-mail: michal.zegrodnik@gmail.com, ufspalek@if.uj.edu.pl, buenemann@gmail.com

Abstract. An orbitally degenerate two-band Hubbard model is analyzed with inclusion of the Hund's rule induced spin-triplet even-parity paired states and their coexistence with magnetic ordering. The so-called *statistically consistent Gutzwiller approximation* (SGA) has been applied to the case of a square lattice. The superconducting gaps, the magnetic moment, and the free energy are analyzed as a function of the Hund's rule coupling strength and the band filling. Also, the influence of the intersite hybridization on the stability of paired phases is discussed. In order to examine the effect of correlations the results are compared with those calculated earlier within the Hartree-Fock (HF) approximation combined with the Bardeen-Cooper-Schrieffer (BCS) approach. Significant differences between the two used methods (HF+BCS vs. SGA+real-space pairing) appear in the stability regions of the considered phases. Our results supplement the analysis of this canonical model used widely in the discussions of pure magnetic phases with the detailed elaboration of the stability of the spin-triplet superconducting states and the coexistent magnetic-superconducting states. At the end, we briefly discuss qualitatively the factors that need to be included for a detailed quantitative comparison with the corresponding experimental results.

PACS numbers: 74.20.-z, 74.25.Dw, 75.10.Lp

Submitted to: *New J. Phys.*

1. Introduction

The question of coexistence of magnetism and superconductivity appears very often in correlated electron systems. In this context, both the spin-singlet and the spin-triplet paired states should be considered. A general motivation for considering the spin-triplet pairing is provided by the discoveries of superconductivity in Sr_2RuO_4 [1, 2], UGe_2 [3, 4], URhGe [5], UIr [6], and UCoGe [7, 8, 9]. In the last four compounds, superconductivity indeed coexists with ferromagnetism. Moreover, for both, the spin-singlet high-temperature superconductors and the heavy-fermion systems, the antiferromagnetism and the superconductivity can have the same origin. Hence, it is natural to ask whether ferromagnetism and spin-triplet superconductivity also have the same origin in the itinerant uranium ferromagnets. A related and a very nontrivial question is concerned with the coexistence of antiferromagnetism with triplet superconducting state as in UNi_2Al_3 [10, 11, 12] and UPt_3 [13, 14].

It has been argued earlier [15, 17, 18, 19] that for the case of indistinguishable fermions, the intra-atomic Hund's rule exchange can lead in a natural manner to the coexistence of spin-triplet superconductivity with magnetic ordering - ferromagnetism or antiferromagnetism in the simplest situations. This idea has been elaborated subsequently by us [20, 21, 22] by means of the combined Hartree-Fock(HF)-Bardeen-Cooper-Shrieffer(BCS) approach. In particular, the phase diagrams have been determined which contain regions of stability of the pure superconducting phase of type A (i.e., the equal-spin-paired phase), as well as superconductivity coexisting with either ferromagnetism or antiferromagnetism.

The HF approximation, as a rule, overestimates the stability of phases with a broken symmetry. Therefore, in this work, we apply the Gutzwiller approximation for the same selection of phases in order to go beyond the HF-BCS analysis and examine explicitly the effects of interelectronic correlations. The extension of the Gutzwiller method to the multi-band case [23, 24, 25] provides us with the so-called renormalization factors for our degenerate two-band model. With these factors, we construct an effective Hamiltonian by means of the *statistically consistent Gutzwiller approximation*, SGA, in which additional constraints are added to the standard Gutzwiller approximation (GA) and with the incorporation of which the single-particle state has been determined (see [26, 27, 28, 29] for exemplary applications of the SGA method). The detailed phase diagram and the corresponding order parameters are calculated as functions of the microscopic parameters such as the band filling, n, the Hund's rule exchange integral, J, and the intra- and inter-orbital Hubbard interaction parameters, U and U', respectively. The obtained results are compared with those coming out from the Hartree-Fock approximation. In this manner, the paper extends the discussion of itinerant magnetism within the canonical (extended Hubbard) model, appropriate for this purpose, to the analysis of pure and coexisting superconducting-magnetic states within a single unified approach. It should be noted that theoretical investigations regarding the spin-triplet pairing have been performed recently also for other systems

[30, 31, 32, 33, 34, 35].

The present model is based on assuming that the starting (bare) bands originate from equivalent orbitals and become inequivalent when the interband hybridization is included. The real $3d$ or $4d$ orbitals are anisotropic, so the model requires some extensions to become applicable in a quantitative manner for real materials. We can say that here we discuss thus some universal stability conditions of the paired and coexistent magnetic-paired states, as well as provide some basic quantitative characteristics. This is because, as we show explicitly below, the order parameters and related other quantities are determined by a minimization of the ground-state or free-energy functional which is obtained by integrating $\ln Z$, where Z is the effective grand-canonical partition function, over the single-particle effective band energies. Hence, the global energies are averaged out over the band states. In other words, the present model with symmetric bands can be regarded as reflecting qualitative features of Sr_2RuO_4 within a two-band approximation. Nevertheless, it is directly applicable for discussing the superfluidity and magnetism in the two-orbital SU(4) model of multicomponent ultracold fermions [36, 37, 38] as there the orbitals are identical and the general orbital and the spin symmetry combine to SU(N) symmetry.

The extension of the present model to the uranium system such as UGe_2 would require considering orbitally degenerate and correlated $5f^2 - 5f^3$ quasi-atomic states due to U and hybridized with the uncorrelated conduction band states. This means that we must have minimally a three-orbital system with two partially occupied $5f$ quasi-atomic states (so the Hund's rule becomes operative) and at least one extra conduction band. Such situation may lead to a partial Mott-localization phenomenon, i.e., to a spontaneous decomposition of $5f^n$ $(n > 1)$ configuration of electrons into the localized and the itinerant parts [39]. In such a situation, it is possible that the localized electrons are the source of ferromagnetism, whereas the itinerant particles are paired [9]. This is not the type of coexistent phase we have in mind here, since in the model considered by us all the system electrons are indistinguishable in the quantum-mechanical sense. These considerations lead to the conclusion that one would require minimally a periodic Anderson model with degenerate $5f^n$ states, to mimic the uranium-based ferromagnetic superconductors. This variant of the multiple-band model is also very useful in the discussion of heavy-fermion compounds. Moreover, in the systems represented by this model, the coexistence of antiferromagnetism and superconductivity has been shown to appear in both experiment [40] and theory [41].

In relation to the even-parity spin-triplet real-space pairing induced by the Hund's rule, one should also mention the spin fluctuations (SF) as another possible mechanism of spin-triplet pairing in liquid ^{3}He systems [42]. In that case the spin-triplet pairing is taking place in a single band system and thus the pair states must be of odd-parity. Within the present approach the spin fluctuations should be treated as quantum fluctuations around the present self-consistently renormalized mean field state [43]. The real-space and the spin-fluctuation contributions may become of comparable magnitude in the close vicinity of the quantum critical point, where the ferro- or antiferro- states

disappear under e.g. pressure.

The paper is composed as follows. In Sec. II we provide the principal aspects of real-space spin-triplet pairing induced by the Hund's rule coupling, and introduce the band-renormalization factors for our two-band model. Furthermore, in subsections A and B of Sec. II we explain how the effective Hamiltonian is constructed, according to the statistically consistent Gutzwiller approximation, for all the phases considered in this work. In Sec. III we discuss the phase diagram, and the principal order parameters in the considered phases, whereas Sec. IV contains the concluding remarks.

2. Model and method

We consider the extended orbitally-degenerate Hubbard Hamiltonian, which has the form

$$\begin{aligned}\hat{H} = & \sum_{ij(i\neq j)ll'\sigma} t_{ij}^{ll'}\hat{c}_{il\sigma}^{\dagger}\hat{c}_{jl'\sigma} + (U'+J)\sum_{i}\hat{n}_{i1}\hat{n}_{i2} \\ & + U\sum_{il}\hat{n}_{il\uparrow}\hat{n}_{il\downarrow} - J\sum_{ill'(l\neq l')}\left(\hat{\mathbf{S}}_{il}\cdot\hat{\mathbf{S}}_{il'} + \frac{3}{4}\hat{n}_{il}\hat{n}_{il'}\right) \\ & = \hat{H}^{0} + \hat{H}^{at} \,,\end{aligned} \tag{1}$$

where $l = 1, 2$ label the orbitals and the first term describes electron hopping between atomic sites i and j. For $l \neq l'$ this term represents electron hopping with change of the orbital (i.e., hybridization in momentum space). The next two terms describe the Coulomb interactions between electrons on the same atomic site. However the second term contains also the contribution, originating from the exchange interaction (J). The last term expresses the Hund's rule i.e., the ferromagnetic exchange between electrons localized on the same site, but on different orbitals. This term contributes to magnetic coupling and is responsible for the spin-triplet pairing leading to magnetic ordering, superconductivity and coexistent magnetic-superconducting phases. In the Hamiltonian (1), we have disregarded the pair hopping term $(J/2)\sum_{il\neq l'}\hat{c}_{il\uparrow}^{\dagger}\hat{c}_{il\downarrow}^{\dagger}\hat{c}_{il'\downarrow}\hat{c}_{il'\uparrow}$ and the so-called correlated hopping term $\sim V\sum_{il\neq l'}\hat{n}_{il\bar{\sigma}}(\hat{c}_{il\sigma}^{\dagger}\hat{c}_{il'\sigma} + H.C.)$. This is because their magnitude depends on the double occupancy probability which is small for $U > W$ (see below), where W is the bare bandwidth. Additionally the coupling constant V for e_g, $3d$ orbitals is smaller than $J \approx 4V$ [44].

In our variational method we assume that the correlated state $|\Psi_G\rangle$ of the system can be expressed in the following manner

$$|\Psi_G\rangle = \hat{P}_G|\Psi_0\rangle \,, \tag{2}$$

where $|\Psi_0\rangle$ is the normalized non-correlated state to be determined later and $\hat{P}_G$ is the Gutzwiller correlator selected in the following form

$$\hat{P}_G = \prod_i \hat{P}_{G|i} = \prod_i \sum_{I,I'} \lambda_{I,I'}^{(i)} |I\rangle_{ii}\langle I'| \,. \tag{3}$$

Here, $\lambda^{(i)}_{I,I'}$ are the variational parameters, which are assumed to be real. In the two-band situation the local basis consists of 16 states (see Table 5), which are defined as follows

$$|I\rangle_i = \hat{C}^{\dagger}_{i,I}|0\rangle_i \equiv \prod_{\gamma\in I}\hat{c}^{\dagger}_{i\gamma}|0\rangle_i = \hat{c}^{\dagger}_{i\gamma_1}...\hat{c}^{\dagger}_{i\gamma_{|I|}}|0\rangle_i \ , \tag{4}$$

where $\gamma = 1, 2, 3, 4$ labels the four spin-orbital states (in the $l\sigma$ notation: $1\uparrow, 1\downarrow, 2\uparrow, 2\downarrow$, respectively) and $|I|$ is the number of electrons in the local state $|I\rangle$. In general, an index I can be interpreted as a set in the usual mathematical sense. The creation operators in (4) are placed in ascending order, i.e., $\gamma_1 < ... < \gamma_{|I|}$. In an analogous manner, one can define the product of annihilation operators

$$\hat{C}_{i,I} = \prod_{\gamma\in I}\hat{c}_{i\gamma} = \hat{c}_{i\gamma_1}...\hat{c}_{i\gamma_{|I|}} \ , \tag{5}$$

which are placed in descending order $\gamma_1 > ... > \gamma_{|I|}$.

Table 1. The local basis consisting of 16 configurations containing $N_e = 0, ..., 4$ electrons, which are enumerated as shown below.

$\|0,0\rangle$	1	$\|0,\downarrow\rangle$	5	$\|\downarrow,\downarrow\rangle$	9	$\|\uparrow\downarrow,\uparrow\rangle$	13
$\|\uparrow,0\rangle$	2	$\|\uparrow\downarrow,0\rangle$	6	$\|\uparrow,\downarrow\rangle$	10	$\|\downarrow,\uparrow\downarrow\rangle$	14
$\|0,\uparrow\rangle$	3	$\|0,\uparrow\downarrow\rangle$	7	$\|\downarrow,\uparrow\rangle$	11	$\|\uparrow\downarrow,\downarrow\rangle$	15
$\|\downarrow,0\rangle$	4	$\|\uparrow,\uparrow\rangle$	8	$\|\uparrow,\uparrow\downarrow\rangle$	12	$\|\uparrow\downarrow,\uparrow\downarrow\rangle$	16

The operator $|I\rangle_{ii}\langle I'|$ can be expressed in terms of $\hat{C}^{\dagger}_I$ and $\hat{C}_I$ in the following manner

$$\hat{m}_{I,I'|i} \equiv |I\rangle_{ii}\langle I'| = \hat{C}^{\dagger}_{i,I}\hat{C}_{i,I'}\hat{n}^h_{I\cup I'|i} \ , \tag{6}$$

where

$$\hat{n}^h_{I\cup I'|i} = \prod_{\gamma\in\overline{I\cup I'}}(1-\hat{n}_{i\gamma}) \ . \tag{7}$$

In the subsequent discussion, we write expectation values with respect to $|\Psi_0\rangle$ as

$$\langle\hat{O}\rangle_0 = \langle\Psi_0|\hat{O}|\Psi_0\rangle \ , \tag{8}$$

while the expectation values with respect to $|\Psi_G\rangle$ will be denoted by

$$\langle\hat{O}\rangle_G = \frac{\langle\Psi_G|\hat{O}|\Psi_G\rangle}{\langle\Psi_G|\Psi_G\rangle} \ . \tag{9}$$

The most important step within the Gutzwiller approach is to derive the formula for the expectation value of the Hamiltonian $\hat{K} = \hat{H} - \mu\hat{N}$ with respect to $|\Psi_G\rangle$. This can be done in the limit of infinite dimensions by a diagrammatic approach [25] which uses the variational analog of Feynmann diagrams. By applying this method to the interaction part of the Hamiltonian (1), which is completely of intra-site character, one obtains

$$\langle\hat{H}^{at}\rangle_G = L\sum_{I_1,I_4}\bar{E}_{I_1,I_4}\langle\hat{m}_{I_1,I_4}\rangle_0 \ , \tag{10}$$

where

$$\bar{E}_{I_1,I_4} = \sum_{I_2,I_3} \lambda_{I_1,I_2}\lambda_{I_3,I_4}\langle I_2|\hat{H}^{at}|I_3\rangle \ , \tag{11}$$

and L is the number of atomic sites. In (10) we have assumed that our system is homogeneous. Note that, with the use of Wick's theorem, the purely local expectation values $\langle \hat{m}_{I_1,I_4}\rangle_0$ can be expressed in terms of the local single-particle density matrix elements $\langle \hat{c}^{\alpha}_{i\gamma}\hat{c}^{\alpha'}_{i\gamma'}\rangle_0$. Here, $\hat{c}^{\alpha}_{i\gamma}$ are either creation or annihilation operators.

The expectation value of the single-particle part in the Hamiltonian (1) can be cast to the form

$$\langle \hat{H}^0\rangle_G = \sum_{ij(i\neq j)}\sum_{\gamma\gamma'\tilde{\gamma}\tilde{\gamma}'} t_{ij}^{\gamma\gamma'}\left(q_{\gamma\tilde{\gamma}}q_{\gamma'\tilde{\gamma}'} - \bar{q}_{\gamma\tilde{\gamma}}\bar{q}_{\gamma'\tilde{\gamma}'}\right)\langle \hat{c}^{\dagger}_{i,\tilde{\gamma}}\hat{c}_{j,\tilde{\gamma}'}\rangle_0 \tag{12}$$

where we have assumed that the renormalization factors q and $\bar{q}$ are real numbers and $t^{\gamma\gamma'} = t^{\gamma'\gamma}$. Moreover, in the equation above we have neglected the part containing the inter-site pairing terms $\langle \hat{c}^{\dagger}_{i,\gamma}\hat{c}^{\dagger}_{j,\gamma'}\rangle_0$ and $\langle \hat{c}_{i,\gamma}\hat{c}_{j,\gamma'}\rangle_0$ as we are going to concentrate on the Hund's rule induced intra-site spin-triplet paired states. The inter-site pairing amplitudes are much smaller than the intra-site terms, in the considered model. The renormalization factors, introduced in (12), have the form

$$q_{\gamma\tilde{\gamma}} = \sum_{I(\tilde{\gamma}\notin I)}\left[\sum_{I'}\mathrm{fsgn}(\tilde{\gamma},I)m^{0(\tilde{\gamma})}_{I,I'}c^{*}_{I\cup\tilde{\gamma},I'|\gamma} + \sum_{I'(\tilde{\gamma}\notin I')}\mathrm{fsgn}(\tilde{\gamma},I)m^{0}_{I',I\cup\tilde{\gamma}}c^{*}_{I',I|\gamma}\right] , \tag{13}$$

where $m^0_{I,I'} = \langle \hat{m}_{I,I'}\rangle_0$ and $m^{0(\tilde{\gamma})}_{I,I'} = \langle \hat{m}^{(\tilde{\gamma})}_{I,I'}\rangle_0$. Here we have introduced the operator

$$\hat{m}^{(\gamma)}_{I,I'} = \hat{C}^{\dagger}_{i,I}\hat{C}_{i,I'}\hat{n}^{h}_{I\cup I'\cup\gamma|i} \ . \tag{14}$$

The parameters $c^{*}_{I_1,I_2|\gamma}$ in (13) are defined as

$$c^{*}_{I_1,I_2|\gamma} = \sum_{I(\gamma\notin I)}\mathrm{fsgn}(\gamma,I)\lambda_{I_1,I\cup\gamma}\lambda_{I,I_2} \ , \tag{15}$$

where we introduced the fermionic sign function

$$\mathrm{fsgn}(\gamma,I) \equiv \langle I\cup\gamma|\hat{c}^{\dagger}_{\gamma}|I\rangle \ . \tag{16}$$

The renormalization factors $\bar{q}_{\gamma\tilde{\gamma}}$ have to be included in (12), when there are nonzero gap parameters ($\langle \hat{c}^{\alpha}\hat{c}^{\alpha}\rangle_0 \neq 0$) in $|\Psi_0\rangle$, which is the case considered here. The form of $\bar{q}_{\gamma\tilde{\gamma}}$ is as follows

$$\bar{q}_{\gamma\tilde{\gamma}} = \sum_{I(\tilde{\gamma}\notin I)}\left[\sum_{I'}\mathrm{fsgn}(\tilde{\gamma},I)m^{0(\tilde{\gamma})}_{I',I}c^{*}_{I',I\cup\tilde{\gamma}|\gamma} + \sum_{I'(\tilde{\gamma}\notin I')}\mathrm{fsgn}(\tilde{\gamma},I)m^{0}_{I\cup\tilde{\gamma},I'}c^{*}_{I,I'|\gamma}\right] . \tag{17}$$

The remaining part of $\langle \hat{K}\rangle_G$ that has to be derived is the expectation value $\langle \hat{N}\rangle_G$. Also in this case, the diagrammatic evaluation in infinite dimensions gives the proper formula,

$$\langle \hat{N}\rangle_G = \sum_{i\gamma}\langle \hat{n}_{i\gamma}\rangle_G \ , \tag{18}$$

where

$$\langle \hat{n}_{i\gamma} \rangle_G = \sum_{I_1,I_4} N^{\gamma}_{I_1,I_4} m^0_{I_1,I_4} \ , \tag{19}$$

and

$$N^{\gamma}_{I_1,I_4} = \sum_{I(\gamma \notin I)} \lambda_{I_1,I\cup\gamma} \lambda_{I\cup\gamma,I_4} \ . \tag{20}$$

The pairing densities in the correlated state that are going to be useful in the subsequent discussion can be expressed in the following way

$$\langle \hat{c}_{i\gamma} \hat{c}_{i\gamma'} \rangle_G = \sum_{I_1,I_4} S^{\gamma\gamma'}_{I_1,I_4} m^0_{I_1,I_4} \ , \tag{21}$$

where

$$S^{\gamma\gamma'}_{I_1,I_4} = \sum_{I(\gamma\gamma' \notin I)} \lambda_{I_1,I} \lambda_{I\cup(\gamma\gamma'),I_4} \mathrm{fsgn}(\gamma, I) \mathrm{fsgn}(\gamma', I) \mathrm{fsgn}(\gamma', \gamma) \ . \tag{22}$$

Using (10), (12), and (18) one can express $\langle \hat{K} \rangle_G$ in terms of the variational parameters $\lambda_{I,I'}$, local and non-local single particle density matrix elements ,$\langle \hat{c}^{\alpha}_{i\gamma} \hat{c}^{\alpha'}_{i\gamma'} \rangle_0$, $\langle \hat{c}^{\dagger}_{i,\gamma} \hat{c}_{j,\gamma'} \rangle_0$, and the matrix elements of the atomic part of the atomic Hamiltonian represented in the local basis $\langle I | \hat{H}^{at} | I' \rangle$.

The formula for $\langle \hat{K} \rangle_G$, obtained in the way described above, can be written as an expectation value of an effective Hamiltonian $\hat{K}_{GA}$, evaluated with respect to $|\Psi_0\rangle$

$$\begin{aligned} \hat{K}_{GA} = & \sum_{ij(i\neq j)} \sum_{\gamma\gamma'\tilde{\gamma}\tilde{\gamma}'} t^{\gamma\gamma'}_{ij} \left(q_{\gamma\tilde{\gamma}} q_{\gamma'\tilde{\gamma}'} - \bar{q}_{\gamma\tilde{\gamma}} \bar{q}_{\gamma'\tilde{\gamma}'} \right) \hat{c}^{\dagger}_{i,\tilde{\gamma}} \hat{c}_{j,\tilde{\gamma}'} \\ & - \mu \sum_{i\gamma} q^s_{\gamma} \hat{n}_{i\gamma} + L \sum_{I_1,I_4} \bar{E}_{I_1,I_4} \langle \hat{m}_{I_1,I_4} \rangle_0, \end{aligned} \tag{23}$$

where $q^s_{\gamma} = \langle \hat{n}_{i\gamma} \rangle_G / \langle \hat{n}_{i\gamma} \rangle_0$. There is no guarantee that the condition

$$\langle \hat{n}_{i\gamma} \rangle_G = \langle \hat{n}_{i\gamma} \rangle_0 \ , \tag{24}$$

is fulfilled. It turns out that it is fulfilled for the paramagnetic and the magnetically ordered phases of our two-band system, however it is not for the superconducting phases. Physically it is most sensible to fix $\langle \hat{n} \rangle_G$ instead of $\langle \hat{n} \rangle_0$, during the minimization. This is the reason why we include the term $-\mu \hat{N}$ already at the beginning of our derivation in $\langle \hat{K} \rangle_G$. In this manner the chemical potential μ refers to the initial correlated system, not to the effective non-correlated one (for which the chemical potential can be different).

Having in mind that there are 16 states in the local basis there could be up to $16 \times 16 = 256$ variational parameters $\lambda_{I,I'}$. However, for symmetry reasons many of these parameters are zero. The finite parameters can be identified by the following rule

$$\lambda_{I,I'} \neq 0 \Leftrightarrow \langle \hat{m}_{I,I'} \rangle_0 \neq 0 \vee \langle I | \hat{H}^{at} | I' \rangle \neq 0; \, . \tag{25}$$

It should also be noted that, as shown in [25], the variational parameters are not independent since they have to obey the constrains

$$\begin{aligned} \langle \hat{P}^2_{G|i} \rangle_0 &= 1, \\ \langle \hat{c}^\dagger_{i\gamma} \hat{P}^2_{G|i} \hat{c}_{i\gamma'} \rangle_0 &= \langle \hat{c}^\dagger_{i\gamma} \hat{c}_{i\gamma'} \rangle_0, \\ \langle \hat{c}^\dagger_{i\gamma} \hat{P}^2_{G|i} \hat{c}^\dagger_{i\gamma'} \rangle_0 &= \langle \hat{c}^\dagger_{i\gamma} \hat{c}^\dagger_{i\gamma'} \rangle_0, \\ \langle \hat{c}_{i\gamma} \hat{P}^2_{G|i} \hat{c}_{i\gamma'} \rangle_0 &= \langle \hat{c}_{i\gamma} \hat{c}_{i\gamma'} \rangle_0 \ , \end{aligned} \tag{26}$$

which are going to be used to fix some of the parameters $\lambda_{I,I'}$.

The results presented in this work have been obtained for the case of a square lattice with the band dispersions

$$\epsilon_{1\mathbf{k}} = \epsilon_{2\mathbf{k}} \equiv \epsilon_{\mathbf{k}} = 2t(\cos(k_x) + \cos(k_y)) \ , \tag{27}$$

and also

$$\epsilon_{12\mathbf{k}} = \epsilon_{21\mathbf{k}} = \beta_h \epsilon_{\mathbf{k}} \ , \tag{28}$$

where $\beta_h \in [0, 1]$. The orbital degeneracy and spatial homogeneity allow us to write

$$\begin{aligned} \langle \hat{n}_{i1} \rangle_G &= \langle \hat{n}_{i2} \rangle_G \equiv n_G/2, \\ \langle \hat{S}^z_{i1} \rangle_G &= \langle \hat{S}^z_{i2} \rangle_G \equiv S^z_G \ , \end{aligned} \tag{29}$$

where

$$\begin{aligned} \hat{S}^z_{il} &\equiv \frac{1}{2}\big(\hat{n}_{il\uparrow} - \hat{n}_{il\downarrow}\big), \\ \hat{n}_{il} &\equiv \hat{n}_{il\uparrow} + \hat{n}_{il\downarrow} \ . \end{aligned} \tag{30}$$

Similar expressions as in (29) can be introduced for the expectation values in the non-correlated state $|\Psi_0\rangle$.

Before discussing the principal magnetic and/or spin-triplet superconducting phases, we introduce first the exact expression of the full exchange operator (the last term of our Hamiltonian) via the local spin-triplet pairing operators ($\hat{A}^\dagger_{im}$, $\hat{A}_{im}$) namely

$$\sum_{ll'(l \neq l')} \left(\hat{\mathbf{S}}_{il} \cdot \hat{\mathbf{S}}_{il'} + \frac{3}{4} \hat{n}_{il} \hat{n}_{il'} \right) = \sum_m \hat{A}^\dagger_{im} \hat{A}_{im} \ , \tag{31}$$

where

$$\hat{A}^\dagger_{i,m} \equiv \begin{cases} a^\dagger_{i1\uparrow} a^\dagger_{i2\uparrow} & m = 1 \\ a^\dagger_{i1\downarrow} a^\dagger_{i2\downarrow} & m = -1 \\ \frac{1}{\sqrt{2}} (a^\dagger_{i1\uparrow} a^\dagger_{i2\downarrow} + a^\dagger_{i1\downarrow} a^\dagger_{i2\uparrow}) & m = 0 \ . \end{cases} \tag{32}$$

We see that those two representations are mathematically equivalent, so the phase with $S^z_G = \langle \hat{S}^z_{il} \rangle_G \neq 0$ and that with the corresponding off-diagonal order parameter $\langle \hat{A}_{im} \rangle_G \neq 0$ (or $\langle \hat{A}^\dagger_{im} \rangle_G \neq 0$) should be treated on equal footing.

2.1. Statistically-consistent Gutzwiller method for superconducting and coexistent superconducting-ferromagnetic phases

In this subsection we will describe the SGA approach as applied to the selected phases characterized by the following order parameters

- Superconducting phase of type A1 coexisting with ferromagnetism (A1+FM): $S^z_{G|u} \neq 0$, $\Delta^G_1 \neq 0$, $\Delta^G_{-1} = \Delta^G_0 = 0$,
- Pure type A superconducting phase (A): $S^z_{G|u} = 0$, $\Delta^G_1 = \Delta^G_{-1} \neq 0$, $\Delta^G_0 = 0$,
- Pure ferromagnetic phase (FM): $S^z_{G|u} \neq 0$, $\Delta^G_1 = \Delta^G_{-1} = \Delta^G_0 = 0$,
- Paramagnetic phase (NS): $S^z_{G|u} = 0$, $\Delta^G_1 = \Delta^G_{-1} = \Delta^G_0 = 0$,

where $S^z_{G|u}$ refers to the uniform magnetic moment and

$$\Delta^G_m = \langle \hat{A}_{im} \rangle_G, \quad (\Delta^G_m)^* = \langle \hat{A}^\dagger_{im} \rangle_G \ , \tag{33}$$

are the spin-triplet local gap parameters which are assumed as real here.

The (correlated) order parameters which have been used above to define the relevant phases can also be defined for the non-correlated state $|\Psi_0\rangle$. With these, we can determine which of the matrix elements $\langle \hat{m}_{I,I'} \rangle_0$ are equal to zero for the considered phases. The assumption (25) then allows us to choose the non-diagonal variational parameters, $\lambda_{I,I'}$, that have to be taken into account during the calculations. We list their indexes (I, I') in Table 2.

Table 2. Nonzero, off-diagonal local variational parameters ($\lambda_{I,I'} = \lambda_{I',I}$) that are used in the calculations for the considered phases.

I	1	2	3	4	5	8	9	8	10	1	1
I'	16	15	14	13	12	16	16	9	11	8	9

As one can see from Table 2, the off-diagonal variational parameters correspond to the creation or annihilation of the Cooper pair in the proper spin-triplet states $|1\uparrow, 2\uparrow\rangle$ and $|1\downarrow, 2\downarrow\rangle$ (phase A). Because in the A1 phase only electrons with spin-up are paired one can assume that $\lambda_{1,16}$, $\lambda_{2,15}$, $\lambda_{3,14}$, $\lambda_{8,16}$, $\lambda_{8,9}$ are zero (and their transoposed corespondants - $\lambda_{I,I'} = \lambda_{I',I}$). For the FM and NS unpaired states only $\lambda_{10,11}$ and $\lambda_{11,10}$ are nonzero. They correspond to the two non-diagonal matrix elements of the atomic Hamiltonian, $\langle I|\hat{H}^{at}|I'\rangle$. With the information contained in Table 2, one obtains the following relations regarding the band-narrowing renormalization factors

$$\begin{aligned} q_{l\sigma,l'\sigma'} \neq 0 \Leftrightarrow l = l' \wedge \sigma = \sigma', \\ \bar{q}_{l\sigma,l'\sigma'} \neq 0 \Leftrightarrow l \neq l' \wedge \sigma = \sigma' \ , \end{aligned} \tag{34}$$

where we have again used the $\gamma = l\sigma$ notation. Due to the degeneracy of our bands we find

$$\begin{aligned} q_{1\sigma,1\sigma} &= q_{2\sigma,2\sigma} \equiv q_\sigma \ , \\ \bar{q}_{1\sigma,2\sigma} &= -\bar{q}_{2\sigma,1\sigma} \equiv \bar{q}_\sigma \ , \\ q^s_{1\sigma} &= q^s_{2\sigma} \equiv q^s_\sigma \ . \end{aligned} \tag{35}$$

Using the equations above we can rewrite the Hamiltonian (23) in the more explicit form, in reciprocal space

$$\hat{K}_{GA} = \sum_{\mathbf{k}l\sigma} (Q_\sigma \epsilon_{\mathbf{k}} - q^s_\sigma \mu) \hat{n}_{\mathbf{k}l\sigma} + \sum_{\mathbf{k}ll'(l\neq l')\sigma} Q_\sigma \epsilon_{\mathbf{k}12} \hat{c}^\dagger_{\mathbf{k}l\sigma} \hat{c}_{\mathbf{k}l'\sigma} + L \sum_{I_1,I_4} \bar{E}_{I_1,I_4} \langle \hat{m}_{I_1,I_4} \rangle_0 \ , \tag{36}$$

where the renormalization factors Q_σ are defined as

$$Q_\sigma \equiv q^2_\sigma - \bar{q}^2_\sigma \ . \tag{37}$$

Having the formula for $\hat{K}_{GA}$, given by (36), one can introduce next the so-called *statistically-consistent Gutzwiller approximation* (SGA). In this method, the mean fields (such as the expectation values for magnetization or superconducting gaps) are treated as variational mean-field order parameters with respect to which the energy of the system is minimized. However, in order to make sure that they coincide with the corresponding values calculated self-consistently, additional constraints have to be introduced with the help of the Lagrange-multiplier method [26, 27, 28, 29]. This leads to supplementary terms in the effective Hamiltonian of the following form

$$\begin{aligned} \hat{K}_\lambda = \hat{K}_{GA} &- \sum_{m=\pm 1} \left[\lambda_m \left(\sum_{\mathbf{k}} \hat{A}_{\mathbf{k}m} - L\Delta^0_m \right) + H.C. \right] \\ &- \lambda_S \left(\sum_{\mathbf{k}l} \hat{S}^z_{\mathbf{k}l} - 2LS^z_0 \right) - \lambda_n \left(\sum_{\mathbf{k}l\sigma} q^s_{l\sigma} \hat{n}_{kl\sigma} - Ln_G \right) \ , \end{aligned} \tag{38}$$

where the Lagrange multipliers λ_m, λ_s, and λ_n are introduced to assure that the averages $\langle \hat{A}_{\mathbf{k}m} \rangle$, $\langle \hat{S}_{\mathbf{k}l} \rangle$ and $\langle \hat{n}_{\mathbf{k}l\sigma} \rangle$ calculated either from the corresponding self-consistent equations or variationally, coincide with each other, which guarantees the fulfillment of the fundamental Bogoliubov principle (otherwise violated in some cases [29]). In this manner we do not alter any of the infinite-dimension features of the approach, used to derive the effective ground-state (or the free energy) functional, but instead form the consistent (renormalized) mean field theory of the correlated fermion system at hand.

Introducing the four-component representation of single-particle operators

$$\hat{\mathbf{f}}^\dagger_{\mathbf{k}\sigma} = (\hat{c}^\dagger_{\mathbf{k}1\sigma}, \hat{c}^\dagger_{\mathbf{k}2\sigma}, \hat{c}_{-\mathbf{k}1\sigma}, \hat{c}_{-\mathbf{k}2\sigma}) \ , \tag{39}$$

we can write down the effective Hamiltonian in the following form

$$\begin{aligned} \hat{K}_\lambda = &\frac{1}{2} \sum_{\mathbf{k}\sigma} \hat{\mathbf{f}}^\dagger_{\mathbf{k}\sigma} \hat{\mathbf{M}}_{\mathbf{k}\sigma} \hat{\mathbf{f}}_{\mathbf{k}\sigma} + \sum_{\mathbf{k}\sigma} \tilde{\epsilon}_{\mathbf{k}\sigma} + 2L \sum_{m=\pm 1} \lambda_m \Delta^0_m + 2L\lambda_S S^z_0 + L\lambda_n n_G \\ &+ L \sum_{I_1,I_4} \bar{E}_{I_1,I_4} \langle \hat{m}_{I_1,I_4} \rangle_0 \ , \end{aligned} \tag{40}$$

where $\hat{\mathbf{M}}_{\mathbf{k}\sigma}$ is a 4x4 orthogonal matrix

$$\hat{\mathbf{M}}_{\mathbf{k}\sigma} = \begin{pmatrix} \tilde{\epsilon}_{\mathbf{k}\sigma} & Q_\sigma \epsilon_{\mathbf{k}12} & 0 & \lambda_\sigma \\ Q_\sigma \epsilon_{\mathbf{k}12} & \tilde{\epsilon}_{\mathbf{k}\sigma} & -\lambda_\sigma & 0 \\ 0 & -\lambda_\sigma & -\tilde{\epsilon}_{\mathbf{k}\sigma} & -Q_\sigma \epsilon_{\mathbf{k}12} \\ \lambda_\sigma & 0 & -Q_\sigma \epsilon_{\mathbf{k}12} & -\tilde{\epsilon}_{\mathbf{k}\sigma} \end{pmatrix} . \tag{41}$$

Here we introduced $\lambda_\uparrow$ and $\lambda_\downarrow$ which correspond to the Lagrange parameters $\lambda_{m=1}$ and $\lambda_{m=-1}$, respectively. The bare quasiparticle energies $\tilde{\epsilon}_{\mathbf{k}l\sigma}$ are defined as

$$\tilde{\epsilon}_{\mathbf{k}\sigma} = Q_\sigma \epsilon_{\mathbf{k}} - q_\sigma^s(\mu + \lambda_n) - \frac{1}{2}\sigma\lambda_S . \tag{42}$$

The diagonalization of the matrix (41) yields the quasiparticle eigen-energies in the paired states of the following form

$$\begin{aligned} E_{\mathbf{k}1\sigma} &= \sqrt{\tilde{\epsilon}_{\mathbf{k}\sigma}^2 + \lambda_\sigma^2} - Q_\sigma \epsilon_{\mathbf{k}12} , \\ E_{\mathbf{k}2\sigma} &= \sqrt{\tilde{\epsilon}_{\mathbf{k}\sigma}^2 + \lambda_\sigma^2} + Q_\sigma \epsilon_{\mathbf{k}12} , \\ E_{\mathbf{k}3\sigma} &= -\sqrt{\tilde{\epsilon}_{\mathbf{k}\sigma}^2 + \lambda_\sigma^2} - Q_\sigma \epsilon_{\mathbf{k}12} , \\ E_{\mathbf{k}4\sigma} &= -\sqrt{\tilde{\epsilon}_{\mathbf{k}\sigma}^2 + \lambda_\sigma^2} + Q_\sigma \epsilon_{\mathbf{k}12} . \end{aligned} \tag{43}$$

The first two energies correspond to the doubly degenerate spin-split quasiparticle excitations in the A phase, whereas the remaining two are their quasihole correspondents.

Even though the Gutzwiller approach was derived for zero temperature, we may construct the grand-potential function F_λ (per atomic site) that corresponds to the effective Hamiltonian (40), i.e.,

$$\begin{aligned} F_\lambda = &-\frac{1}{L\beta}\sum_{\mathbf{k}l\sigma} \ln\left[1 + e^{-\beta E_{\mathbf{k}l\sigma}}\right] + \frac{1}{L}\sum_{\mathbf{k}\sigma} \tilde{\epsilon}_{\mathbf{k}\sigma} + 2\sum_{m=\pm 1} \lambda_m \Delta_m^0 + 2\lambda_S S_0^z + (\lambda_n + \mu) n_G \\ &+ \sum_{I_1, I_4} \bar{E}_{I_1, I_4} \langle \hat{m}_{I_1, I_4} \rangle_0 . \end{aligned} \tag{44}$$

The values of the mean fields, the variational parameters, and the Lagrange multipliers are found by minimizing the F_λ functional, i.e., the necessary conditions for minimum are

$$\frac{\partial F_\lambda}{\partial \vec{A}} = 0 , \quad \frac{\partial F_\lambda}{\partial \vec{\Lambda}_V} = 0 , \quad \frac{\partial F_\lambda}{\partial \vec{\Lambda}_L} = 0 , \tag{45}$$

where $\vec{A}$, $\vec{\Lambda}_V$, $\vec{\Lambda}_L$ denote collectively the mean fields in the non-correlated state, the variational parameters and the Lagrange multipliers respectively. Additionally, the chemical potential, μ enters through the relation

$$\frac{\partial F_\lambda}{\partial n_G} = \mu . \tag{46}$$

After solving the complete set of equations, one still has to calculate the mean fields in the correlated state with the use of their analogs in the non-correlated state and the variational parameters using (19) and (21).

With the SGA method one minimises the variational ground state energy $\langle \hat{K} \rangle_G$ with respect to the variational parameters $\lambda_{I,I'}$ and the single-particle states $|\Psi_0\rangle$. Note that an alternative way for this minimization has been introduced, e.g., in [45]. Beyond the ground-state properties of $\hat{K}$ one is often also interested in the (effective) single-particle Hamiltonian (40) because its eigenvalues are interpreted as quasi-particle excitation energies [46].

2.2. Statistically-consistent Gutzwiller method for the coexistent antiferromagnetic-spin-triplet superconducting phase

To consider antiferromagnetism in the simplest case, we divide our system into two interpenetrating sublattices A and B. In accordance with this division, we define the annihilation operators on the sublattices

$$\hat{c}_{il\sigma} = \begin{cases} \hat{c}_{il\sigma A} & \text{for i} \in A \ , \\ \hat{c}_{il\sigma B} & \text{for i} \in B \ . \end{cases} \tag{47}$$

The same holds for the creation operators. Next, the Gutzwiller correlator can be expressed in the form

$$\hat{P}_G = \prod_{i(A)} \hat{P}^{(A)}_{G|i} \prod_{i(B)} \hat{P}^{(B)}_{G|i} \ , \tag{48}$$

where

$$\hat{P}^{(A/B)}_{G|i} = \sum_{I,I'} \lambda^{(A/B)}_{I,I'} |I\rangle_{ii}\langle I'| \ . \tag{49}$$

If we assume that charge ordering is absent, we have

$$\langle \hat{S}^z_{ilA} \rangle_G \equiv S^z_{G|s}, \quad \langle \hat{S}^z_{ilB} \rangle_G \equiv -S^z_{G|s} \ , \tag{50}$$

$$\langle \hat{n}_{ilA} \rangle_G = \langle n_{ilB} \rangle_G \equiv n_G/2 \ . \tag{51}$$

Similar expressions can be obtained for the case of expectation values taken in the state $|\Psi_0\rangle$. As one can see from (49), we have introduced separate sets of variational parameters ($\lambda^A_{I,I'}$ and $\lambda^B_{I,I'}$) for the two sublattices. Fortunately, it does not mean that we have twice as many variational parameters as in the preceding subsection. The parameters $\lambda^A_{I,I'}$ are related to the corresponding $\lambda^B_{I,I'}$ through

$$\lambda^{(A)}_{I_1,I_2} = \lambda^{(B)}_{I_3,I_4} \ , \tag{52}$$

where the states I_1 and I_2 have opposite spins to those in the I_3 and I_4 states, respectively. The same division has to be made for the renormalization factors q, $\bar{q}$

and q^s. They fulfill the transformation relations

$$\begin{aligned} q^A_{\gamma,\gamma'} &= q^B_{\bar{\gamma},\bar{\gamma}'}, \\ \bar{q}^A_{\gamma,\gamma'} &= \bar{q}^B_{\bar{\gamma},\bar{\gamma}'}, \\ q^s_{\gamma A} &= q^s_{\bar{\gamma}B} \ , \end{aligned} \tag{53}$$

where γ and $\bar{\gamma}$ are spin-orbitals with opposite spins. The coexistent superconducting-antiferromagnetic phase (SC+AF) can be defined in the following way

$$\begin{aligned} \Delta^G_{1A} = \Delta^G_{-1B} \equiv \Delta^G_+ \neq 0 \ , \\ \Delta^G_{-1A} = \Delta^G_{1B} \equiv \Delta^G_- \neq 0 \ , \\ S^z_{G|s} \neq 0 \ . \end{aligned} \tag{54}$$

Considerations analogical to those presented in subsection 2 lead to the conclusion that for both sublattices the non-diagonal variational parameters, $\lambda^A_{I,I'}$ and $\lambda^B_{I,I'}$, that have to be used in the calculations, appropriate for the SC+AF phase, are the same as those listed in Table 2. This fact, and the degeneracy of our bands, allow us to apply (35) for both sets of renormalization factors (for A and B sublattices), as we have

$$\begin{aligned} & q^A_{1\sigma,1\sigma} = q^A_{2\sigma,2\sigma} = q^B_{1\bar{\sigma},1\bar{\sigma}} = q^B_{2\bar{\sigma},2\bar{\sigma}} \equiv q_\sigma \ , \\ & \bar{q}^A_{1\sigma,2\sigma} = -\bar{q}^A_{2\sigma,1\sigma} \equiv \bar{q}_\sigma; \quad \bar{q}^B_{1\bar{\sigma},2\bar{\sigma}} = -\bar{q}^B_{2\bar{\sigma},1\bar{\sigma}} \equiv \bar{q}_\sigma \ , \\ & q^s_{1\sigma A} = q^s_{2\sigma A} = q^s_{1\bar{\sigma}B} = q^s_{2\bar{\sigma}B} \equiv q^s_\sigma \ , \end{aligned} \tag{55}$$

where $\bar{\sigma}$ represents the spin opposite to σ. Now, we can write down the Hamiltonian $\hat{K}_{GA}$ for the case of SC+AF phase

$$\begin{aligned} \hat{K}_{GA} = & \sum_{\mathbf{k}l\sigma} Q\epsilon_{\mathbf{k}} (\hat{c}^\dagger_{\mathbf{k}l\sigma A}\hat{c}_{\mathbf{k}l\sigma B} + \hat{c}^\dagger_{\mathbf{k}l\sigma B}\hat{c}_{\mathbf{k}l\sigma A}) + \sum_{\mathbf{k}ll'(l\neq l')\sigma} Q\epsilon_{\mathbf{k}12} (\hat{c}^\dagger_{\mathbf{k}l\sigma A}\hat{c}_{\mathbf{k}l'\sigma B} + \hat{c}^\dagger_{\mathbf{k}l\sigma B}\hat{c}_{\mathbf{k}l'\sigma A}) \\ & - \mu \sum_{\mathbf{k}l\sigma} (q^s_\sigma \hat{n}_{\mathbf{k}l\sigma A} + q^s_{\bar{\sigma}} \hat{n}_{\mathbf{k}l\sigma B}) + \frac{L}{2} \sum_{I_1,I_4} \bar{E}^A_{I_1,I_4} \langle \hat{m}^A_{I_1,I_4} \rangle_0 + \frac{L}{2} \sum_{I_1,I_4} \bar{E}^B_{I_1,I_4} \langle \hat{m}^B_{I_1,I_4} \rangle_0 \ , \end{aligned} \tag{56}$$

where

$$Q = q_\uparrow q_\downarrow - \bar{q}_\uparrow \bar{q}_\downarrow \ . \tag{57}$$

It should be noted that the sums in (56) are taken over all $L/2$ independent $\mathbf{k}$ states. As before, we apply the SGA method which leads to the effective Hamiltonian with the statistical-consistency constraints of the form

$$\begin{aligned} \hat{K}_\lambda = \hat{K}_{GA} & - \lambda_S \left[\sum_{\mathbf{k}l\sigma} \frac{1}{2} \sigma (\hat{n}_{\mathbf{k}l\sigma A} - \hat{n}_{\mathbf{k}l\sigma B}) - 2LS^z_{0|s} \right] \\ & - \lambda_+ \left[\sum_{\mathbf{k}} (\hat{A}_{\mathbf{k}1A} + \hat{A}_{\mathbf{k}-1B}) - L\Delta^0_+ + H.C. \right] \\ & - \lambda_- \left[\sum_{\mathbf{k}} (\hat{A}_{\mathbf{k}-1A} + \hat{A}_{\mathbf{k}1B}) - L\Delta^0_- + H.C. \right] \\ & - \lambda_n \left[\sum_{\mathbf{k}l\sigma} (q^s_\sigma \hat{n}_{\mathbf{k}l\sigma A} + q^s_{\bar{\sigma}} \hat{n}_{\mathbf{k}l\sigma B}) - Ln_G \right] \end{aligned} \tag{58}$$

Introducing now the eight-component composite operator

$$\hat{\mathbf{f}}^{\dagger}_{\mathbf{k}\sigma} \equiv (\hat{c}^{\dagger}_{\mathbf{k}1\sigma A}, \hat{c}^{\dagger}_{\mathbf{k}2\sigma A}, \hat{c}^{\dagger}_{\mathbf{k}1\sigma B}, \hat{c}^{\dagger}_{\mathbf{k}2\sigma B}, \hat{c}_{-\mathbf{k}1\sigma A}, \hat{c}_{-\mathbf{k}2\sigma A}, \hat{c}_{-\mathbf{k}1\sigma B}, \hat{c}_{-\mathbf{k}2\sigma B}) \ , \tag{59}$$

we can write down the effective Hamiltonian $\hat{K}_{\lambda}$ in the following form

$$\begin{aligned} \hat{K}_{\lambda} = & \frac{1}{2}\sum_{\mathbf{k}\sigma} \hat{\mathbf{f}}^{\dagger}_{\mathbf{k}\sigma} \hat{\mathbf{M}}_{\mathbf{k}\sigma} \hat{\mathbf{f}}_{\mathbf{k}\sigma} - (\mu + \lambda_n)(q^s_{\uparrow} + q^s_{\downarrow})L \\ & + 2L\lambda_{+}\Delta^0_{+} + 2L\lambda_{-}\Delta^0_{-} + 2L\lambda_S S^z_{0|s} + L\lambda_n n_G \\ & + \frac{L}{2}\sum_{I_1,I_4} \bar{E}^A_{I_1,I_4} \langle \hat{m}^A_{I_1,I_4} \rangle_0 + \frac{L}{2}\sum_{I_1,I_4} \bar{E}^B_{I_1,I_4} \langle \hat{m}^B_{I_1,I_4} \rangle_0 \ , \end{aligned} \tag{60}$$

where the explicit form of the 8x8 matrix is

$$\hat{\mathbf{M}}_{\mathbf{k}\sigma} = \begin{pmatrix} \eta^{-}_{\sigma} & 0 & Q\epsilon_{\mathbf{k}} & Q\epsilon_{\mathbf{k}12} & 0 & \lambda^A_{\sigma} & 0 & 0 \\ 0 & \eta^{-}_{\sigma} & Q\epsilon_{\mathbf{k}12} & Q\epsilon_{\mathbf{k}} & -\lambda^A_{\sigma} & 0 & 0 & 0 \\ Q\epsilon_{\mathbf{k}} & Q\epsilon_{\mathbf{k}12} & -\eta^{+}_{\sigma} & 0 & 0 & 0 & 0 & \lambda^B_{\sigma} \\ Q\epsilon_{\mathbf{k}12} & Q\epsilon_{\mathbf{k}} & 0 & -\eta^{+}_{\sigma} & 0 & 0 & -\lambda^B_{\sigma} & 0 \\ 0 & -\lambda^A_{\sigma} & 0 & 0 & -\eta^{-}_{\sigma} & 0 & -Q\epsilon_{\mathbf{k}} & -Q\epsilon_{\mathbf{k}12} \\ \lambda^A_{\sigma} & 0 & 0 & 0 & 0 & -\eta^{-}_{\sigma} & -Q\epsilon_{\mathbf{k}12} & -Q\epsilon_{\mathbf{k}} \\ 0 & 0 & 0 & -\lambda^B_{\sigma} & -Q\epsilon_{\mathbf{k}} & -Q\epsilon_{\mathbf{k}12} & \eta^{+}_{\sigma} & 0 \\ 0 & 0 & \lambda^B_{\sigma} & 0 & -Q\epsilon_{\mathbf{k}12} & -Q\epsilon_{\mathbf{k}} & 0 & \eta^{+}_{\sigma} \end{pmatrix} \ , \tag{61}$$

and

$$\begin{aligned} \lambda^A_{\uparrow} = \lambda^B_{\downarrow} \equiv \lambda_{+} \ ; \quad \lambda^A_{\downarrow} = \lambda^B_{\uparrow} \equiv \lambda_{-} \ , \\ \eta^{-}_{\sigma} = -\frac{1}{2}\sigma\lambda_S - q^s_{\sigma}(\mu + \lambda_n) \ ; \quad \eta^{+}_{\sigma} = -\frac{1}{2}\sigma\lambda_S + q^s_{\sigma}(\mu + \lambda_n) \ . \end{aligned} \tag{62}$$

Diagonalization of (61) leads to the quasi-particle energies $E_{\mathbf{k}l\sigma}$ $(l = 1, 2, 3, ..., 8)$. The corresponding grand potential function F_{λ} per atomic site now has the form

$$\begin{aligned} F_{\lambda} = & -\frac{2}{L\beta}\sum_{\mathbf{k}l\sigma} \ln\left[1 + e^{-\beta E_{\mathbf{k}l\sigma}}\right] - \mu(q^s_{\uparrow} + q^s_{\downarrow}) \\ & + 2\lambda_{+}\Delta^0_{+} + 2\lambda_{-}\Delta^0_{-} + 2\lambda_S S^z_{0|s} + (\lambda_n + \mu)n_G \\ & + \frac{L}{2}\sum_{I_1,I_4} \bar{E}^A_{I_1,I_4} \langle \hat{m}^A_{I_1,I_4} \rangle_0 + \frac{L}{2}\sum_{I_1,I_4} \bar{E}^B_{I_1,I_4} \langle \hat{m}^B_{I_1,I_4} \rangle_0 \ . \end{aligned} \tag{63}$$

As before, we minimize the F_{λ} function to determine the values of the mean fields, the variational parameters and the Lagrange parameters. The necessary conditions for the minimum are again expressed by (45) and (46). In the subsequent discussion we consider also the pure antiferromagnetic phase (AF), for which $S^z_{G|s} \neq 0$ but $\Delta_{+} = \Delta_{-} \equiv 0$. The number of equations that need to be solved is different for different phases considered in this work. In Table III we show how many equations are included in (45) and (46) for all phases discussed.

Table 3. Number of equations that have to be solved in the case of all considered here phases. To reduce the number of equations for particular phases we have used certain symmetry relations regarding the mean field parameters, the Lagrange multipliers, and the variational parameters.

phase	A	A1+FM	SC+AF	AF	NS	FM
No. of Eqs.	16	17	22	12	8	13

3. Results and discussion

Equations (45) and (46) have been solved numerically for all phases by means of the hybrd1 subroutine from the MINPACK library, which performs a modification of the Powell hybrid method. The maximal estimated error of the procedure was set to 10^{-7}. The derivatives in Eq. (45) and (46) were computed by using a 5-step stencil method with the step equal to $x = 10^{-4}$. For the sake of clarity, we have provided the acronyms representing the considered here phases In Table 4.

Table 4. Acronyms representing the considered phases.

A	pure type A superconducting phase
A1+FM	superconducting phase type A1 coexisting with ferromagnetism
SC+AF	superconducting phase coexisting with antiferromagnetism
FM	Pure ferromagnetic phase
AF	Pure antiferromagnetic phase
NS	Paramagnetic phase

We concentrate now on the detailed numerical analysis of the phase diagram and the microscopic characterization of the stable phases. Having in mind that for 3d orbitals $U' = U - 2J$, one obtains the HF condition for the pairing to occur, $U < 3J$ (see [22]). We discuss thus first and foremost the limit $U < 3J$, as it allows for a direct comparison of SGA with the HF solution. In this manner we can single out explicitly the role of correlations in stabilizing the relevant phases. One should note that in the considered regime ($U < 3J$) we have a model with intraatomic interorbital attractions leading to spin-triplet pairs. As the main attractive force is of intraatomic nature, we focus here on the local (s-wave) type of pairing only. In other words, as we discuss the situation with no or small hybridization, the intersite part of the pairing can be disregarded.

The calculations have been carried out for $U' = U - 2J$, $U = 2.2J$, $k_BT/W = 10^{-4}$. This leaves us still with three independent microscopic parameters in our model: n_G, J, and β_h. All the energies have been normalized to the bare band-width $W = 8|t|$ (as we consider the square lattice with nearest neighbor hopping). For comparison, we also show the results calculated by means of the combined HF-BCS≡HF approximation. This method is described in detail in our previous paper for the same model as considered here. We can also reproduce the HF results by using the Gutzwiller method described in this work and setting $\lambda_{I,I'} = \delta_{I,I'}$.

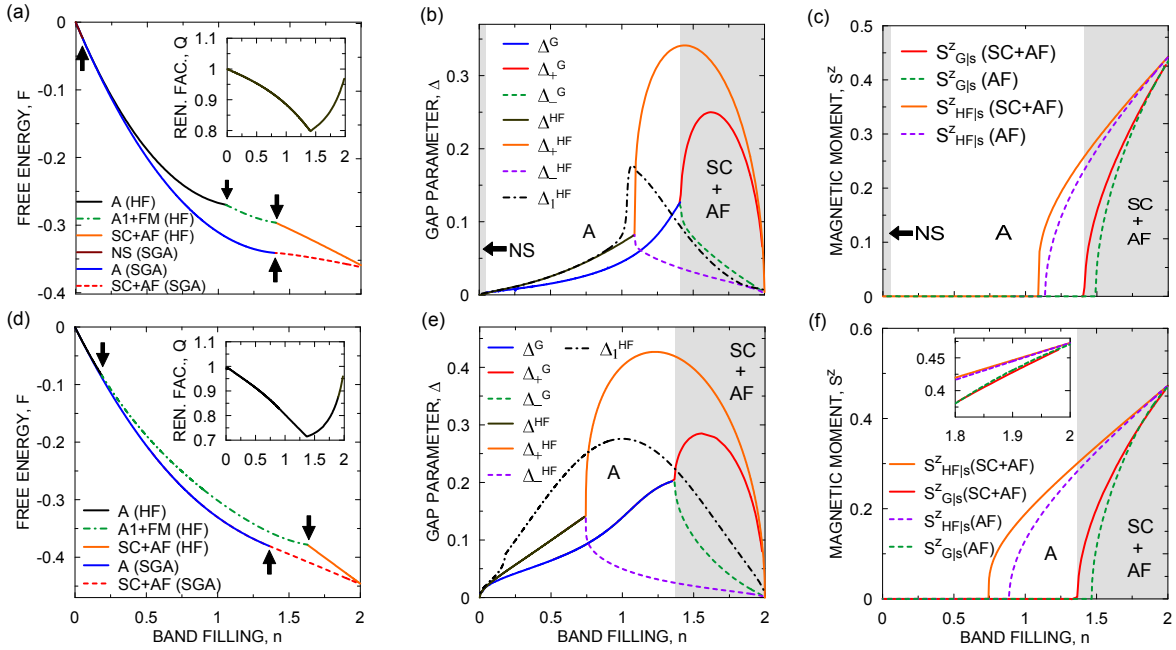

Figure 1. (Color online) Stable phases evolution vs. band filling. The superconducting gap parameter, magnetic moment and free energies as a function of band filling both for the HF and SGA, for $J = 0.299$: a, b, c and $J = 0.4545$: d, e, f. The results are for $\beta_h = 0.0$. The shaded regions represent the stability regions of the respective phases according to the SGA calculations. In Figs. a and d we show only the free energies of stable phases. The arrows in a and d mark the transitions points between phases.

In Fig. 1 we display the free energy, superconducting gaps, and magnetic moments for the two values $J = 0.299$ and $J = 0.4545$. As one can see from the free-energy plots (Figs. 1a and 1d), below some certain value of band filling, the pure superconducting phase of type A is stable for the SGA method. The increase of the number of electrons in the system, enhances the gap in this region (Figs. 1b and 1e). Above the critical band filling n_c, the staggered moment structure is created and a division into two gap parameters (Δ_+ and Δ_-) appears, as can be seen in Figs. 1b, 1e, 1c, and 1f. In this regime the SC+AF phase becomes stable.

When approaching half filling, both gaps gradually approach zero and for $n = 2$ we are left with a pure AF phase, which is of Slater insulating type evolving towards the Mott-Hubbard insulating state with the increasing U. As the staggered magnetic moment is rising (with the increase of n_G), the renormalization factor is approaching unity (cf. Insets to Fig. 1a and 1d). This is a consequence of the fact that for large values of S^z_G, the configurations with two electrons of opposite spin, on the same orbital, are ruled out.

Comparing Figs. 1a, 1b, 1c with Figs. 1d, 1e, 1f one sees that by increasing J we make the value of n_c smaller. However, the decrease in n_c is not as significant in SGA as it is in the HF case. In general the results presented Figs. 1b, 1c, 1e, 1f

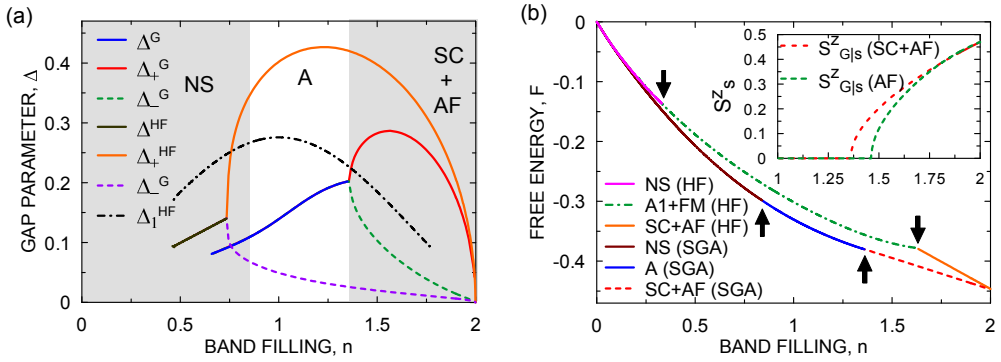

Figure 2. (Color online) The superconducting gaps (a) and the free energies (b) as a function of band filling for $J = 0.4545$ and $\beta_h = 0.1$. The shaded regions represent stability of respective phases according to the SGA calculations. The vertical arrows mark the phase borders.

look similar from the qualitative point of view for both methods. For SGA, the onset of antiferromagnetically ordered phase appears closer to half filling than for the HF method. Another difference between HF and SGA is that for the former the staggered moment in the SC+AF phase is increased by the appearance of SC for the whole range of band fillings, whereas in SGA calculations the staggered moment is slightly stronger in the AF phase than in the SC+AF phase for a small region close to the half-filled situation (inset of Fig. 1f).

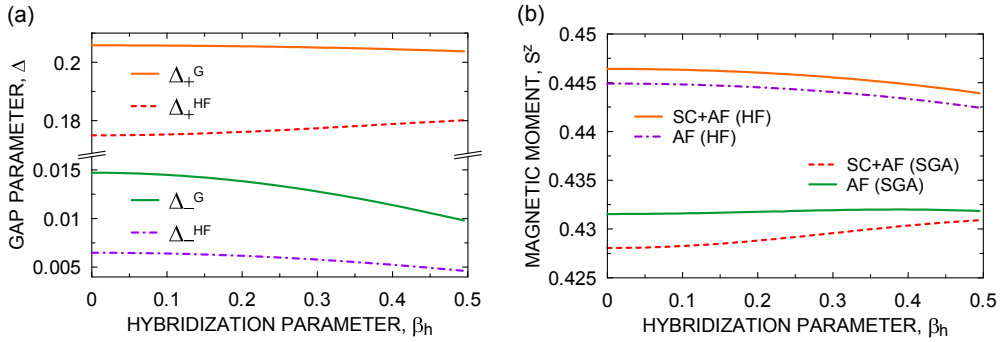

Figure 3. (Color online) The superconducting gaps and magnetic moment as a function of the hybridization strength, β_h, for $n = 1.9$, $J = 0.4545$, for the case of SC+AF and AF phases.

Significant differences between HF and SGA can be seen in Figs. 1c and 1f. While changing the band filling from 0 to 2, in the case of SGA calculations we move consecutively through the regions of stability of NS (for $J = 0.299$), A, SC+AF phases, and for $n = 2$ we have pure antiferromagnetism. The situation is different in the HF approximation, where in between the regions of stability of A and SC+AF phase, we have also the stable A1+FM phase. It should be also noted that the free energy calculated in SGA is lower than the one for the HF situation, as one should expect, since the correlations are accounted more accurately in the former method. It is also

very interesting that having the system with $U < 3J$, no pure ferromagnetism appears in this canonical model of itinerant magnetism.

In Fig. 2, we present the results for the case with nonzero hybridization parameter, $\beta_h = 0.1$. In this case there are no pure superconducting solutions below some certain value of the band filling (cf. Fig. 2a) and an extended region of NS stability occurs. The influence of the hybridization on the antiferromagnetically ordered phases is weak, as can be seen more clearly in Fig. 3. The changes in the superconducting gap and the magnetic moment in the coexistent phase triggered by the hybridization, are quite small even for larger values of β_h. It should be noted that the hybridization leads to inequivalent bands. Hence the pairing is robust against the Fermi wave vector mismatch for the carriers composing the Cooper pair, at least not for too large β_h.

Next, we discuss the J dependence of the superconducting gap, the free energy and the magnetic moment for selected values of band filling. As in the case of n-dependences the gap parameters and the magnetic moments in both SGA and HF approximation are qualitatively similar. In Fig. 4 we can see that for $n = 1.9$ even the free-energy plots and regions of stability of certain phases are comparable for both calculation schemes used. For the quarter-filled case (cf. Fig. 5) the A1+FM phase is stable above some value of J, according to the HF results. However, this is not the case in the SGA approximation, where the A phase has lower free energy even than the saturated ferromagnetic phase coexisting with superconductivity. Comparing Figs. 5b and 5d (as well as 1d and 2b) one sees that the region of stability of the A phase narrows down in favor of the NS phase, due to the influence of hybridization.

It is important to check whether the itinerant magnetic phases are stable in the regime $U' > J$ ($U > 3J$), i.e., when the superconductivity is absent in the HF approximation. For this purpose, in Fig. 6 we provide the band-filling dependence of the free energy corresponding to stable phases for $U = 4J$. Indeed, the paramagnetic and the magnetically ordered phases are stable for both methods of calculations. Therefore, for $U > 3J$ we recover the magnetic phase diagram for this model, which was

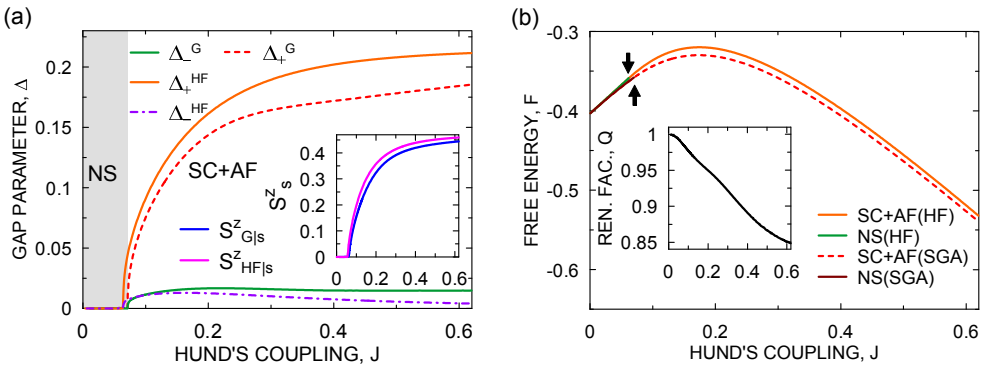

Figure 4. (Color online) The superconducting gaps in the SC+AF phase (a) and free energies of stable phases (b) as a function of Hund's coupling for $n = 1.9$ and $\beta_h = 0.1$. The shaded region represent the stability of NS phase according to the SGA results.

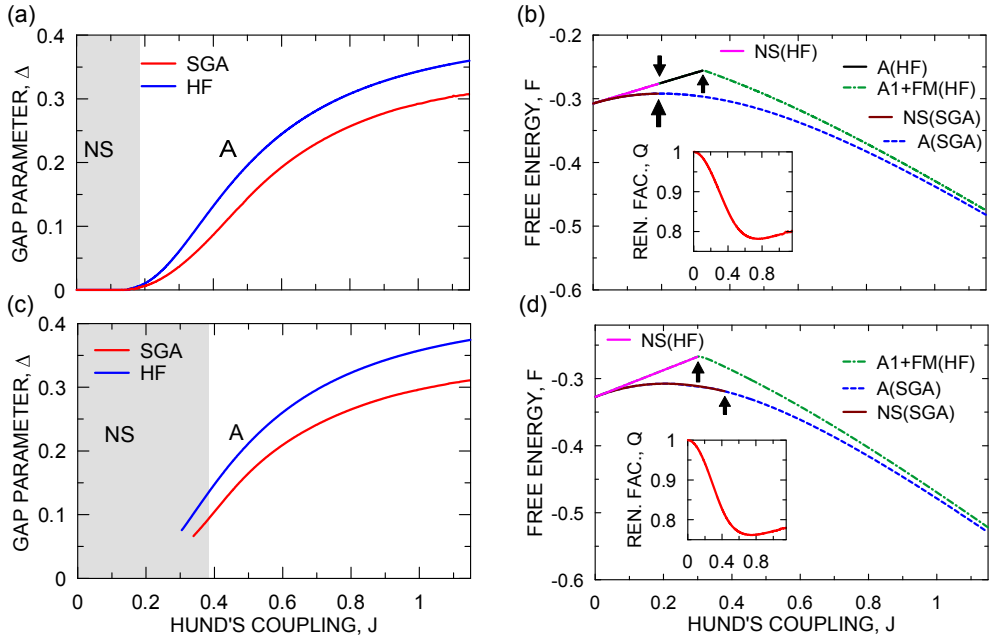

Figure 5. (Color online) The superconducting gaps in the A phase as a function of the Hund's coupling for $n = 1.0$ (a-for $\beta_h = 0.0$ and c-for $\beta_h = 0.1$) and free energies of stable phases corresponding to SGA and HF approximations (b-for $\beta_h = 0.0$ and d-for $\beta_h = 0.1$). The shaded regions represent the stability of the NS phase according to the SGA. The vertical arrows mark the border points between respective phases. Insets: Bandwidth renormalization factor for $\beta_h = 0$ (upper) and $\beta_h = 0.1$ (lower).

considered originally only in the context of magnetism. The free energy of the saturated ferromagnetic phase calculated by the SGA is very close to the one obtained by the HF approach. This is again caused by the circumstance that in the saturated state all of the spins are parallel and the double occupancies on the same orbital are absent. In this situation, the intra-orbital Coulomb interaction is automatically switched off. For the sake of completeness, we have plotted in Fig. 7a and 7b the double occupancy probability d, both in HF (d^0) and SGA (d^G) treatments. One should note a drastic reduction of d in SGA with the increasing J (and hence U). This is the reason why we have neglected both the so-called correlated-hopping and the pair-hopping terms in the starting Hamiltonian. It would be interesting to determine the stability of the coexistent phases in this regime ($U' > J$). Work along this line is in progress.

4. Conclusions

The principal purpose of this paper was to formulate a many-particle method which allows to investigate the spin-triplet real-space pairing in correlated system with an orbital degeneracy. To this end, we have carried out a detailed analysis using the statistically-consistent Gutzwiller approximation (SGA) for the two-band degenerate Hubbard model with the spin-triplet superconductivity and itinerant magnetism included, both treated on equal footing. Also, in our approach we have discussed

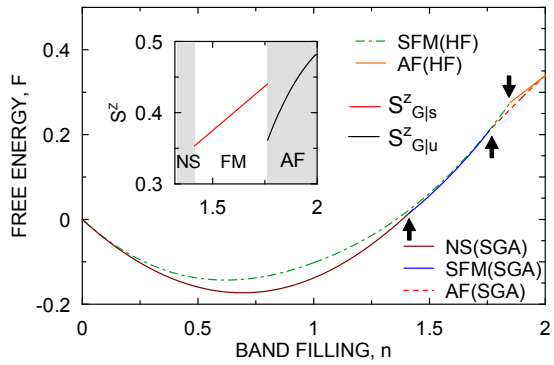

Figure 6. (Color online) The free energies of the stable phases for SGA and HF methods for $J = 0.4$, $U = 1.6$ and $\beta_h = 0$. The shaded regions in the inset mark the stability of certain phases according to the SGA approach. Note the appearance of ferromagnetic phase for $U = 4J$ (i.e., for $U > 3J$) in the filling range $1.45 \div 1.75$, sandwiched in between paramagnetic and antiferromagnetic phases.

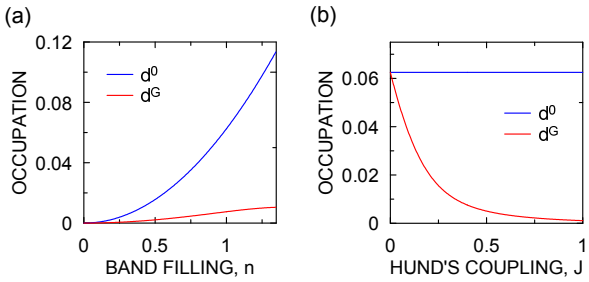

Figure 7. (Color online) The average double occupancies $d^0 = \langle \hat{n}_{il\uparrow}\hat{n}_{il\downarrow}\rangle_0$ and $d^G = \langle \hat{n}_{il\uparrow}\hat{n}_{il\downarrow}\rangle_G$ vs. band filling (a) and Hund's coupling (b) corresponding to the normal state (NS) for the parameters: $J = 0.4$, $U = 1.6$, $\beta_h = 0$ - (a) and $U = 4J$, $n = 1$, $\beta_h = 0$ - (b).

explicitly the nature of ordered phases. Previous analysis [31, 47] carried out in the dynamic mean-field approach addressed only the instability of the normal phase against the formation of the pure paired states. We compare our results with those coming from the Hartree-Fock approximation amended with the Bardeen-Cooper-Schrieffer (BCS) approach. The obtained Hund's coupling and band filling dependences of the magnetic moment and the superconducting gap parameters are often similar from the qualitative point of view with those evaluated by means of the HF approximation. However, the stability regions of the considered phases are significantly different for the two applied methods. In SGA, the stable coexisting superconducting-ferromagnetic phase is absent while it appears in the HF approximation in a certain range of J and n values. Furthermore, the coexistence of the paired state with antiferromagnetism appears much closer to the half-filled situation in SGA than in HF approximation. For $n = 2$ the superconductivity disappears and only the pure antiferromagnetism survives; this state can be termed a correlated Slater-Mott-insulator state, as it evolves gradually into the Mott-Hubbard insulating state with increasing $U > 1$ and $S^z_{G|s} \to 1/2$.

Table 5. Exemplary values of the order parameters, the chemical potential, the free energy, and the band renormalization factors corresponding to the considered phases, for two different sets of values of the microscopic parameters n and J. The underlined values correspond the stable phases. The numerical accuracy is on the level of the last digit specified.

		$n = 1.0$	$n = 1.9$
parameter	phase	$J = 0.299$	$J = 0.299$
Δ	A	<u>0.0450027</u>	0.1701940
Δ	A1+FM	0.0426749	0.1307664
Δ_+	SC+AF	-	<u>0.1638992</u>
Δ_-	SC+AF	-	<u>0.0161868</u>
S_u^z	A1+FM	0.000317	0.1092674
S_s^z	SC+AF	-	<u>0.3902738</u>
S_s^z	AF	-	0.3885899
μ	A	<u>-0.1382377</u>	0.16078601
μ	NS	-0.1377649	0.1875964
μ	A1+FM	-0.1379700	0.18222514
μ	SC+AF	-	<u>-0.0421144</u>
μ	AF	-	-0.0893963
F	A	<u>-0.3106091</u>	-0.3118381
F	NS	-0.3105145	-0.2992516
F	A1+FM	-0.3105586	-0.3020254
F	SC+AF	-	<u>-0.3576542</u>
F	AF	-	-0.3509731
$Q_\uparrow$	A1+FM	0.8845776	0.6751619
$Q_\downarrow$	A1+FM	0.8839251	0.6282452
Q	A	<u>0.8845136</u>	0.6736373
Q	NS	0.8840340	0.6421089
Q	SC+AF	-	<u>0.9211224</u>
Q	AF	-	0.9293567

The influence of hybridization for both approximations is similar. With an increase of the β_h parameter, the region of stability of the superconducting type-A phase narrows down in favor of the NS state. On the other hand, the antiferromagnetic phase is not affected in any significant manner by an increase of β_h.

The band renormalization factors approach unity as the interaction constants J, U and U' tend to zero, what represents an additional test of correctness of our numerical results. Generally, in the weak-coupling limit our present results reduce to those obtained in HF approximation analysed by us in [22], as it should be.

It is important to emphasize that for both approaches (SGA and HF) the phase diagrams have been obtained for $U < 3J$, i.e. for relatively low value of the Hubbard interaction U, or equivalently, for a relatively high value of the Hund's rule exchange

integral. We call this regime as the one with attractive pairing interaction. A complete analysis of the present model would require studying the stability of the spin-triplet superconductivity and its coexistence with magnetic ordering in the complementary regime $U > 3J$, where the magnetism may be favored against superconductivity. This regime has been the subject in a number of earlier papers [24, 48, 49], as then both the intraorbital, as well as the interorbital interaction is repulsive, and lead in a natural manner to magnetic ordering. We should see progress along this line soon.

5. Acknowledgements

Disscusions with Jakub Jędrak and Jan Kaczmarczyk are gratefully acknowledged. M.Z. has been partly supported by the EU Human Capital Operation Program, Polish Project No. POKL.04.0101-00-434/08-00. J.S. acknowledges the financial support from the Foundation for Polish Science (FNP) within project TEAM. The grant MAESTRO from the National Science Center (NCN) was helpful for the PL-DE cooperation within the present project on a unified approach to magnetism and superconductivity in correlated fermion systems.

References

[1] Y. Maeno, H. Hashimoto, K. Yoshida, S. Nishizaki, T. Fujita, J, G. Bednorz and F. Lichtenberg, Nature **372**, 532 (1994).
[2] Y. Maeno, Physica B **281-282**, 865 (2000)
[3] S. S. Saxena, P. Agarwal, K. Ahilan, F. M. Grosche, R. K. W. Haselwimmer, M. J. Steiner, E. Pugh, I. R. Walker, S. R. Julian, P. Monthoux, G. G. Lonzarich, A. Huxley, I. Sheikin, D. Braithwaite and J. Flouquet, Nature **406**, 587 (2000).
[4] A. Huxley, I. Sheikin, E. Ressouche, N. Kemovanois, D. Braithwaite, R. Calemczuk, J. Flouquet, Phys. Rev. B **63**, 144519 (2001).
[5] N. Tateiwa, T. C. Kobayashi, K. Hanazono, K. Amaya, Y. Haga, R. Settai and Y. Onuki, J. Phys.: Condens. Matter **13**, 117 (2001).
[6] T. C. Kobayashi, S. Fukushima, H. Hidoka, H. Kotegawa, T. Akazawa, E. Yamamoto, Y. Haga, R. Settai, and Y. Onuki, Physica B **378-380**, 355 (2006).
[7] N. T. Huy, A. Gasparini, D. E. de Nijs, Y. Huang, J. C. P. Klaasse, T. Gortenmulder, A. de Visser, A. Hamann, T. Görlach, and H. v. Löhneysen, Phys. Rev. Lett. **99**, 067006 (2007).
[8] E. Slooten, T. Naka, A. Gasparini, Y. K. Huang, and A. de Visser, Phys. Rev. Lett. **103**, 097003 (2009).
[9] For review see: A. de Visser in Encyclopedia of Materials Science: Science and Technology (Elsevier, 2010), pp. 1-6.
[10] C. Geibel, S. Thies, D. Kaczorowski, A. Mehner, A. Grauel, B. Seidel, U. Ahlheim, R. Helfrich, K. Petersen, C. D. Bredl, and F. Staglich, Z. Phys. B **83**, 305 (1991).
[11] A. Schröder, J. G. Lussier, B. D. Gaulin, J. D. Garrett, W. J. L. Buyers, L. Rebelski, and S. M. Shapiro, Phys. Rev. Lett. **72**, 136 (1994).
[12] K. Ishida, D. Ozaki, T. Kamatsuka, H. Tou, M. Kyogaku, Y. Kitaoka, N. Tateiwa, N. K. Sato, N. Aso, C. Geibel, and F. Steglich, Phys. Rev. Lett. **89**, 037002 (2002).
[13] G. Aeppli, D. Bishop, C. Broholm, E. Bucher, K. Siemensmeyer, M. Steiner, and N. Stüsser, Phys. Rev, Lett. **63**, 676 (1989)

[14] H. Tou, Y. Kitaoka, K. Asayama, N. Kimura, Y. Onuki, E. Yamamoto, and K. Maezawa, Phys. Rev. Lett. **77**, 1374 (1996)
[15] K. Klejnberg and J. Spałek, J. Phys.: Condens. Matter **11**, 6553 (1999).
[16] K. Klejnberg and J. Spałek, Phys. Rev. B **61**, 15542 (2000).
[17] J. Spałek, Phys. Rev. B **63**, 104513 (2001).
[18] J. Spałek, P. Wróbel, and W. Wójcik, Physica C **387**, 1 (2003).
[19] Previous brief and qualitative considerations about the ferromagnetism and spin-triplet pairing coexistence see: S-Q. Shen, Phys. Rev. **57**, 6474 (1998).
[20] M. Zegrodnik and J. Spałek, Acta Phys. Pol. A **121** 1051 (2011).
[21] M. Zegrodnik and J. Spałek, Acta Phys. Pol. A **121** 801 (2011).
[22] M. Zegrodnik and J. Spałek, Phys. Rev. B **86** 014505 (2012).
[23] J. Bünemann and W. Weber, Phys. Rev. B **55** 4011 (1997).
[24] J. Bünemann, W. Weber and F. Gebhard, Phys. Rev. B **57** 6896 (1998).
[25] Jörg Bünemann, Florian Gebhard, Torsten Ohm, Stefan Weiser, and Werner Weber in *Frontiers in Magnetic Materials* (Springer, Berlin 2005).
[26] J. Jędrak and J. Spałek, Phys. Rev. B **81** 073108 (2010).
[27] J. Kaczmarczyk and J. Spałek, Phys. Rev. B **84** 125140 (2011).
[28] O. Howczak and J. Spałek, J. Phys.: Condens. Matter **24** 205602 (2012).
[29] J. Jędrak, J. Kaczmarczyk and J. Spałek, arXiv:1008:0021v2 [cond-mat.str-el] 18 May 2011.
[30] K. Sano and Y. Ōno, J. Phys. Soc. Jpn., **72**, 1847 (2003).
[31] J. E. Han, Phys. Rev. B **70**, 054513 (2004).
[32] J. Hotta and K. Ueda, Phys. Rev. Lett. **92**, 107007 (2004)
[33] X. Dai, Z. Fang, Y. Zhou, and F-C. Zhang, Phys. Rev. Lett **101**, 057008 (2008).
[34] P. A. Lee and X-G. Wen, Phys. Rev. B **78**, 144517 (2008).
[35] Y. Imai, K. Wakabayashi, M. Sigrist, Phys. Rev. B **85**, 174532 (2012).
[36] A. V. Gorshkov, M. Hermele, V. Gurarie, C. Xu, P. S. Julienne, J. Ye, P. Zoller, E. Demler, M. D. Lukin, A. M. Rey, Nature Physics **6**, 289 (2010).
[37] R. W. Cherng, G. Rafael, and E. Demler, Phys. Rev. Lett. **99**, 130406 (2007).
[38] C. Wu, J. Hu, S.-C. Zhang, Int. Mod. Phys. B **24**, 311 (2009).
[39] G. Zwicknagl, J. Phys. Soc. Japan, **75** Suppl., 226 (2006), and references therein.
[40] For recent review see: G. Knebel, J. Buhot, D. Aoki, G. Laperot, S. Raymond, E. Ressouche, and J. Flouquet, J. Phys. Soc. Jpn. **80**, SA001(2011).
[41] O. Howczak, J. Kaczmarczyk, and J. Spałek, arXiv: 1209.0621 and Phys. Stat. Solidi (b), in press.
[42] D. Fay and J. Appel, Phys. Rev. B **22**, 3173 (1980);
A. Layzer and D. Fay, Inter. J. Magnetism, **1**, 135 (1971).
[43] P. W. Anderson and W. F. Brinkman in *The Physics of Liquid and Solid Helium*, edited by K. H. Bennemann and J. B. Ketterson (J. Wiley, New York, 1977), p. 177ff
[44] J. S. Griffith in *The Theory of Transition Metals and Ions* (Cambridge University Press, 1971), cf. Appendix 6.
[45] J. Bünemann, F. Gebhard, T. Schickling, and W.Weber, phys. stat. sol. (b) **248**, 203 (2010).
[46] J. Bünemann, F. Gebhard, and R. Thul, Phys. Rev. B **67**, 075103 (2003).
[47] S. Sakai, R. Arita, and H. Aoki, Phys. Rev. B **70**, 172504 (2004)
[48] J. Kuneš, I. Leonov, M. Kollar, K. Byczuk, V. I. Anisimov, and D. Vollhardt, Eur. Phys. J. Special Topics, **180**, 5 (2010).
[49] X. Y. Deng, L. Wang, X. Dai, and Z. Fang, Phys. Rev. B **79**, 075114 (2009).

Even-parity spin-triplet pairing for orbitally degenerate correlated electrons by purely repulsive interactions

Michał Zegrodnik,[1,*] Jörg Bünemann,[2,†] and Jozef Spałek[3,‡]

[1] *AGH University of Science and Technology, Faculty of Physics and Applied Computer Science, Al. Mickiewicza 30, 30-059 Kraków, Poland*
[2] *Max-Planck Institute for Solid State Research, Heisenbergstr. 1, D-70569 Stuttgart, Germany*
[3] *Marian Smoluchowski Institute of Physics, Jagiellonian University, ul. Reymonta 4, 30-059 Kraków, Poland*

We demonstrate the stability of a spin-triplet paired s-wave (with an admixture of extended s-wave) state for the case of purely repulsive interactions in a degenerate two-band Hubbard model. We further show that near half-filling the considered kind of superconductivity can coexist with antiferromagnetism. The calculations have been carried out with the use of the so-called *statistically consistent Gutzwiller approximation* for the case of a square lattice. The absence of a stable paired state when analyzed in the Hartree-Fock-BCS approximation allows us to claim that the electron correlations in conjunction with the Hund's rule exchange play the crucial role in stabilizing the spin-triplet superconducting state. A sizable hybridization of the bands suppresses the paired state.

PACS numbers: 74.20.-z, 74.25.Dw, 75.10.Lp

Introduction.—Spin-triplet superconductivity was postulated to occur in Sr_2RuO_4[1,2], in uranium compounds[3–5], and in iron pnictides[6,7]. All these multi-band systems have moderately (Sr_2RuO_4 and the pnictides) or strongly correlated (URhGe, UPt_3) electrons, d and f, respectively. Earlier, the spin-triplet pairing has been used successfully to describe the superfluidity of liquid ^{3}He[8,9] and that of the neutron-star crust[10]. In the last two cases of fermionic systems, which are considered as paramagnets with an enhanced susceptibility, a single-component (a single-band) Landau Fermi-liquid picture was taken as a starting point and the pairing of the odd parity (p-wave) was due to the exchange of a paramagnon. Such an approach is limited to weak correlations and was also applied to weakly ferromagnetic superconducting systems[11] and to Sr_2RuO_4[12].

In the correlated and orbitally degenerate systems the intraatomic ferromagnetic (Hund's rule) exchange interaction of magnitude $J \sim 0.1$eV, appears naturally in the extended Hubbard model and is essential for the description of ferromagnetism, for moderately and strongly correlated electrons. On the other hand, its significance in the spin-triplet pairing has been emphasized in general[13–18], as well as for both the pnictides[6] and Sr_2RuO_4[19–20]. In most cases, the Hund's rule and other local Coulomb interactions are either treated in the Hartree-Fock approximation[21] and/or semi-phenomenological negative-U intersite attraction[22] is introduced. A number of experimental results can be successfully interpreted in this manner, often assuming pairing with odd angular momentum, though the situation in this respect is not yet completely clear. In effect, it is very important to scrutinize a global stability of the spin-triplet phase against an onset of either magnetism or the coexistent states within this canonical model of correlated electrons while treating both the magnetism and the pairing in real space on equal footing.

We have recently analyzed a microscopic model with the Hund's-rule induced spin-triplet pairing, in both the Hartree-Fock[21] and the Gutzwiller approximation[23]. In the Hartree-Fock-BCS limit, the paired states (often coexisting with magnetism) appear only in the limit $U' - J = U - 3J < 0$, where U' is the intraatomic interorbital magnitude of the Coulomb repulsion. This limit can be called as that with attractive interactions. In the correlated Gutzwiller state and under the same conditions, superconductivity, both pure and coexistent with antiferromagnetism, is also stable[23]. The stability of superconducting phases comes not as a surprise in this parameter regime, since it resembles a single band model with negative U. In the course of this study, however, it became apparent to us that the spin-triplet paired state can also become stable in the much more realistic regime of purely repulsive interactions $U' - J > 0$, a typical situation for the correlated $3d$ and $4d$ electrons. This regime has been considered for a similar model with the use of the dynamical mean-field theory in Ref.[16], where only the normal-state instability with respect to the spin-triplet pairing was analyzed. Here we show explicitly that the s-wave (with an admixture of an extended s-wave) solution, i.e., with even parity, is stable (also against ferromagnetism) and therefore should be considered in the analysis of the spin-triplet superconductivity in the orbitally degenerate and correlated systems. We would like to underline that this is a generic microscopic approach in which the electronic correlations play a decisive role in stabilizing the spin-triplet even-parity state. Namely, the superconductivity induced by such pairing mechanism does not appear at all in the Hartree-Fock-BCS type of approach. This situation arises also for high-temperature superconductors, where purely repulsive Hubbard model leads to a spin-singlet d-wave pairing[24].

In connection with the proposed microscopic pairing one should also note the extensive studies of pairing in multicomponent cold-atom fermionic systems (see e.g. Refs.[25–27]). In distinction to those works, we discuss here the spin-triplet paired state in correlated lattice

system and beyond the mean-field (BCS) approximation within a concrete source of pairing (the Hund's rule exchange), as well as analyze explicit its stability (and coexistence) with magnetism.

Model.—The starting Hamiltonian has the form of the extended Hubbard model, i.e.,

$$\hat{H} = \sum_{ij(i\neq j)ll'\sigma} t_{ij}^{ll'} \hat{c}_{il\sigma}^{\dagger} \hat{c}_{jl'\sigma} + U' \sum_{i} \hat{n}_{i1}\hat{n}_{i2} + U \sum_{il} \hat{n}_{il\uparrow}\hat{n}_{il\downarrow} - J \sum_{ill'(l\neq l')} \left(\hat{\mathbf{S}}_{il} \cdot \hat{\mathbf{S}}_{il'} + \frac{1}{4} \hat{n}_{il}\hat{n}_{il'} \right) , \tag{1}$$

where $l = 1, 2$ labels the orbitals. The first term includes intraband ($l = l'$) and interband (hybridization, $l \neq l'$) hopping terms, the second and third represent the interorbital and intraorbital Coulomb repulsion, whereas the last represents the full form of the Hund's rule exchange interaction. The Hamiltonian (1) can be rewritten in a alternative form using the real-space representation for the pairing parts

$$\hat{H} = \sum_{ij(i\neq j)ll'\sigma} t_{ij}^{ll'} \hat{c}_{il\sigma}^{\dagger} \hat{c}_{jl'\sigma} + U \sum_{il} \hat{n}_{il\uparrow}\hat{n}_{il\downarrow} + (U' + J) \sum_{i} \hat{B}_i^{\dagger} \hat{B}_i + (U' - J) \sum_{im} \hat{A}_{im}^{\dagger} \hat{A}_{im} , \tag{2}$$

where the spin-triplet $\hat{A}_{im}$ and spin-singlet $\hat{B}_i$ pairing operators are defined as follows

$$\hat{A}_{i,m}^{\dagger} \equiv \begin{cases} \hat{c}_{i1\uparrow}^{\dagger} \hat{c}_{i2\uparrow}^{\dagger} & m = 1 , \\ \hat{c}_{i1\downarrow}^{\dagger} \hat{c}_{i2\downarrow}^{\dagger} & m = -1 , \\ \frac{1}{\sqrt{2}} (\hat{c}_{i1\uparrow}^{\dagger} \hat{c}_{i2\downarrow}^{\dagger} + \hat{c}_{i1\downarrow}^{\dagger} \hat{c}_{i2\uparrow}^{\dagger}) & m = 0 , \end{cases} \tag{3}$$

$$\hat{B}_i^{\dagger} \equiv \frac{1}{\sqrt{2}} (\hat{c}_{i1\uparrow}^{\dagger} \hat{c}_{i2\downarrow}^{\dagger} - \hat{c}_{i1\downarrow}^{\dagger} \hat{c}_{i2\uparrow}^{\dagger}) . \tag{4}$$

As one can see, for $U' > J$ the interaction energy that corresponds to the creation of a single pair in either spin-triplet or spin-singlet states on a atomic site, is positive. For an orbitally degenerate case, where the standard hierarchy of couplings is $U > U' > J$, the interorbital local spin-triplet type of pairing, if any, may be favored over the singlet one. The factor favoring the triplet over the singlet pairing is the Hund's rule exchange, but as we show, the electronic correlations are equally important to stabilize the paired state globally.

Method.—As said above, electronic correlations turn out to be crucial in this system. To include them in our study we use the modified Gutzwiller approximation. In this method, one assumes that the correlated state $|\Psi_G\rangle$ of the system can be expressed in the following manner

$$|\Psi_G\rangle = \hat{P}_G |\Psi_0\rangle , \tag{5}$$

where $|\Psi_0\rangle$ is the normalized non-correlated state to be defined below, whereas $\hat{P}_G$ is the Gutzwiller correlator, which we have selected in the form

$$\hat{P}_G = \prod_i \hat{P}_{G|i} \equiv \prod_i \sum_{I,I'} \lambda_{I,I'} |I\rangle_{ii} \langle I'| . \tag{6}$$

Here, $\{|I\rangle\}$ is a basis of the local (atomic) Hilbert space (16 states) and $\lambda_{I,I'}$ are variational parameters, which we assume to be real. In the subsequent discussion, we write the expectation values with respect to $|\Psi_0\rangle$ as $\langle \hat{O} \rangle_0 \equiv \langle \Psi_0 | \hat{O} | \Psi_0 \rangle$, while the expectation values with respect to $|\Psi_G\rangle$ will be denoted by

$$\langle \hat{O} \rangle_G \equiv \frac{\langle \Psi_G | \hat{O} | \Psi_G \rangle}{\langle \Psi_G | \Psi_G \rangle} = \frac{\langle \Psi_0 | \hat{P}_G \hat{O} \hat{P}_G | \Psi_0 \rangle}{\langle \Psi_0 | \hat{P}_G^2 | \Psi_0 \rangle} . \tag{7}$$

We focus on the pure superconducting phase of type A for which $\langle \hat{A}_{i,1} \rangle_G = \langle \hat{A}_{i,-1} \rangle_G \neq 0$ and $\langle \hat{A}_{i,0} \rangle_G \equiv 0$. This is because one would expect that the equal spin state (ESP) is favored by the local ferromagnetic exchange. Note that the expectation values in the correlated state, $|\Psi_G\rangle$ of the respective pairing operators are nonzero only if the corresponding expectation values in the noncorrelated state $|\Psi_0\rangle$ are also nonzero. For simplicity, we assume that $t^{11} = t^{22} \equiv t$ and $t^{12} = t^{21} \equiv t'$ for the nearest neighbors. The expectation value of the grand Hamiltonian $\hat{K} = \hat{H} - \mu \hat{N}$ in the correlated state has been derived in the limit of infinite dimensions by a diagrammatic approach[28] and has the form

$$\langle \hat{K} \rangle_G = \sum_{ijl\sigma} Q\, t_{ij} \langle \hat{c}_{il\sigma}^{\dagger} \hat{c}_{jl\sigma} \rangle_0 + \sum_{ijll'\sigma} Q\, t'_{ij} \langle \hat{c}_{il\sigma}^{\dagger} \hat{c}_{jl'\sigma} \rangle_0 + \sum_{ij\sigma} \tilde{Q}\, t_{ij} (\langle \hat{c}_{i1\sigma}^{\dagger} \hat{c}_{j2\sigma}^{\dagger} \rangle_0 + \langle \hat{c}_{j2\sigma} \hat{c}_{i1\sigma} \rangle_0) + L \sum_{I,I'} \bar{E}_{I,I'} \langle \hat{m}_{I,I'} \rangle_0 - \mu \sum_{il\sigma} q_{l\sigma}^s \langle \hat{n}_{il\sigma} \rangle_0 , \tag{8}$$

where Q and $\tilde{Q}$ are the renormalization factors, L is the number of atomic sites, μ refers to the chemical potential, $q_{l\sigma}^s = \langle \hat{n}_{il\sigma} \rangle_G / \langle \hat{n}_{il\sigma} \rangle_0$, and $\hat{m}_{I,I'} \equiv |I\rangle\langle I'|$. The factors Q and $\tilde{Q}$, as well as $\bar{E}_{I,I'}$, can be expressed with the use of the variational parameters $\lambda_{I,I'}$, the local single particle density matrix elements $\langle \hat{c}_{il\sigma}^{\alpha} \hat{c}_{il'\sigma'}^{\alpha'} \rangle_0$, and the matrix elements of the atomic part of (1) represented in the local basis, $\langle I | \hat{H}^{at} | I' \rangle$. Here $\hat{c}_{il\sigma}^{\alpha}$ are either creation or anihilation operators. The expression for $\langle \hat{K} \rangle_G$ can be rewritten as the expectation value of the effective single-particle Hamiltonian $\hat{K}_{GA}$, evaluated with respect to $|\Psi_0\rangle$, i.e.,

$$\hat{K}_{GA} = \sum_{ijl\sigma} Q\, t_{ij} \hat{c}_{il\sigma}^{\dagger} \hat{c}_{jl\sigma} + \sum_{ijll'\sigma} Q\, t'_{ij} \hat{c}_{il\sigma}^{\dagger} \hat{c}_{jl'\sigma} + \sum_{ij\sigma} \tilde{Q}\, t_{ij} (\hat{c}_{i1\sigma}^{\dagger} \hat{c}_{j2\sigma}^{\dagger} + \hat{c}_{j2\sigma} \hat{c}_{i1\sigma}) + L \sum_{I,I'} \bar{E}_{I,I'} \langle \hat{m}_{I,I'} \rangle_0 - \mu \sum_{il\sigma} q_{l\sigma}^s \hat{n}_{il\sigma} . \tag{9}$$

The first three terms of (9) originate from the single particle part of (2), while the fourth originates from its interaction part. It can be seen that the intraatomic part

has been taken as its average, in accordance with the general philosophy of the Gutzwiller approach. Again, the Q and $\tilde{Q}$ factors are the renormalization factors of the respective dynamic processes. The first two refer to the narrowing of the quasiparticle bands, whereas the $\tilde{Q}$ parameter corresponds to the intersite pairing amplitude. It should be emphasized that in our initial Hamiltonian (1) there are no intersite interaction terms and so the intersite pairing that is present in (9) is due to correlations (a non-BCS factor). Also, the factor $\tilde{Q}$ is nonzero only when the local expectation values $\langle \hat{A}_{i,\pm 1}\rangle_G$ (and the corresponding $\langle \hat{A}_{i,\pm 1}\rangle_0$) are also nonzero. As a result, the intersite pairing appears concomitantly with the intrasite one.

In the statistically consistent Gutzwiller approach (SGA)[29−31] the mean fields are treated as variational parameters, with respect to which the free energy of the system is minimized. Hence, in order to assure that the self-consistent and the variational procedures yield the same results, additional constraints have to be introduced with the help of the Lagrange-multiplier method. This leads to supplementary terms in the effective Hamiltonian so that now it takes the form

$$\hat{K}_{\lambda} = \hat{K}_{GA} - \lambda_n\Big(\sum_{il\sigma} q^s_{l\sigma}\hat{n}_{il\sigma} - L\langle\hat{n}\rangle_G\Big) - \sum_{m=\pm 1}\Big[\lambda_m\Big(\sum_i \hat{A}_{im} - L\langle\hat{A}_{im}\rangle_0\Big) + H.C.\Big] , \tag{10}$$

where the Lagrange multipliers λ_m and λ_n are introduced to assure that the averages $\langle\hat{A}_{im}\rangle$ and $\langle\hat{n}\rangle$ calculated either from the corresponding self-consistent equations or variationally, coincide with each other. One should also note that it is natural to fix $\langle\hat{n}\rangle_G$ instead of $\langle\hat{n}\rangle_0$ during the minimization procedure. This is the reason why we put the term $-\mu\hat{N}$ already at the beginning of out derivation. The values of the mean fields, the variational parameters, the and the Lagrange multipliers, are all found by minimizing the free energy functional $\hat{F}_{\lambda}$ that is derived with the help of the effective Hamiltonian $\hat{K}_{\lambda}$ in a standard statistical-mechanical manner. For the considered two-band model there can be up to 256 variational parameters $\lambda_{I,I'}$. Fortunately, for symmetry reasons, one can reduce their number significantly. It should also be noted that not all of the parameters are independent, as certain constraints have to be obeyed[23,28]. In effect, we have to minimize only 16 variables in this pure superconducting state of type A.

From Eqs.(9) and (10) it can be seen that the Lagrange multipliers λ_m have an interpretation of the intrasite gap parameters, while the symmetry of the intersite gap parameter is fully determined by the bare band dispersion relation. By assuming the dispersion relation for a square lattice with nonzero hopping t between nearest neighbors only

$$\epsilon_{\mathbf{k}} = -2t(\cos k_x + \cos k_y) , \tag{11}$$

one obtains the following form of the gap parameter

$$\Delta_{\mathbf{k}} = \Delta^{(0)} + \Delta^{(1)}(\cos k_x + \cos k_y) , \tag{12}$$

where $\Delta^{(0)} \equiv \lambda_1 = \lambda_{-1}$ (as we are considering an ESP state) while $\Delta^{(1)} \equiv 2\tilde{Q}t$ is the intersite pairing amplitude. In this manner, we have obtained a mixture of the s-wave and the extended s-wave pairing symmetry.

In order to check if the stable spin-triplet paired phases can indeed appear in the repulsive-interaction regime, we have performed first the calculations taking into account only the intrasite pairing for the following selection of phases: type A superconducting (**A**), pure ferromagnetic (**FM**), paramagnetic (**NS**), superconducting coexisting with antiferromagnetism (**SC**+**AF**), and pure antiferromagnetic (**AF**). The antiferromagnetic ordering considered by us has a simple two-sublattice form. We have also considered the so-called A1 superconducting phase ($\langle\hat{A}_1\rangle_G \neq 0$ and $\langle\hat{A}_{-1}\rangle_G = \langle\hat{A}_0\rangle_G \equiv 0$) coexisting with ferromagnetism. However, this phase turned out not to be stable for the whole range of model parameters examined. Therefore, it is not included in the subsequent discussion. Detailed information concerning the above phases can be found in[23], where we have analyzed the intrasite paired states in the regime of attractive interaction, i.e., for $U' - J < 0$.

Results.—The calculations have been performed assuming that the hybridization matrix element has the form $\epsilon_{12\mathbf{k}} \equiv \beta_h\epsilon_{\mathbf{k}}$, where $\beta_h \in [0,1]$, specifies the interband hybridization strength. The interorbital Coulomb repulsion constant U' was set to $U' = U - 2J$. All the energies have been normalized to the bare band-width, $W = 8|t|$, and the presented results were obtained for $k_BT/W = 10^{-4}$ emulating the $T = 0$ state.

In Fig. 1 we show that the superconducting phases, both pure and coexisting with antiferromagnetism, are stable for purely repulsive interactions regime ($U' - J > 0$). With the increasing Coulomb repulsion U, the regions of stability of the paired phases are becoming narrower. Note that the Hartree-Fock calculations lead only to the stability of magnetically ordered phases in this regime. The appearance of the paired states is therefore a genuine many-particle effect which is caused by the electronic correlations and taken into account in the SGA method.

Next, we discuss the superconducting A phase with inclusion of the intersite part of the pairing. In Fig. 2 we plot the superconducting gap components as a function of the effective pairing constant $J_{\text{eff}} \equiv U' - J$. As the value of the J_{eff} parameter changes sign to positive, the intrasite interaction corresponding to the spin-triplet-pair creation on a single atomic site changes from attractive to repulsive. As one could expect, according to the Hartree-Fock-BCS results, the intrasite gap parameter vanishes before J_{eff} reaches zero and the intersite pairing does not appear. The situation is different in the SGA. Namely, the paired solution survives for $J_{\text{eff}} > 0$ and the pairing has both the intra- and the inter-site components. However, the $\Delta^{(1)}$ parameter is an order of magnitude smaller

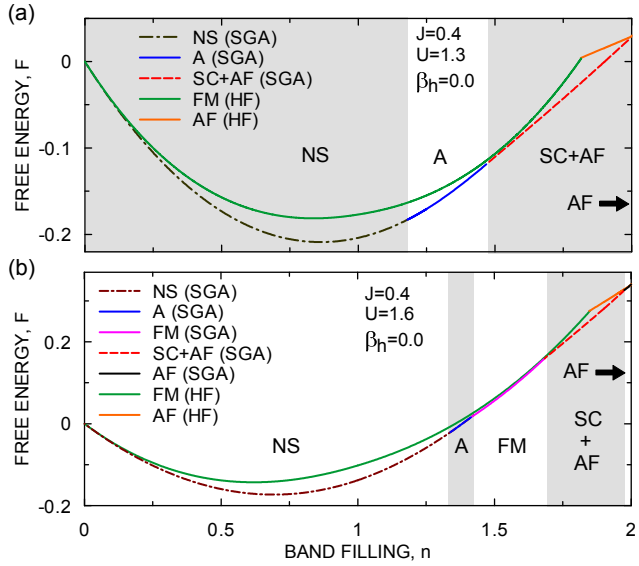

FIG. 1. (Color online) Ground-state energy of stable phases as a function of the band filling for the case when only the intrasite pairing is included (i.e., for $\Delta^{(1)} \equiv 0$). For comparison, plots obtained in the H-F approximation are also shown. The shaded regions mark the stability of corresponding phases according to the SGA method. Pure AF state is stable for $n = 2$ (marked by arrow).

than $\Delta^{(0)}$. The phase A has a lower value of energy than the normal phase for the whole range of $J_{\rm eff}$ presented in Fig. 2. Exemplary values of the order parameters, the renormalization factors, and the free energy for $T \to 0$, are all listed in Table I.

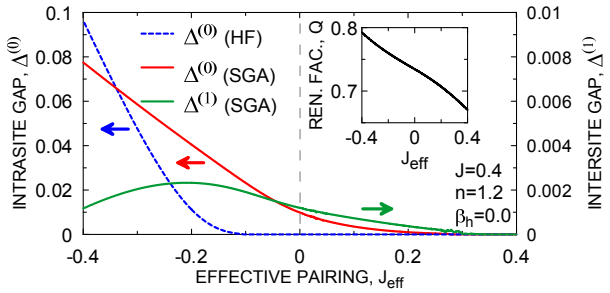

FIG. 2. (Color online) The intrasite (left scale) and the intersite (right scale) gap components as a functionof the effective coupling constant $J_{\rm eff} = U' - J$. For comparison, we provide also the results obtained in the Hartree-Fock approximation. Additionally, the band renormalization factor is shown in the inset. Note that $\Delta^{(1)} = \tilde{Q}/4$.

In Fig. 3a we plot the J dependences of the gap parameters for $J_{\rm eff} = 0.1$. For larger values of J the difference in magnitude between the intra- and the inter-site contributions to the pairing is not that large. The influence of the hybridization on the considered type of superconductivity is shown in Fig. 3b. The superconducting gaps are not affected by the increase of the β_h parameter up

TABLE I. Representative values of the gap parameters, the renormalization factors and the free energies for $J = 0.4$, $n = 1.2$ and $\beta_h = 0.0$, for three different values of the effective pairing constant, $J_{\rm eff}$. For comparison, we have provided the values of the renormalization factor and the free energy for the superconducting phase of type A and the normal phase, NS. The subscripts refer to these two phases. The numerical accuracy is better that the last digit specified.

$J_{\rm eff}$	$\Delta^{(0)}$	$\Delta^{(1)}$	Q_A	Q_{NS}	F_A	F_{NS}
−0.1	0.02325	0.00191	0.74669	0.74401	-0.255481	-0.255067
0.1	0.00357	0.00073	0.72164	0.72157	-0.179725	-0.179705
0.15	0.00200	0.00054	0.71454	0.71453	-0.161874	-0.161867

to the critical value $\beta_h^C \approx 0.0379$ at which both of them suddenly drop to zero. Therefore, a sizable hybridization is detrimental to the spin-triplet pairing and the effect is strong. It means that this type of pairing suppresses the energy gain due the interorbital hopping and hence is possible only for weakly hybridized systems, where the condensation energy is dominant, $2(\Delta^{(0)})^2/J \gtrsim \beta_h/8$.

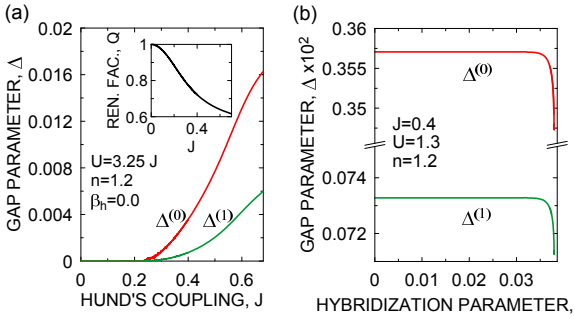

FIG. 3. (Color online) Intrasite ($\Delta^{(0)}$) and intersite ($\Delta^{(1)}$) gap parameters as a function of the Hund's exchange integral (a) and the hybridization parameter (b). In the inset of (a) the J dependence of the band narrowing factor is shown.

Conclusions.—By using the SGA approach, we have shown that the intrasite spin-triplet paired states, both pure (A type) and coexistent with antiferromagnetism (SC+AF phase) can become stable in the orbitally degenerate Hubbard model, in the limit of purely repulsive interactions ($U' - J > 0$). The coexistent SC+AF phase is possible for the systems close to the half filling (the case of pnictides), whereas the pure A phase appears when $n \approx 1.2$ for doubly or when $n \approx 1.8$ for triply degenerate band which corresponds roughly to the case of Sr_2RuO_4 in the hole language. One can say that both the Hund's rule and the correlations induced change of band energy contribute to the spin-triplet pairing mechanism; they correspond to the BCS (potential energy gain) and the non-BCS (kinetic energy gain) factors stabilizing the paired state[32]. The intersite (extended s-wave) part of the pairing is related to the intrasite (s-wave) one. This can be seen from Figs. 2 and 3a, where $\Delta^{(0)}$ and $\Delta^{(1)}$ reach zero for the same values of model parameters. The hybridization is detrimental to the superconducting A-

phase stability when the spin-triplet pairing condensation energy becomes smaller than the Pauli-principle-allowed kinetic-energy gain. The present model, while not being material-specific provides universal features of the pairing. This is because the order parameter is calculated by minimizing the total energy averaged over the band energies. Also, the considered here phase complements the discussion of combined spin-orbital ordering in the strong-correlation limit[33].

M.Z. has been partly supported by the EU Human Capital Operation Program, Polish Project No. POKL.04.0101-00-434/08-00. This work has been partly supported by the Foundation for Polish Science (FNP) within project TEAM and partly by the National Science Center (NCN), through scheme MAESTRO, Grant No. DEC-2012/04/A/ST3/00342. We are also grateful to Karol I. Wysokiński for helpful discussions.

* michal.zegrodnik@gmail.com
† buenemann@gmail.com
‡ ufspalek@if.uj.edu.pl

[1] A. P. Mackenzie and Y. Maeno, Rev. Mod. Phys. **75**, 657 (2003).
[2] T. M. Rice and M. Sigrist, J. Phys.: Condens Matter **7**, L643 (1994).
[3] S. S. Saxena, P. Agarwal, K. Ahilan, F. M. Grosche, R. K. W. Haselwimmer, M. J. Steiner, E. Pugh, I. R. Walker, S. R. Julian, P. Monthoux, G. G. Lonzarich, A. Huxley, I. Sheikin, D. Braithwaite and J. Flouquet, Nature **406**, 587 (2000).
[4] A. Huxley, I. Sheikin, E. Ressouche, N. Kemovanois, D. Braithwaite, R. Calemczuk, J. Flouquet, Phys. Rev. B **63**, 144519 (2001).
[5] N. Tateiwa, T. C. Kobayashi, K. Hanazono, K. Amaya, Y. Haga, R. Settai and Y. Onuki, J. Phys.: Condens. Matter **13**, 117 (2001).
[6] X. Dai, Z. Fang, Y. Zhou, and F-C. Zhang, Phys. Rev. Lett **101**, 057008 (2008).
[7] P. A. Lee and X-G. Wen, Phys. Rev. B **78**, 144517 (2008).
[8] P. W. Anderson and W. F. Brinkman, Phys. Rev. Lett. **30**, 1108 (1973).
[9] P. W. Anderson and W. F. Brinkman in *Physics of Liquid and Solid Helium*, edited by K. H. Bennemann, and J. B. Ketterson (J. Wiley & Sons, New York, 1978) Part II, pp. 177-286.
[10] D. Pines and A. Alpar, Nature **316**, 27 (1985).
[11] D. Fay and J. Appel, Phys. Rev. B **22**, 3173 (1980).
[12] I. I. Mazin and D. I. Singh, Phys. Rev. Lett. **79**, 733 (1997).
[13] J. Spałek, Phys. Rev. B **63**, 104513 (2001).
[14] A. Klejnberg and J. Spałek, J. Phys. C: Condens. Matter **11**, 6553 (1999).
[15] J. E. Han, Phys. Rev. B **70**, 054513 (2004).
[16] S. Sakai, R. Arita, and H. Aoki, Phys. Rev. B **70**, 172504 (2004).
[17] K. Sano and Y. Ono, J. Phys. Soc. Jpn **72**, 1847 (2003).
[18] C. M. Puetter and H-Y. Kee, Eur. Phys. Lett. **98**, 27010 (2012).
[19] T. Takimoto, Phys. Rev. B **62**, R14641 (2000).
[20] S. Koikegami, Y. Yoshida, and T. Yanagisawa, Phys. Rev. B **67**, 134517 (2003).
[21] M. Zegrodnik and J. Spałek, Phys. Rev. B **86** 014505 (2012).
[22] J. F. Annett, B. L. Györffy, G. Litak, and K. I. Wysokiński, Eur. Phys. J. B **36**, 301 (2003)
[23] M. Zegrodnik, J. Spałek, and J. Bünemann, arxiv: 1304.4478, unpublished
[24] D. J. Scalapino, *Handbook of High-Temperature Superconductivity*, edited by J. R. Schrieffer and J. S. Brooks (Springer, New York, 2007) Chap. 13
[25] R. W. Cherng, G. Refael, and E. Demler, Phys. Rev. Lett. **99**, 130406 (2007).
[26] A. V. Gorshkov, M. Hermele, V. Gurarie, C. Xu, P. S. Julienne, J. Ye, P. Zoller, E. Demler, M. D. Lukin, A. M. Rey, Nature Physics **6**, 289 (2010).
[27] C. Wu, J. Hu, S.-C. Zhang, Int. J. Mod. Phys. B **24**, 311 (2009).
[28] J. Bünemann, F. Gebhard, T. Ohm, S. Weiser, and W. Weber in *Frontiers in Magnetic Materials* (Springer, Berlin 2005).
[29] J. Jędrak, J. Kaczmarczyk, J. Spałek, arxiv:1008.002
[30] J. Jędrak and J. Spałek, Phys. Rev. B **81** 073108 (2010).
[31] J. Kaczmarczyk and J. Spałek, Phys. Rev. B **84** 125140 (2011).
[32] J. Kaczmarczyk, J. Spałek, T. Schickling, and J. Bünemann, arXiv: 1210.6249
[33] A. Klejnberg and J. Spałek, Phys. Rev. B **61**, 15542 (2000).

Spin-triplet paired state induced by the Hund's rule coupling and correlations: fully statistically consistent Gutzwiller approach

J Spałek and M Zegrodnik

AGH University of Science and Technology, Faculty of Physics and Applied Computer Science, Al. Mickiewicza 30, PL-30-059 Kraków, Poland

E-mail: ufspalek@if.uj.edu.pl, michal.zegrodnik@gmail.com

Abstract. The intrasite and intersite spin-triplet pairing gaps induced by the interband Hund's rule coupling and the correlations are analyzed in the doubly degenerate Hubbard Hamiltonian. To include the effect of correlations the Statistically Consistent Gutzwiller (SGA) approximation is used. In this approach the consistency means that the averages calculated from the self-consistent equations and those determined variationally coincide with each other. The emphasis is put on the solution for which the average particle number is conserved when carrying out the Gutzwiller projection. The method leads to a stable equal-spin paired state in the so-called repulsive interactions limit ($U > 3J$) in the regime of moderate correlations. The interband hybridization introduces an inequivalence of the bands which, above a critical magnitude, suppresses the paired state due to both the Fermi-wave vector mismatch for the Cooper pair and the Pauli-principle-allowed interband hopping.

PACS numbers: 74.20.-z, 74.25.Dw, 75.10.Lp

Submitted to: *J. Phys.: Condens. Matter*

1. Introduction

The theoretical investigations concerning spin-triplet pairing are motivated by the discoveries of the superconducting phases in Sr_2RuO_4 [1, 2], in iron pnictides [3, 4], and in uranium compounds [5, 6, 7]. It has been proposed [8, 9, 10, 11, 12] that the Hund's rule exchange coupling can lead in a natural manner to various spin-triplet paired states in the orbitally degenerate systems. In our recent papers we have investigated this kind of pairing mechanism in the doubly degenerate Hubbard model with inclusion of the interband hybridization by using both Hartree-Fock (HF) [13] and the statistically consistent Gutzwiller (SGA) [14, 15] approximations. It has been shown that by applying the latter method one obtains a combination of intrasite and intersite contributions to the pairing in the so-called purely repulsive interactions regime. However, the method applied in those calculations does not guarantee the conservation of the average particle number when carrying out the Gutzwiller projection, which transforms the system composed of noncorrelated electrons into a nonstandard quasiparticle Fermi liquid representing effectively the correlated state. The average particle number conservation should be a characteristic of the Fermi liquid and it is worth a separate analysis. This is because at the outset of the Landau Fermi-liquid theory is the one-to-one correspondence of the bare and quasiparticle states. This matter has already been discussed [17, 18, 19] with respect to the original Gutzwiller approximation for a single band. In these considerations the so-called fugacity factors have been introduced, which compensate the particle-number reduction appearing during the execution of the Gutzwiller projection. The fugacity factors were also used by Gebhard [20], Laughlin [21], and Wang et al [22]. Moreover, a similar approach, but in conjunction with the SGA method, has been performed recently to study the coexistence of antiferromagnetism and superconductivity both in the $t-J$ model [23] as well as in the Anderson-Kondo lattice model [24, 25]. It should be noted that different choices of fugacity factors have been considered, imposing local and global as well as spin-dependent and spin-independent forms of the particle-number conservation. They all have been compared by Fukushima [19]. Moreover, it seems reasonable to say that in the case of multiband models the orbital-dependence of the fugacity factors should also be introduced. However, the differences between all these approaches are immaterial when one considers the situation of a homogeneous system without either magnetic or orbital ordering, as is the case here. The present formulation allows us to compare our results with those obtained earlier and in this manner discuss explicitly a degree of insensitivity of the Gutzwiller approach to the solution details. In any case, the incorporation of the fundamental principle makes the SGA approach we have proposed fully statistically consistent.

In this paper we focus on the particle number conservation with respect to the statistically consistent Gutzwiller approximation that has been used by us recently in the study of the Hund's rule induced spin-triplet pairing in the doubly degenerate Hubbard model. As described in the following section, we propose the inclusion of an additional term in the effective Hamiltonian that forces the particle number conservation

without introducing the fugacity factors [19]. We discuss also the role of the interorbital hybridization, which introduces the bads inequivalence and is detrimental to the stability of the considered kind of paired phase when sufficiently strong.

2. Model and method

We consider the doubly degenerate Hubbard Hamiltonian, which has the form

$$\begin{aligned}\hat{H} = &\sum_{ijll'\sigma} t_{ij}^{ll'} \hat{c}_{il\sigma}^{\dagger} \hat{c}_{jl'\sigma} + U' \sum_{i} \hat{n}_{i1} \hat{n}_{i2} \\ &+ U \sum_{il} \hat{n}_{il\uparrow} \hat{n}_{il\downarrow} - J \sum_{ill'(l\neq l')} \left(\hat{\mathbf{S}}_{il} \cdot \hat{\mathbf{S}}_{il'} + \frac{1}{4} \hat{n}_{il} \hat{n}_{il'} \right) ,\end{aligned} \tag{1}$$

where $l = 1, 2$ labels the orbitals. The first term corresponds to intraband ($l = l'$) and interband (hybridization, $l \neq l'$) hopping terms, the second and the third include the direct interorbital and intraorbital Coulomb repulsion, whereas the last represents the Hund's rule exchange interaction. One has to mention that in the interaction part we have neglected both the so-called local correlated hopping and the two-particle hopping terms, as they are very small for $U > W$ (W is the bare bandwidth) limit which is considered here. We can rewrite the Hamiltonian (1) in the alternative form

$$\begin{aligned}\hat{H} = &\sum_{ijll'\sigma} t_{ij}^{ll'} \hat{c}_{il\sigma}^{\dagger} \hat{c}_{jl'\sigma} + U \sum_{il} \hat{n}_{il\uparrow} \hat{n}_{il\downarrow} \\ &+ (U' + J) \sum_{i} \hat{B}_{i}^{\dagger} \hat{B}_{i} + (U' - J) \sum_{im} \hat{A}_{im}^{\dagger} \hat{A}_{im} ,\end{aligned} \tag{2}$$

where the spin-triplet $\{\hat{A}_{im}\}$ and the spin-singlet $\hat{B}_i$ local pairing operators are defined as follows

$$\hat{A}_{i,m}^{\dagger} \equiv \begin{cases} \hat{c}_{i1\uparrow}^{\dagger} \hat{c}_{i2\uparrow}^{\dagger} & m = 1 , \\ \hat{c}_{i1\downarrow}^{\dagger} \hat{c}_{i2\downarrow}^{\dagger} & m = -1 , \\ \frac{1}{\sqrt{2}} (\hat{c}_{i1\uparrow}^{\dagger} \hat{c}_{i2\downarrow}^{\dagger} + \hat{c}_{i1\downarrow}^{\dagger} \hat{c}_{i2\uparrow}^{\dagger}) & m = 0 , \end{cases} \tag{3}$$

$$\hat{B}_{i}^{\dagger} \equiv \frac{1}{\sqrt{2}} (\hat{c}_{i1\uparrow}^{\dagger} \hat{c}_{i2\downarrow}^{\dagger} - \hat{c}_{i1\downarrow}^{\dagger} \hat{c}_{i2\uparrow}^{\dagger}) . \tag{4}$$

From the above form of the starting Hamiltonian one can intuitively see that the spin-triplet pairing, if any, is favored as $U' = U - 2J$ for $3d$ and $4d$ orbitals. This can be considered as obvious in the $U < 3J$ limit when we have an effectively attractive interaction ($U' - J < 0$) which leads to the pairing in a straightforward manner. We do not make this assumption here and consider the case when $U > 3J$, since it is more realistic for $3d$ and $4d$ orbitals. As in our previous paper, we are using the SGA method in which one starts from the correlated Gutzwiller state $|\Psi_G\rangle$ of the system in the following form [16]

$$|\Psi_G\rangle = \hat{P}_G |\Psi_0\rangle , \tag{5}$$

where $|\Psi_0\rangle$ is the non-correlated reference state with broken symmetry, as discussed below, whereas $\hat{P}_G$ is the Gutzwiller projection operator, which has been selected in the form

$$\hat{P}_G = \prod_i \hat{P}_{G|i} \equiv \prod_i \sum_{I,I'} \lambda_{I,I'} |I\rangle_{ii}\langle I'| \; . \tag{6}$$

Here, $\lambda_{I,I'}$ are the variational parameters which are assumed to be real and $\{|I\rangle\}$ is the basis of the local (atomic) Fock space composed of 16 states containing $N_e = 0, 1, ..., 4$ electrons. Such choice of the projection operator allows for the situation in which the expectation values of the number of particles before and after the projection may differ for some states. The presented here approach is thus so far the same as the one we have used earlier [14, 15]. We briefly summarize it and next show the modification of the method which guarantees the average particle number conservation. In the following discussion we denote the expectation values with respect to $|\Psi_0\rangle$ as $\langle\hat{O}\rangle_0 \equiv \langle\Psi_0|\hat{O}|\Psi_0\rangle$, whereas the expectation values with respect to $|\Psi_G\rangle$ are determined as

$$\langle\hat{O}\rangle_G \equiv \frac{\langle\Psi_G|\hat{O}|\Psi_G\rangle}{\langle\Psi_G|\Psi_G\rangle} = \frac{\langle\Psi_0|\hat{P}_G\hat{O}\hat{P}_G|\Psi_0\rangle}{\langle\Psi_0|\hat{P}_G^2|\Psi_0\rangle} \equiv \frac{\langle\hat{P}_G\hat{O}\hat{P}_G\rangle_0}{\langle\hat{P}_G^2\rangle_0} \; . \tag{7}$$

The term on the right has a principal importance, as it expresses the average of the operator $\hat{O}$ in the correlated state through the averages in the non-correlated state and thus can be factorized into the single-particle (two-site at most) contributions (according to the Wick's theorem). The particle conservation condition can be now expressed simply as $\langle\hat{n}\rangle_0 = \langle\hat{n}\rangle_G$, where $\hat{n} = \sum_{il\sigma} \hat{n}_{il\sigma}/L$ (L is the number of atomic sites).

The superconducting A phase (the equal spin polarized state, ESP) which we consider in this paper is defined by the relations $\langle\hat{A}_{i,1}\rangle_G = \langle\hat{A}_{i,-1}\rangle_G \neq 0$ and $\langle\hat{A}_{i,0}\rangle_G \equiv 0$. These definitions are analogical when taken with respect to $|\Psi\rangle_0$, namely $\langle\hat{A}_{i,1}\rangle_0 = \langle\hat{A}_{i,-1}\rangle_0 \neq 0$ and $\langle\hat{A}_{i,0}\rangle_0 \equiv 0$. As shown earlier [14, 15] the paired A phase is stable against ferromagnetism and the coexistent superconducting-ferromagnetic phase in the proper range of model parameters. In order to simplify the situation, we assume equivalence of the orbitals $t^{11} = t^{22} \equiv t$ and $t^{12} = t^{21} \equiv t'$. It has been argued [14, 15] that the expectation value of the initial grand Hamiltonian $\hat{K} = \hat{H} - \mu\hat{N}$ in the correlated state can be considered as an expectation value of the effective grand Hamiltonian $\hat{K}_{GA}$ in the non-correlated state ($\langle\hat{K}\rangle_G = \langle\hat{K}_{GA}\rangle_0$) in the limit of infinite dimensions. Explicitly, the effective Hamiltonian has the following form

$$\begin{aligned} \hat{K}_{GA} = & \sum_{ijl\sigma} Q\; t_{ij}\hat{c}^\dagger_{il\sigma}\hat{c}_{jl\sigma} + \sum_{ijll'(l\neq l')\sigma} Q\; t'_{ij}\hat{c}^\dagger_{il\sigma}\hat{c}_{jl'\sigma} \\ & + \sum_{ij\sigma} \tilde{Q}\; t_{ij}(\hat{c}^\dagger_{i1\sigma}\hat{c}^\dagger_{j2\sigma} + \hat{c}_{j2\sigma}\hat{c}_{i1\sigma}) \\ & + L\sum_{I,I'} \bar{E}_{I,I'}\langle\hat{m}_{I,I'}\rangle_0 - \mu q_s \sum_{il\sigma}\langle\hat{n}_{il\sigma}\rangle_0 \; , \end{aligned} \tag{8}$$

where L is the number of atomic sites, $q_s = \langle\hat{n}\rangle_G/\langle\hat{n}\rangle_0$, whereas Q and $\tilde{Q}$ are the renormalization factors of the respective dynamic processes. The first two terms of (8)

correspond to the hopping in the renormalized quasiparticle bands and the third term is responsible for the intersite spin-triplet pairing which is induced by both the intrasite Hund's coupling and the correlations. The fourth term originates from the intraatomic interaction part of the initial Hamiltonian (1) and is taken as an average, in accordance with the general philosophy of the Gutzwiller approach. Here, $\hat{m}_{I,I'} \equiv |I\rangle\langle I'|$, whereas the q_s, Q, $\tilde{Q}$, and $\bar{E}_{I,I'}$ parameters can be expressed by the mean field parameters, variational parameters, and the matrix elements of the atomic part of (1) represented in the local basis, $\langle I|\hat{H}^{at}|I'\rangle$. These expressions were derived by using the diagrammatic approach in the limit of infinite dimensions [16]. Note that for $q_s < 1$, we have a reduction of the average site occupancy in the correlated state, a very nontrivial situation, which is taken care of by introducing the particle conservation constraint as shown below.

Now, we can construct the $\hat{K}^a_\lambda$ effective Hamiltonian according to the statistically consistent variant of the Gutzwiller approximation (SGA). In this approach, the mean-field averages are treated as variational parameters with respect to which the free energy of the system is minimized. Such procedure is equivalent to selecting the type of the noncorrelated wave function $|\Psi_0\rangle$. Additionally, we introduce the supplementary terms (called the statistical-consistency conditions) to the effective Hamiltonian so that the averages $\langle\hat{A}_{im}\rangle$ and $\langle\hat{n}\rangle$ calculated either from the corresponding self-consistent equations or variationally, coincide with each other. For this purpose, the Lagrange multiplier method is used. As a result, the next-generation effective Hamiltonian $\hat{K}^a_\lambda$ takes the following form

$$\begin{aligned}\hat{K}^a_\lambda \equiv \hat{K}_{GA} &- \lambda_n\big(q_s\sum_{il\sigma}\hat{n}_{il\sigma} - L\langle\hat{n}\rangle_G\big) \\ &- \sum_{m=\pm1}\big[\lambda_m\big(\sum_i \hat{A}_{im} - L\langle\hat{A}_{im}\rangle_0\big) + H.C.\big]\ ,\end{aligned} \tag{9}$$

where λ_n and λ_m are the Lagrange multipliers. In the considered method all the mean fields, the variational parameters and the Lagrange multipliers are found by minimizing the free energy functional obtained from the $\hat{K}^a_\lambda$ Hamiltonian. Since usually the correlated state is the one that we want to discuss, it is convenient to fix $\langle\hat{n}\rangle_G$ instead of $\langle\hat{n}\rangle_0$. That is why the effective Hamiltonian contains the Lagrange constraint with the average particle number in the correlated state (the second term of $\hat{K}^a_\lambda$). In this manner $\langle\hat{n}\rangle_G$ is treated as a model parameter (the band filling) and $\langle\hat{n}\rangle_0$ is adjusted during the minimization procedure.

At this point we make the final modification which guarantees the fulfillment of the condition $\langle\hat{n}\rangle_0 = \langle\hat{n}\rangle_G$. With this respect a constraint to the Hamiltonian is added with yet another Lagrange multiplier Λ, i.e.,

$$\hat{K}^b_\lambda \equiv \hat{K}^a_\lambda - \Lambda(\langle n\rangle_0 - \langle n\rangle_G)\ . \tag{10}$$

One can see that the superscripts a and b differentiate the Hamiltonians without and with the constraint on the particle number conservation, respectively. It should be noted

that the additional term in (10) does not contain any operators, but only expectation values. In this manner, it is introduced in the same spirit, as the Gutzwiller variational parameters. The minimization over the Lagrange parameter Λ is going to assure that the average particle number is conserved during the projection operation even though the explicit form of the projection operator is not changed with respect to that used earlier [14, 15]. This constitutes the difference between this approach and the one which modifies the projection operator by introducing the fugacity factors [19]. Nevertheless, one additional equation has to be solved when applying this method. Note that the presence of the condition $\langle \hat{n} \rangle_0 = \langle \hat{n} \rangle_G$ restricts the parameter space of available solutions and hence makes the appearance of any broken-symmetry state less favorable. In effect, the free energy of the ground-state within the present approach may not be lower than that discussed by us earlier. It should be also noted that in general, to make the method proposed here consistent with the one that uses the spin/orbital-dependent or position-dependent fugacity factors [19], one would have to impose similar dependences on the respective Lagrange parameters. However, as it has already been said, in the present situation of a homogeneous system with no magnetic/orbital ordering, the mentioned corrections are not required. The model with the effective Hamiltonian (10) constitutes our fully statistically consistent Gutzwiller approach (f-SGA).

The Hund's rule coupling, together with the correlations taken into account in SGA, lead to the s-wave pairing (intrasite) with an admixture of the extended s-wave pairing (intersite). The respective gap parameter has the form

$$\Delta_{\mathbf{k}} = \Delta^{(0)} + \Delta^{(1)}(\cos k_x + \cos k_y) \; , \tag{11}$$

where $\Delta^{(0)} \equiv \lambda_1 = \lambda_{-1}$ (as we are considering an ESP state) and $\Delta^{(1)} \equiv 2\tilde{Q}t$ is the intersite pairing amplitude. As one can see, the Lagrange parameters $\lambda_{\pm 1}$ have the interpretation of the intrasite gap parameters. The symmetry of the intersite gap parameter is fully determined by the bare band dispersion relation, which has been chosen in the form

$$\epsilon_{\mathbf{k}} = -2t(\cos k_x + \cos k_y) \; , \tag{12}$$

and corresponds to the square lattice with the nearest-neighbor electron hopping only. In the ESP state, after performing the full diagonalization of the effective Hamiltonian (10), one obtains the following dispersion relations

$$E_{\mathbf{k}} = \pm \sqrt{(\epsilon_{\mathbf{k}} - \mu - \lambda_n)^2 + \Delta_{\mathbf{k}}^2} + \epsilon_{12\mathbf{k}} \; , \tag{13}$$

which correspond to the quasiparticle (+) and quasihole (−) excitations. Here, $\epsilon_{12\mathbf{k}}$ is the hybridization matrix element. In what follows, we solve the model, what amounts of solving 16 integral equations with the method and accuracy characterized earlier [14, 15].

3. Results and discussion

The calculations were performed for the interorbital Coulomb repulsion constant U' set to $U' = U - 2J$ and assuming that the hybridization matrix element has the form $\epsilon_{12\mathbf{k}} \equiv \beta_h \epsilon_{\mathbf{k}}$, where $\beta_h \in [0, 1]$, specifies the interband hybridization strength. Moreover, all the energies have been normalized to the bare band-width, $W = 8|t|$ and the reduced temperature was set to $k_B T/W = 10^{-4}$ emulating the $T = 0$ state. In this section the results corresponding to $\langle \hat{n} \rangle_0 \neq \langle \hat{n} \rangle_G$ ($q_s < 1$) and $\langle \hat{n} \rangle_0 = \langle \hat{n} \rangle_G$ ($q_s = 1$) cases are compared explicitly. They have been obtained by using the Hamiltonians $\hat{K}^a_\lambda$ and $\hat{K}^b_\lambda$, respectively. It should be noted that in the calculations without the average particle number constraint, the band filling n refers to $\langle \hat{n} \rangle_G$, whereas $\langle \hat{n} \rangle_0$ is adjusted when carrying out the minimization procedure.

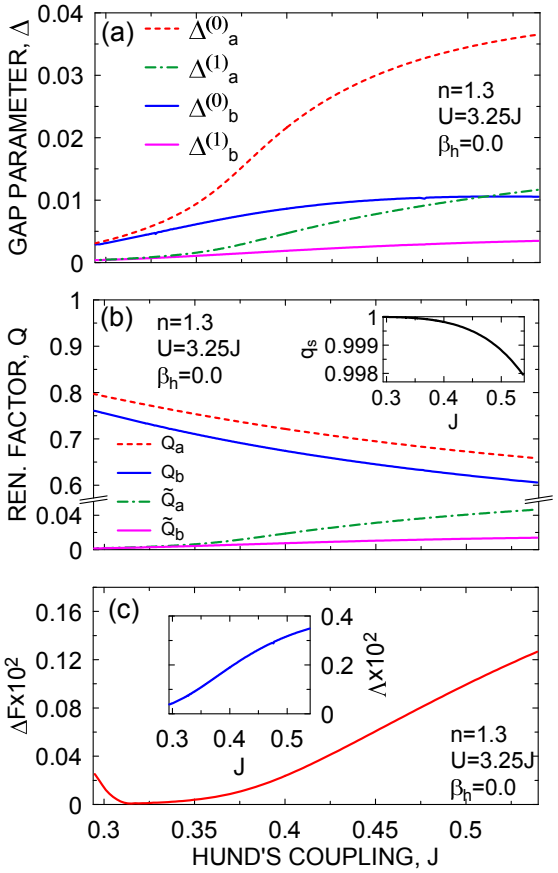

Figure 1. The Hund's rule coupling dependence of the intrasite ($\Delta^{(0)}$) and intersite ($\Delta^{(1)}$) gap parameters (a), the renormalization factors (b), and the free energy difference $\Delta F = F^b - F^a$ (c). The results that correspond to the solution with $n_G \neq n_0$ are labeled with the a index, whereas those corresponding to the $n_G = n_0$ solution are labeled with the index b. In the inset to (b) the J dependence of the ratio $q_s = n_G/n_0$ is shown and the Lagrange multiplier Λ is presented in the inset to (c).

In Fig. 1a we have plotted the superconducting gap components $\Delta^{(0)}$ and $\Delta^{(1)}$ vs. Hund's exchange coupling J. Their magnitudes are essentially reduced when the particle

conservation constraint is imposed. The differences between these two approaches is getting smaller, as the value of the J parameter diminishes and the superconductivity is becoming weaker. The renormalization factors are displayed in Fig. 1b, where also the particle number ratio $q_s = \langle n \rangle_G / \langle n \rangle_0$ is presented in the inset. It should be noted that in the normal state the constraint added in $\hat{H}^b_\lambda$ is not needed as the condition $\langle \hat{n} \rangle_0 = \langle \hat{n} \rangle_G$ is fulfilled automatically. Fig. 1c exhibits that the free energy of the solution corresponding to $\hat{H}^a_\lambda$ is smaller than that corresponding to $\hat{H}^b_\lambda$, which does not come as a surprise, since the available variational parameter space is richer in the former case. However, the superconducting solution in both situations has lower values of the free energy than either the normal or the ferromagnetic phases within the range of model parameters studied.

The following physical conclusions should be drawn from the results shown in Fig. 1. First, a small deviation of the value q_s (renormalizing the occupancy) from unity (cf. inset in b) leads to the essential reduction of the gap components so, while the coupling constant J remains the same, to bring their magnitude to realistic values, it may be necessary to preserve the particle conservation, on expense of the computing time and increased complexity. Second, as discussed already [15], this solution for physically significant regime ($U > 3J$) does not appear in the Hartree-Fock approximation so the paired state is driven to an equal extent by the Hund's rule and the correlations. Moreover, this mechanism leads not only to intra- but also to inter-site pairing component.

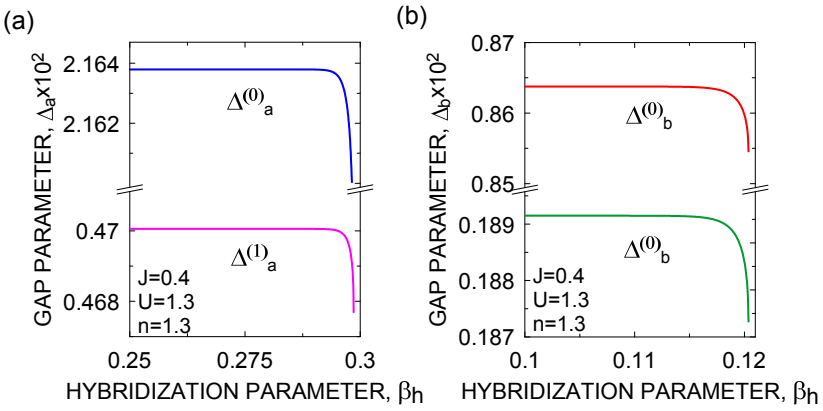

Figure 2. Hybridization magnitude β_h dependence of the gap parameters for the case when $n_G \neq n_0$ (a) and $n_G = n_0$ (b). The hybridization is detrimental to the superconductivity.

Next, we analyze the influence of the hybridization on the stability of the paired state. The corresponding dependence of the gap vs. β_h is plotted in Fig. 2. No qualitative differences are seen between the $\langle \hat{n} \rangle_0 = \langle \hat{n} \rangle_G$ and $\langle \hat{n} \rangle_0 \neq \langle \hat{n} \rangle_G$. In both cases a sizable hybridization is detrimental to the pairing. However, for the case indicated by the a index superconductivity survives for substantially larger values of the β_h parameter, because the gap parameters obtained in this situation are larger (by factor 2÷3). There

are two reasons why the hybridization is detrimental to the superconductivity. First, the bands become inequivalent when $\beta_h \neq 0$. This fact is demonstrated explicitly by

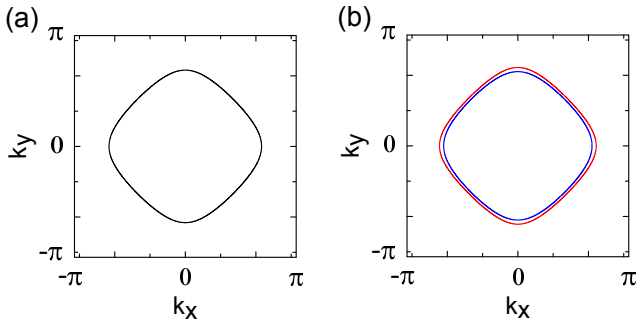

Figure 3. Fermi surface topology in to the normal state for the model parameters $U = 1.3$, $J = 0.4$, $n = 1.3$ for two different values of the hybridization strenght $\beta_h = 0$ - (a) and $\beta_h = 0.11$ - (b). The two Fermi surface sheets are visible for the case with non-zero hybridization corresponding to bonding and antibonding states. The distance between the sheets defines the Fermi-wave-vector mismatch which is small in this circumstances.

plotting the Fermi surface topology for $n \approx 4/3$ in Fig. 3. We see that in the case $\beta_h \neq 0$ we have two Fermi surface sheets corresponding to the inequivalent hybridized bands $\tilde{\epsilon}_{\mathbf{k}1,2} = \epsilon_{\mathbf{k}} \pm \epsilon_{12\mathbf{k}}$. Therefore, the corresponding Fermi wave vectors are different, $\mathbf{k}_{F1} \neq \mathbf{k}_{F2}$. As we have the symmetry $\tilde{\epsilon}_{\mathbf{k}\alpha} = \tilde{\epsilon}_{-\mathbf{k}\alpha}$, there is a Fermi wave-vector mismatch between $\mathbf{k}_{F1}$ and $-\mathbf{k}_{F2}$ when the Cooper pair is formed within our interband pairing mechanism. This is the reason of the superconducting state disappearance at critical value of $\Delta\mathbf{k} \equiv \mathbf{k}_{F1} - \mathbf{k}_{F2}$. The collapse of the homogeneous Cooper-pair state at the critical value of β_h may signal a possibility of a spontaneous formation of the Fulde-Ferrell-Larkin-Ovchinnikov (FFLO) type of inhomogeneous state with the wave vector $\mathbf{Q} = \pm\Delta\mathbf{k}$. This state has not been analyzed in the present paper.

The additional reason why the homogeneous ESP state collapses at critical β_h is caused by the circumstance that by breaking the inter-band ESP state we enhance the inter-band hopping for the opposite spins of electrons and thus diminish the system energy in the normal state. These processes will also destabilize orbitally ordered state, which is disregarded here as for the considered band filling the itineracy destabilizes an alternant occupancy of the orbitals (antiferromagnetic orbital ordering).

For the sake of completeness, we have plotted in Fig 4 the renormalized band structure, both in the normal (a) and in the superconducting (b-d) states. The bands are narrowed by the factor of $Q \approx 0.7$ with respect to the bare band states. Furthermore, in the superconducting phase the gaps are of the same magnitude still for $\beta_h = 0.11$, so the Fermi wave vector mismatch is not yet strong enough to destabilize the uniform superconducting state in a almost discontinuous manner (cf. Fig. 2b).

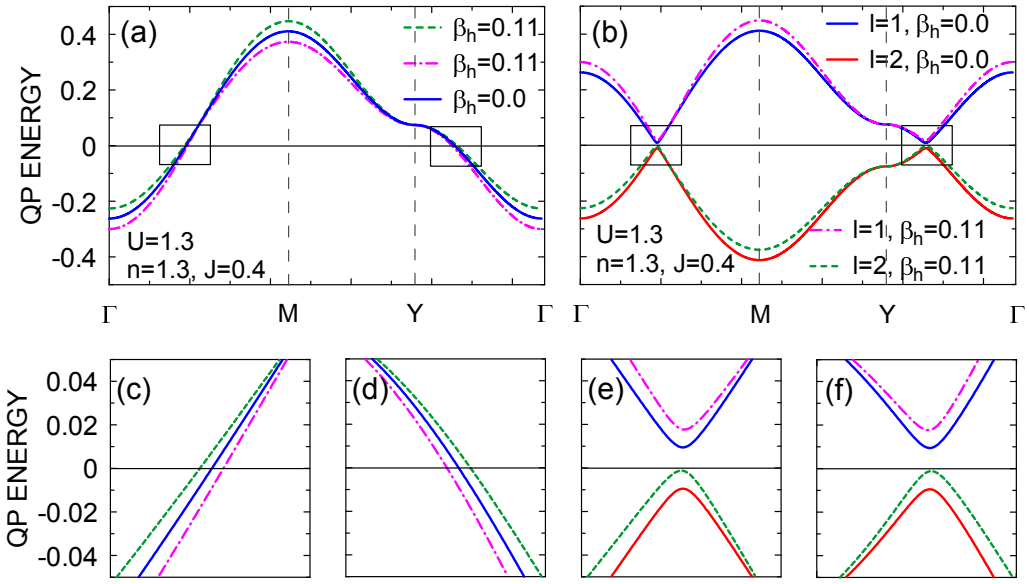

Figure 4. The quasiparticle energies in the normal state - (a) and the superconducting A phase (for $\langle\hat{n}\rangle_0 = \langle\hat{n}\rangle_G$) - (b) for two values of the β_h parameter. For a given set of model parameters one can see the doubly degenerate spin-split quasiparticle excitation and its quasihole correspondent in (b). The characteristic points of the Brillouin zone are the following: $\Gamma = (0,0)$, $M = (\pi,\pi)$, $Y = (0,\pi)$. In (c), (d), (e), and (f) the QP energies are shown zoomed around two points of the Brillouin zone that are marked by squares in (a) and (b).

4. Conclusions

We have proposed a modified SGA approach in which we impose the condition for the average particle number conservation when carrying out the Gutzwiller projection to the correlated state. The calculated results were compared with those obtained earlier [15]. It has been shown that the differences between these two methods are significant when the superconducting pairing is strong. The gap parameter is strongly reduced in the case when the condition $\langle n\rangle_0 = \langle n\rangle_G$ is imposed for larger coupling constants, J. It is amazing that a small free energy difference $\Delta F \sim 10^{-3}W \sim 1$meV leads to such remarkable quantitative differences of the physically meaningful parameters even though their qualitative trends remains similar. It should be also noted that the average number of particle ratio q_s is very close to unity. The influence of the interband hybridization is qualitatively similar for both approaches. The Fermi-surface topology and the quasiparticle energies have been also analyzed. Large Fermi wave vector mismatch between the hybridized bands can be the source of a transition to a spontaneous inhomogeneous spin-triplet state of the FFLO type, which has not been analyzed here.

In our study we have taken the band filling $n \equiv 1.3 \approx 4/3$. Due to the electron-hole symmetry the same results should be obtained for $n \approx 8/3$. Such band filling emulates the corresponding band filling $n \approx (4/3)(3/2) = 2$ or $n \approx 4$ in the electron-hole symmetric systems with three bands. The last filling corresponds to that of $3d^4$

configuration of a triply-degenerate-band state for Sr_2RuO_4. The modeling of this system via a doubly-degenerate band state has been discussed in [26].

The stable ESP solution can be obtained in the Hatree-Fock approximation only for $U < 3J$ [15], while in the SGA approach, i.e., when the correlations are taken into account, this rather stringent and unrealistic condition is unnecessary. In connection with this we should mention the two papers [29, 30] in which the instability of the normal state with respect spin-triplet state has been discussed within the Dynamical Mean Field Approximation. In our paper, we analyze explicitly the ordered phase. This is an essential extension of the whole approach as it can provide a starting microscopic basis for the analysis of the spin-triplet pairing in e.g. Sr_2RuO_4. So far the successful models for this compound are based on negative-U assumption [27, 28] which may turn unrealistic in this case of $4d$ orbitals due to the Ru atoms. Obviously, to make our model quantitatively valid we have to include the strongly anisotropic nature of the $4d$ orbitals, as well as a sizable spin orbit coupling. Nevertheless, the present approach represents, in our view, the first complete microscopic treatment in a model situation which may form a staring point for calculations in a realistic situation. These realistic calculations will contain many more Gutzwiller variational parameters which may make the numerics quite cumbersome. Nonetheless, the overall features should be preserved as the variational calculations require only total energy, averaged out over quasiparticle bands. Also, it is rewarding that the considered microscopic pairing mechanism allows for the formation of not only the pure spin-triplet superconducting phase, but also the superconductivity coexisting with magnetic ordering [15], depending on the value of microscopic parameters, as well as, most probably, on the details of the band structure.

5. Acknowledgements

M.Z. has been partly supported by the EU Human Capital Operation Program, Polish Project No. POKL.04.0101-00-434/08-00. This work has been partly supported by the Foundation for Polish Science (FNP) within project TEAM and partly by the National Science Center (NCN), through scheme MAESTRO, Grant No. DEC-2012/04/A/ST3/00342. We are also grateful to Jörg Bünemann for helpful discussions.

References

[1] A. P. Mackenzie and Y. Maeno, Rev. Mod. Phys. **75**, 657 (2003).
[2] T. M. Rice and M. Sigrist, J. Phys.: Condens Matter **7**, L643 (1994).
[3] Y. Kamihara, T. Watanabe, M. Hirano, and H. Hosono 2008, J. Am. Chem. Soc. **130**, 3296 (2008).
[4] Y. Nakai, S. Kitagawa, K. Ishida, Y. Kamihara, M. Hirano, and H. Hosono, N. J. Phys. **11**, 045004 (2009).
[5] S. S. Saxena, P. Agarwal, K. Ahilan, F. M. Grosche, R. K. W. Haselwimmer, M. J. Steiner, E. Pugh, I. R. Walker, S. R. Julian, P. Monthoux, G. G. Lonzarich, A. Huxley, I. Sheikin, D. Braithwaite and J. Flouquet, Nature **406**, 587 (2000).
[6] A. Huxley, I. Sheikin, E. Ressouche, N. Kemovanois, D. Braithwaite, R. Calemczuk, J. Flouquet, Phys. Rev. B **63**, 144519 (2001).

[7] N. Tateiwa, T. C. Kobayashi, K. Hanazono, K. Amaya, Y. Haga, R. Settai and Y. Onuki, J. Phys.: Condens. Matter **13**, 117 (2001).
[8] K. Klejnberg and J. Spałek, J. Phys.: Condens. Matter **11**, 6553 (1999).
[9] K. Klejnberg and J. Spałek, Phys. Rev. B **61**, 15542 (2000).
[10] J. Spałek, Phys. Rev. B **63**, 104513 (2001).
[11] J. Spałek, P. Wróbel, and W. Wójcik, Physica C **387**, 1 (2003).
[12] For previous brief and qualitative considerations about the ferromagnetism and spin-triplet pairing coexistence see: S-Q. Shen, Phys. Rev. **57**, 6474 (1998).
[13] M. Zegrodnik and J. Spałek, Phys. Rev. B **86** 014505 (2012).
[14] M. Zegrodnik, J. Spałek, J. Bünemann, arxiv: 1305.2806
[15] M. Zegrodnik, J. Bünemann, J. Spałek, arxiv: 1304.4478
[16] J. Bünemann, F. Gebhard, T. Ohm, S. Weiser, and W. Weber in *Frontiers in Magnetic Materials* (Springer, Berlin 2005).
[17] P. W. Anderson and N. P. Ong, J.Phys. Chem. Solids **67**, 1 (2006).
[18] B. Edegger, N. Fukushima, C. Gros, and V. N. Muthukumar, Phys. Rev. B **72**, 134504 (2005).
[19] N. Fukushima, Phys. Rev. B **78**, 115105 (2008).
[20] F. Gebhard, Phys. Rev. B **41**, 9452 (1990).
[21] R. B. Laughlin, Philos. Mag. **86**, 1165 (2006).
[22] Q.-H. Wang, Z. D. Wang, Y. Chen, and F. C. Zhang, Phys. Rev. B **73**, 092507 (2006).
[23] J. Kaczmarczyk and J. Spałek, Phys. Rev. B **84**, 125140 (2011).
[24] O. Howczak, J. Spałek, J. Phys.: Condens. Matt. **24**, 205602 (2012).
[25] O. Howczak, J. Kaczmarczyk, and J. Spałek, Phys. Status Solidi **250**, 609-614 (2013).
[26] Y. Imai, K. Wakabayashi, M. Sigrist, Phys. Rev. B **85**, 174532 (2012).
[27] J. F. Annett, B. L. Györffy, G. Litak, and K. I. Wysokiński, Eur. Phys. J. B **36**, 301 (2003).
[28] J. F. Annett, B. L. Györffy, and K. I. Wysokiński, New J. Phys. **11**, 055063 (2009).
[29] J. E. Han, Phys. Rev. B **70**, 054513 (2004).
[30] S. Sakai, R. Arita, and H. Aoki, Phys. Rev. B **70**, 172504 (2004).